ANL-5732

ARGONNE NATIONAL LABORATORY
P. O. Box 299
Lemont, Illinois

BIOLOGICAL AND MEDICAL RESEARCH DIVISION SEMIANNUAL REPORT

January through June, 1957

July, 1957

Preceding Reports:
ANL-5696 - October, November, December, 1956
ANL-5655 - July, August, September, 1956

Operated by The University of Chicago
under
Contract W-31-109-eng-38

DISCLAIMER

TABLE OF CONTENTS

TABLE OF CONTENTS

TABLE OF CONTENTS

TABLE OF CONTENTS

TABLE OF CONTENTS

TABLE OF CONTENTS

PROGRESS REPORT: RADIATION-INDUCED DIVISION DELAY

II. Preliminary Studies on Gamma-Ray Dose-Rate Effects and on Fission Neutron Effects

Howard S. Ducoff

X-irradiated nitrogen-depleted suspensions of Chilomonas paramecium exhibit a division delay, upon restoration to complete medium, that is equal to the sum of the lag time of unirradiated suspensions returned to complete medium and the fission delay induced in exponentially growing cultures exposed to the same dose of X-rays.[1] This indicates that no recovery takes place in the absence of the nitrogen source; the total damage to the division process accumulating during a relatively extended period of time becomes manifest, and may be quantitatively determined, after restoration to the complete medium. It has thus been possible to study the effect on duration of division block of various Co^{60} γ-ray rates with exposure times which constitute a significant fraction of, or which even exceed, the normal interdivision time. For example, 90 min of exposure at a dose rate of 150 r/min results in the same division delay as 10 min at 1000 r/min. In addition, it has been possible to study the division-blocking effects of irradiation with fission neutrons of the CP-5 reactor. These studies proved that, just as with X- and γ-ray exposures, neutron irradiation results in a division delay from which there is no detectable recovery in the absence of a utilizable nitrogen source.

Acknowledgement: I should like to thank Dr. H. H. Vogel, Jr. for performing the neutron irradiations.

Reference

1. Ducoff, H. S. Factors affecting radiation-induced division delay in Chilomonas paramecium. Physiol. Zool. In press.

PRELIMINARY REPORT: EFFECT OF LIGHT AND X-RAY UPON THE GERMINATION OF TOBACCO SEED

Norbert J. Scully

In a number of plant species, germination of seed is known to be promoted by visible light. Recent studies confirm that this effect of light upon germination is a widespread phenomenon.(1) It has been clearly demonstrated with the more light-sensitive species that a reversible photoreaction is involved in the regulation of germination.(2) In these cases, water-soaked seed that fail to germinate in the dark are induced to germinate by exposure to red (6550 A) light, and the effect is reversed if the exposure is followed by exposure to far red (7350 A) light. A reversible photoreaction of this general type has been recently noted for tobacco (Nicotiana tabacum) although the complete visible-light action spectrum has not been detailed.(3)

The present report deals with the cultural and white light requirements for germination of tobacco (Nicotiana tabacum var. One-sucker), as well as the relative sensitivity of this light mechanism to X-irradiation.

Experimental

Tobacco seeds were kept on filter paper moistened with 2 ml of distilled water in 5-cm glass Petri dishes, with 50 seeds per dish. All dishes were kept in light-tight containers except at time of light treatment, and the temperature was maintained at 76°F except during X-ray treatment. These cultural conditions resulted in 100% germination when adequate light treatments were applied. Germination of the soaked seed is first apparent two days after light treatment, at the time at which the radicle ruptures the seed coat; germination data reported here are based on observations made 3-6 days after light treatment.

Since the light sensitivity for germination of tobacco seed is known to vary from variety to variety of this species, the sensitivity of the One-sucker variety was first ascertained. When dishes of soaked seed were maintained in darkness for 8 days, no germination was observed. Later studies indicated no germination if the period was extended to 22 days.

The seed are not light-sensitive when in dry dormant condition but they respond as early as 15 min after the initiation of the water soak treatment, if given 8000 fcm (500 foot-candles for 16 min) of light from a combined fluorescent and incandescent mazda source. When seed were soaked for 24, 48, or 72 hr, under the described cultural conditions, and then exposed to incandescent Mazda light varying in dose from 0.07-5000 fcm,

their light sensitivity increased with increasing duration of imbibition (Table 1). The tobacco variety seed used was measurably sensitive to light in the range of 0.07-1.0 fcm.

TABLE 1

Effect of imbibition period and light dose on germination of tobacco seed

Each value represents data obtained from one dish containing 50 seeds. Results are expressed as % germination.

Light dose,* fcm	Water imbibition period		
	24 hr	48 hr	72 hr
0	0	0	0
0.07	0	2	2
1.0	2	16	2
10.0	4	28	18
100.0	32	72	26
1000.0	64	88	86
5000.0	100	96	98

*The 0.07-fcm and 1.0-fcm exposures were at an intensity of 0.8 foot-candles and the remainder were at 42 foot-candles.

On the basis of the information obtained in these preliminary studies, the effect of X-irradiation upon the germination of this seed was investigated. Seed, 50 per dish, were soaked for 48 hr and then exposed to X-ray doses of 0, 500, 1000, 2500, 5000, 7500, and 10,000 r, with 2 dishes per dose group. Following irradiation, one dish from each dose group was placed in darkness while the other was immediately exposed to 10,000 fcm (500 fc for 20 minutes) to a fluorescent and incandescent Mazda light source, and all dishes were placed in darkness. The results are shown in Table 2, where germination of seed for all treatment groups is reported as per cent germination at 6 days after X-irradiation.

The data indicate that X-ray treatment under these conditions does not modify the normal failure to germinate in dark. Neither did it alter the capacity of a light dose (10,000 fcm) exceeding that required for 100% germination to promote full germination. However, the stage of germination attained by X-irradiated seed was measurably altered with increasing dose. The control, 500 and 1000 r groups were of comparable stages of development, while successively retarded stages were exhibited by seed given increasing dose in the 2500, 5000, 7500, and 10,000 r groups.

TABLE 2

Effect of light and X-ray dose on germination of tobacco seed

Each value represents data obtained from one dish containing 50 seeds. Results are expressed as % germination.

X-ray dose, r	Light treatment	
	Light	Dark
0	98	0
500	100	0
1000	100	0
2500	100	0
5000	94	0
7500	94	0
10000	98	0

Further study will be made of the effect of X-ray treatment upon the light sensitivity of both dry and soaked seeds. Subsequently, such seed will be given light doses which will promote approximately 50% germination, thereby affording opportunity to measure increase or decrease resulting from X-ray treatment. The detailed action spectrum for promotion of germination of this seed will be investigated.

References

1. Evanari, M. Seed germination, in Radiation Biology, Vol. III, A. Hollaender, ed., McGraw-Hill, New York (1956).

2. Borthwick, H. A., S. B. Hendricks, E. H. Toole, and V. K. Toole. Action of light on lettuce-seed germination. Botan. Gaz. 115:205-225 (1954).

3. Toole, E. H., H. A. Borthwick, S. B. Hendricks, and V. K. Toole. Physiological studies on the effects of light and temperature on seed germination. Compt. rend. assoc. intern essais semences 18:267-276 (1953).

PROGRESS REPORT. BACTERIAL MUTATION

Mean Delay Period in the Induction of the Mutant Phenotype

Herbert E. Kubitschek

In a previous report[1] the mean delay period for the expression of resistance to the bacteriophage T5 was found to be a time equivalent to 3.4 generations of growth of the parent culture of bacteria in Escherichia coli, strain B/1, t. This result does not imply that the cells undergoing the change from sensitivity to resistance also required 3.4 divisions, on the average, to express the mutant phenotype, since the growth rate of these cells in transition is not known.

A measurement of the mean growth rate of these cells with the latent phenotype (mutant genotype but wildtype phenotype) can be made that will allow the calculation of the actual mean number of divisions which the new mutant must undergo before resistance is expressed. The growth rate of cells of the mutant phenotype B/1, t/5 is the same as that of the parent culture. It can be shown that the number of divisions, D, undergone by the latent mutant is given by the solution of the transcendental equation

$$m^* (D - 3.4) = \left\{ 1 - \exp (D - 3.4) \right\} \quad L \frac{dm}{dt}$$

where m^* is the titer for cells of the latent phenotype, L is the duration of the latent period and $\frac{dm}{dt}$ is the observed mutation rate. Thus the measurement of D involves the measurement of m^*. In practice, this can be accomplished by allowing bacteria from chemostat samples to grow for a period long enough so that all mutants can express the mutant phenotype, and then to applying the test for phage resistance.

The measurement of the mean delay period in terms of the number of divisions required by the newly-formed mutants is in progress.

Reference

1. Kubitschek, H. E., and H. E. Bendigkeit. The mean delay in the appearance of the phenotype for phage resistance in Escherichia coli. Quarterly Report of the Biological and Medical Research Division, Argonne National Laboratory. ANL-5655, pp. 36-38 (1956).

12

PROGRESS REPORT: BACTERIAL MUTATION

Delay Period in the Induction of Phage Resistance

Herbert E. Kubitschek and Harold E. Bendigkeit

Previously[1] we have indicated that the mean delay period in the production of resistance to the phage T5 in E. coli, strain B/1, t is 3.4 generations of parental growth. It is shown below that the newly-formed mutant undergoes the same number of divisions; that is, the newly-formed mutant has a growth rate very close to that of both the parent cell and the cell with the mutant phenotype.

The data leading to the above conclusion are shown in Figure 1.

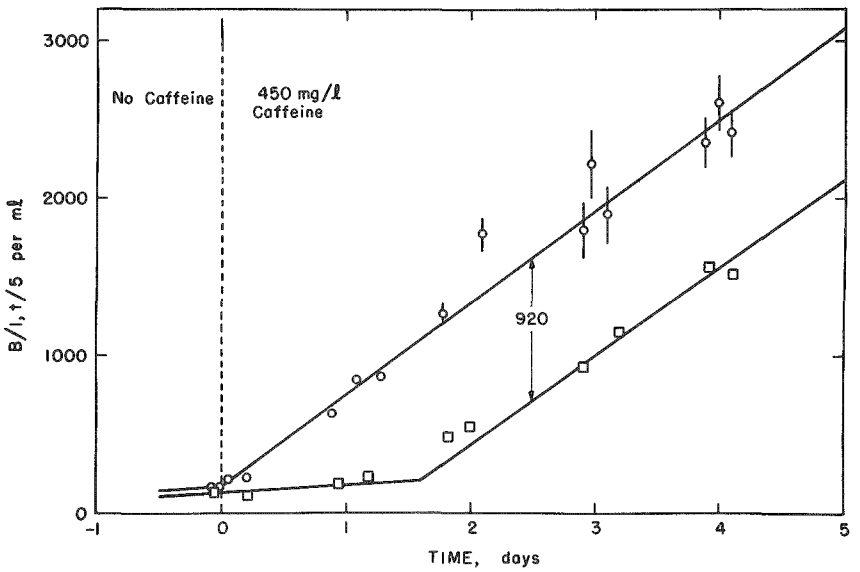

Figure 1. Accumulation of T5-resistant bacteria in a chemostat to which caffeine has been added. □, titers of bacteria with the mutant phenotype; O, sum of bacteria with mutant phenotype plus those with mutant genotype but wild phenotype. Vertical bars represent standard errors greater than 5%, considering counting errors only.

The lines here represent different kinds of measurements upon the same chemostat: (a) the squares indicate titers of bacteria with the phage-resistant phenotype, and are obtained by applying phage immediately upon taking a sample from the chemostat; (b) the circles include titers of all bacteria capable of developing phage resistance as well as titers of the expressed mutants, and these data are obtained by applying phage after 3 hr of growth (about six generations) on nutrient agar. The difference

between the two sets of data indicates the number of bacteria which have not expressed the mutant phenotype. If they are not under selection, then their equilibrium number in the chemostat should be the number of mutants produced in 3.4 generations. On the basis of the observed mutation rate of 580/day from Figure 1 and the generation time of 11.4 hours, the number of mutants produced in 3.4 generations should be 940. The observed difference between the two lines, 920, is shown in the figure. We conclude that the induction of the mutation has little or no effect upon the growth rate of the bacterium.

The data of Figure 1 have further implications. A single event establishes the mutant genotype. These events occur at random in the population. Following the stimulus to mutation, the mean delay period for the appearance of a mutant genotype is small, less than half a generation.

Reference

1. Kubitschek, H E., and H. E. Bendigkeit The mean delay in the appearance of the phenotype for phage resistance in Escherichia coli. Quarterly Report of Biological and Medical Research Division, Argonne National Laboratory. ANL-5655, pp. 36-38 (1956).

PROGRESS REPORT: BACTERIAL MUTATION

Filamentous Growth of *Escherichia coli* Exposed to Caffeine

Herbert E. Kubitschek and Harold E. Bendigkeit

At slow and medium growth rates of *E. coli*, strain B/1,t in the chemostat (Friedlein medium with tryptophan limiting the growth rate), these bacteria have a conventional appearance: they are rod-shaped and about 2 to 4 μ long. Only a minute fraction shows filamentous forms. At very rapid growth rates, near generation times of 2 hr, most of the bacterial mass is in the filamentous form.

In the presence of caffeine, which is a mutagen inducing resistance to the bacterial virus T5, filament formation occurs at slower growth rates. At any given growth rate the filament fraction increases with caffeine concentration. Thus, the physiological effect of caffeine, growth without customary division, now corresponds to that observed for other mutagens, such as ultraviolet light and X-rays.

In addition, in the presence of sufficient concentrations of the antimutagens adenosine or guanine the filament-producing effect of the caffeine is lost.

RADIOSTRONTIUM AT "OPTIMUM CARCINOGENIC LEVEL" IN THE DOG: EFFECT UPON MORBIDITY OF TOTAL BLOOD EXCHANGE SHORTLY AFTER INJECTION

Miriam P. Finkel, Robert J. Flynn, Juanita Lestina, and Dorice M. Czajka

It is an established fact that radiostrontium is a potent skeletal carcinogen when it is deposited in adequate amount within the bones of several mammalian species. The lowest effective dose is not yet known; the highest effective dose is determined by the acute and subacute response to irradiation of the several species that have been studied. For example, in our long-term mouse experiment the median-lethal 30-day dose of Sr^{90} (in equilibrium with Y^{90}) was 6 μc/g; acute irradiation disease appeared in all mice that received 4.3 μc/g; most of the animals that survived the early stages of poisoning with 2.2 μc/g died with malignant bone tumors; and 91% of those that received 0.9 μc/g died with one or more grossly visible bone tumors.[1,2] On the other hand, the 30-day LD_{50} for the dog was found to be approximately 0.15 μc/g,[3] at which dose less than 20% of a mouse population would be expected to show bone malignancies. One osteogenic sarcoma has already appeared among the six dogs that survived the acute effects of this dose.[4]

One of the major problems associated with radiocarcinogenesis concerns the length of time between the administration of the isotope and the appearance of malignant change. Present data suggest that the length of this latent period does not vary with the radioelement, with the size of the dose (except insofar as survival time decreases and tumor incidence increases with increasing dose), or with the age of the animal at the time of treatment.[5] But there is very little evidence bearing upon the question of whether the length of the latent period is constant for all mammalian species. This information is lacking primarily because no species other than the mouse has received internal emitters at levels that have an almost absolute probability of inducing bone tumors. For example, 167 days is the shortest length of time between injection of Sr^{90} and death of a mouse with a malignant bone tumor (2.2 μc/g), but 2.8 years elapsed before the first dog died with a similar neoplasm (0.15 μc/g). To date the shortest latent period reported for the dog is 1.8 years after 0.841 μc/kg of radiothorium.[6]

As an approach to the question of variation of latent period with species, we are investigating possible methods of subjecting all or a portion of the dog skeleton to levels of irradiation from Sr^{90} that have been shown to be potently carcinogenic in the mouse. In the latter species intravenously injected doses of from about 0.5 to 1.0 μc/g result in a great number of bone tumors and constitute the "optimum carcinogenic range." Since this range exceeds the 30-day LD_{50} for the dog by a factor of from 3 to 7, some

means must be found either to protect the animal from acute irradiation death or to treat only a small portion of the skeleton. Our first attempt, which was to deliver a total intravenous dose of 0 5 mc/kg in the course of several months by fractionation, terminated fatally after two doses of 0.1 mc/kg each. Our second attempt was based upon the propositions that (a) the major factor in acute irradiation disease is the initial injury resulting from the irradiation of the entire animal by the circulating radioisotope immediately after injection, and (b) some protection might be afforded by withdrawing the material still in the blood stream 2 hr after injection. The results will be reported here.

Experiment

An adult, male, mongrel dog, weighing 10.5 kg, was anesthetized with Nembutal® and prepared for transfusion into the right jugular vein and for bleeding from the right femoral artery. Five ml of solution, containing 5.05 mc of Sr^{90} in equilibrium with Y^{90}, were injected into the left saphenous vein. Blood samples were withdrawn for radioanalysis at various intervals thereafter. Starting at 146 min after injection, approximately 100 ml of blood was withdrawn from the femoral artery, and immediately thereafter 100 ml of pooled serum and whole blood from three donor dogs was introduced into the jugular vein. This procedure was repeated 12 times during the next 40 min, the only variation being the final introduction of 300 rather than 100 ml in order to compensate for the withdrawal of blood samples during the first 140 min. The right jugular vein and femoral artery were ligated and severed, the flesh wounds were sutured, and the dog was given a prophylactic dose of 600,000 units of penicillin. Within a short time swelling was noted about the mouth and eyes, and a generalized allergic response became evident Adrenalin ® was administered subcutaneously, and the swelling was negligible 24 hours later.

Terramycin® was substituted for penicillin as a therapeutic antibiotic, and recovery from surgery was uneventful. The total leucocyte count fell to 500/mm^3 by the eleventh day, and rectal temperature rose to 103.6° by the 13th day, the animal seemed somewhat weak and ate poorly. No oral petechiae were seen, and the general appearance was good. One hundred ml of fresh blood was injected into the left saphenous vein. Beginning with the 14th day streptomycin was given, as well as Sulfathalidine ®, sulfathiazole, Hemogen Hextabs ®, menadione, and ascorbic acid. On the 17th day death seemed imminent, but there was a sudden change in the course of a few hours, and on the 18th day the temperature was normal and the appetite good. From the 20th through the 25th day medication consisted of Hemogen Hextabs ®, ascorbic acid, and Terramycin ®. Since that time there have been periods of elevated temperature and occasional evidence of weakness and loss of appetite. Fresh blood was given on the 42nd day (100 ml), and 6 ml of femoral bone marrow from a donor dog was introduced into the marrow cavity of the right femur on the 57th day. At present (70 days

after injection) the dog appears to be in good condition except for the hematological findings, which are presented in Figures 2 and 3. The slight suggestion of improvement after the administration of bone marrow leads to some interesting speculations and prompts further experimentation, which is now being planned.

That we did not succeed in diminishing total-body irradiation by replacing strontium-carrying blood with fresh blood is evident in Figure 4. In plotting these data it has been assumed that at the moment the injection was completed the entire dose was in the blood, that 7.5-8% of the total body weight was blood,(7) and that the blood volume changed in the course of the experiment only by the amount withdrawn and injected. The solid line indicates the observed reduction with time of the total dose in the circulating blood; the dashed line indicates the reduction expected during the period of alternate bleeding and transfusing. It is obvious that there was a delicate balance between the concentration of radiostrontium in the blood and in the tissues (bone, primarily), and that the material that had been deposited was so lightly held that it was readily available to the circulation. Approximately 650 μc, or 12.9% of the total dose, was removed from the dog by bleeding during the three hours after injection. However, if all the blood had been drained from the animal at 146 min, only about 250 μc would have been removed. These additional 400 μc must have returned to the circulation from the bone. Thus it appears that the deposition of radiostrontium can be influenced by the blood-exchange procedure but that the blood level cannot be changed appreciably.

The first blood sample taken $1\frac{1}{2}$ min after injection indicated that 35.7% of the injected dose was in the blood at that time (Figure 5). This gives a half-time value of one min, and is consistent with the assumptions that (1) 10% of the total blood volume reaches bone during a single circulation cycle, (2) all the radiostrontium that reached bone remained there, and (3) deposition in soft tissues was negligible, and (4) circulation time in the dog was 9 sec. At 6 min, 22% of the total dose remained in the blood, whereas only 1.5% would be expected if the above conditions were maintained. This emphasizes the fact that the strontium was only very loosely held and could readily shift from bone to blood and back again at this short interval after injection.

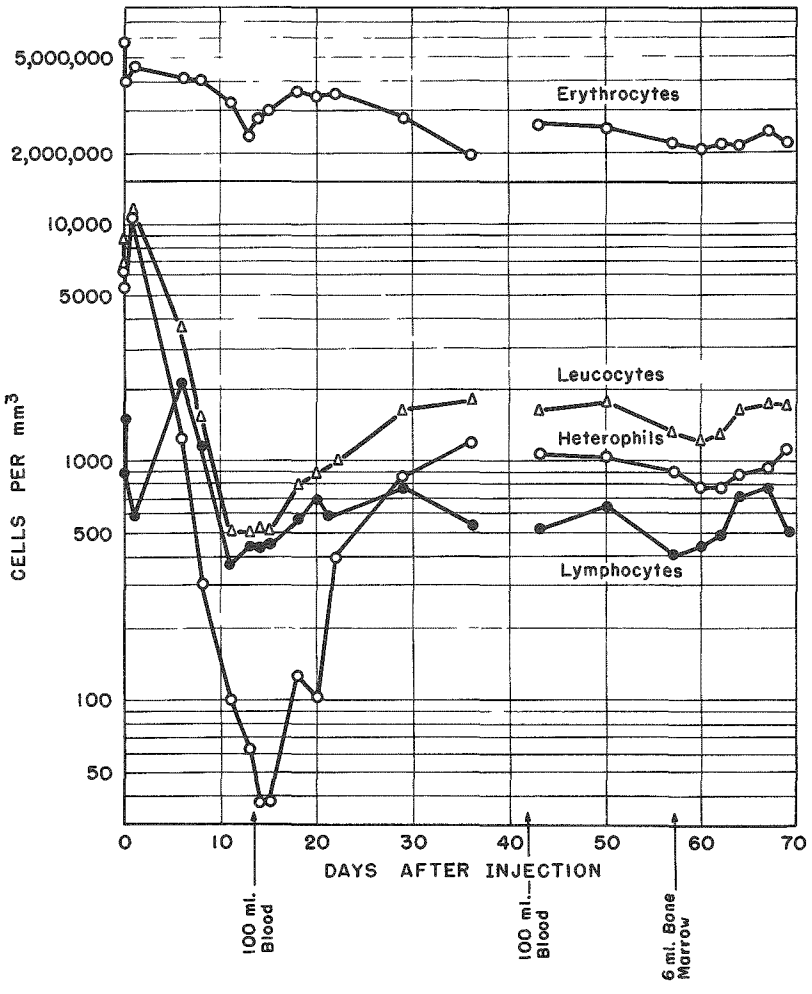

Figure 2. Response of the hematopoietic system as measured by the erythrocyte and leucocyte counts of the peripheral blood.

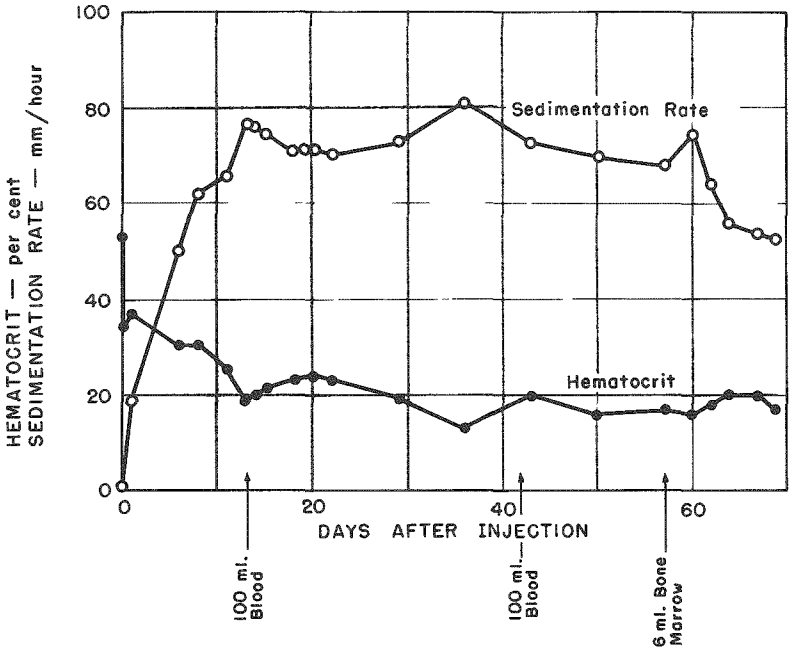

Figure 3. Hematocrit and sedimentation rate of the peripheral blood after injection.

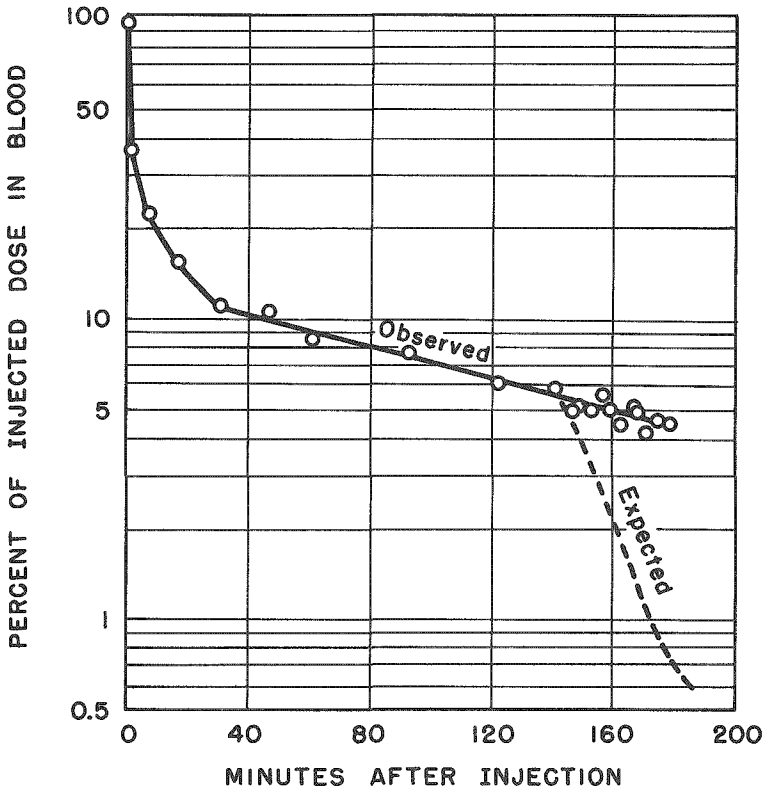

Figure 4

Percentage of the total dose in the circulating blood during the 3 hours after injection.

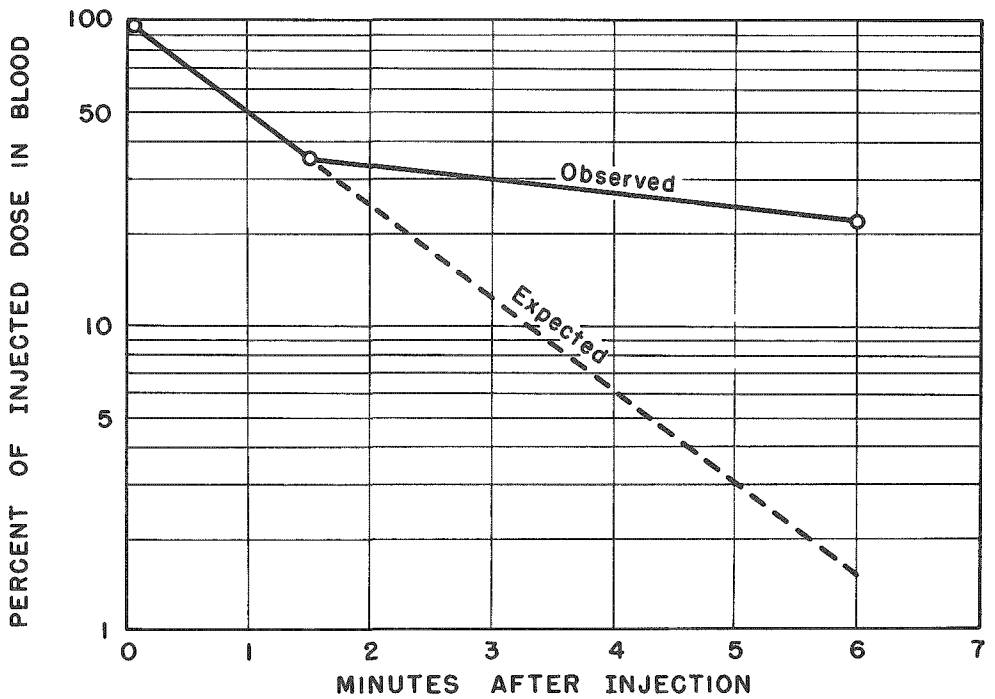

Figure 5. Percentage of the total dose observed in the blood 1-1/2 and 6 minutes after injection and the percentage expected if the material once deposited in bone could not return to the circulation.

References

1. Finkel, M., and G. Scribner. Toxicity of strontium-90 and calcium-45 in mice. I. Status of experiments 200-300 days after injection. Quarterly Report of Biological and Medical Research Division, Argonne National Laboratory. ANL-5456, pp. 36-37 (1955).

2. Finkel, M., and G. Scribner. Toxicity of strontium-90 and calcium-45 in mice. II. Status of experiments 625 days after injection. Quarterly Report of Biological and Medical Research Division, Argonne National Laboratory. ANL-5597, pp. 16-20 (1956).

3. Finkel, M., J. Lestina, G. Scribner, H. Lisco, R. Flynn, and A. Brues. Toxicity of radiostrontium in dogs: Current status of the long-term experiments. Quarterly Report of Biological and Medical Research Division, Argonne National Laboratory. ANL-5426, pp. 33-35 (1955).

4. Finkel, M., R. Flynn, J. Clark, G. Scribner, J. Lestina, H. Lisco and A. Brues. Toxicity of radiostrontium in carnivores: Current status of the long-term cat and dog experiments. Quarterly Report of Biological and Medical Research Division, Argonne National Laboratory. ANL-5696, pp. 16-20 (1957).

5. Finkel, M. Internal emitters and tumor induction. (International Conference on the Peaceful Uses of Atomic Energy, Geneva) Peaceful Uses of Atomic Energy, Vol. 11, pp. 160-164. United Nations, New York (1955).

6. Arnold, J. Pathology report. Annual Progress Report, Radiobiology Laboratory, University of Utah, College of Medicine, pp. 29-34 (1956).

7. Maloney, M. Personal communication.

THE INFLUENCE OF DOSAGE PATTERN UPON THE TOXICITY OF Sr^{90} IN MICE

I. Preliminary Experiment and 212-day Survey of the Long-term Study

Miriam P. Finkel, Betty J. Tellekson, Juanita Lestina, and Birute O. Biskis

The maximum permissible levels of radioisotopes in man are stated in terms of the retained dose, or the body burden. However, it has been our custom to refer to the toxicity of radioisotopes in mouse populations in terms of the injected dose rather than the retained dose. There are several reasons for this practice: First, although the amount of material that is administered to each animal is known with some degree of accuracy, the amount remaining at the time of death can only be assumed from average retention curves because the assay of each animal in a large toxicity experiment is not feasible. Second, the body burden is not constant but decreases with time. Third, the relative contributions of the administered dose and the retained dose in bringing about the ultimate pathological changes are not known, so there is no more reason to use one reference point than the other. This last problem, which is of considerable theoretical importance, might be attacked by eliminating the peak irradiation that follows immediately upon the administration of the total dose in a single injection. This can be accomplished by dividing the total dose into several fractions given at time intervals so spaced that the body level increases gradually and does not at any time approach 100% of the total dose.

The administration of a bone-seeking radioisotope in divided doses rather than in a single dose adds another variable in an area where information is meager. Although it is known that radiostrontium is deposited unevenly in bone composed of typical haversian systems, and it may be anticipated that dividing the dose will increase the number but decrease the intensity of the so-called "hot spots," we do not know whether a similar uneven distribution occurs in mouse bone, where typical haversian systems are lacking. Of even greater importance is the fact that the significance of these more radioactive areas in tumorigenesis has not been established. This complication can be alleviated, and in fact, some answers to the general questions may be gained by dividing the total dose still further into many smaller fractions so that a completely uniform distribution of the radioisotope in bone will be approached.

Materials and Methods

CF No. 1 female mice, which were approximately 70 days old at the beginning of the experiment, were given Sr^{90} (in equilibrium with Y^{90}) as the chloride in normal saline at pH 5.5, by intravenous injection. Three dose levels were used: 1.0 $\mu c/g$, which has been shown to induce malignant bone tumors in 100% of 150-day survivors, 0.5 $\mu c/g$ (expected 80% incidence of bone tumors), and 0.25 $\mu c/g$ (expected 25% incidence of bone tumors).[1] The total dose was administered in a single injection, in 5 equal fractions at 7-day intervals, or in 20 equal fractions 5 days a week for 4 weeks.

Table 3 gives the plan of the retention and distribution studies. The amount of Sr^{90} present in the living mice was determined by measuring the bremsstrahlung produced by the beta emanations of its Y^{90} daughter. A sodium iodide crystal $2\frac{1}{2}$ in. long and $1\frac{1}{2}$ in. in diameter was used.* At the end of the counting period the radiostrontium content of 19 of these animals was verified by ash analysis.** Animals in the autoradiographic series were killed with Nembutal ® at specified times, and representative bones were dehydrated in acetone and ether, embedded in Scotchcast Resin No. 2 (Minnesota Mining and Manufacturing Co., St. Paul, Minn.),[2] and ground to approximately 100 μ in thickness. Exposures were made on duPont X-ray Safety Film, Industrial Type 510.

TABLE 3

Plan of the preliminary experiment

Total dose, $\mu c/g$	Number of injections	Dose per injection, $\mu c/g$	Number of animals		
			Retention	Autography	Ash analysis
1.0	1	1 0	10	(2)‡	(5)
0.5	1	0.5	10	10(5)	(3)
0 25	1	0.25	10	(2)	(5)
0.5	5†	0.1	10	10(5)	(3)
0.5	20††	0.025	10	10(5)	(3)

†One per week for 5 weeks. ††Five per week for 4 weeks.

‡Numbers in parentheses were derived after 58 or 100 days from animals used for retention estimates.

*We are indebted to P. Gustafson for his assistance in assembling and operating the physical apparatus.

**These analyses were done by F. Smetana.

The plan of the long-term toxicity experiment is given in Table 4. The animals are being maintained in accordance with the routine procedures established for length-of-life studies with radioisotopes in our laboratory. When natural death is imminent, the mice are killed with Nembutal ® and examined for evidence of gross and microscopic pathology.

TABLE 4

Plan of the long-term toxicity experiment

Group	Total dose, $\mu c/g$	Number of injections	Dose per injection, $\mu c/g$	Number of animals
1	1.0	1	1.0	30
2	0.5	1	0.5	30
3	0.25	1	0.25	45
4	1.0	5*	0.2	45
5	0.5	5	0.1	60
6	0.25	5	0.05	75
7	1.0	20**	0.05	60
8	0.5	20	0.025	75
9	0.25	20	0.0125	90
10	0	1	0	90

*One per week for 5 weeks.

**Five per week for 4 weeks.

Results of the Preliminary Experiment

Body Burden. The amount of Sr^{90} in the living mice at various times is expressed as the percentage of the total dose on a log-log grid in Figure 6. Each point represents the average of 10 animals. The values following a single injection can be represented by a straight line extending from the day after injection until the termination of the experiment at 100 days. The bremsstrahlung from the last 3 survivors of a former Sr^{90} study[1,3] were counted in similar fashion 992 days after injection, and the values obtained fit an extension of this straight line within the range of expected variation. The apparent inverse relationship between retention and size of dose during the first 10 days is not significant since the differences are no greater than the variability of the data.

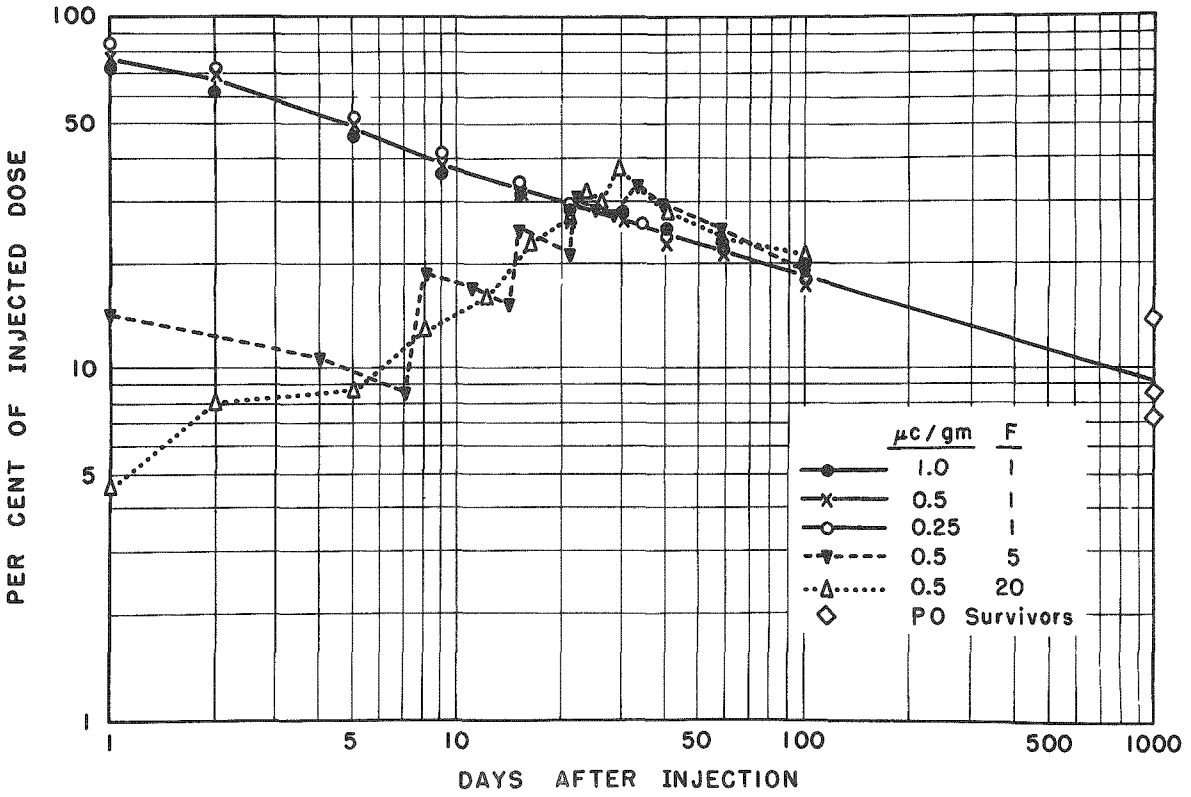

Figure 6. Body burden as a function of dosage pattern and time.
F = number of fractions.

The measured body burdens of those animals that received the total dose in 5 or in 20 fractions followed the expected, calculated values. The peak percentages are not recorded in Figure 6 since the bremsstrahlung were counted before each reinjection rather than after. However, these can be estimated from the available data so that comparisons of dose-rate can be made. For example, the maximum body content was 47.5% of the total dose immediately after the last of 5 fractions had been given, and it was 35% after the last of 20 fractions had been given; this is in contrast to 100% of the total dose present immediately after a single injection. Necessarily, all 3 dosage patterns ultimately resulted in equal average daily body burdens, as summarized in Table 5. These data show that the primary objective of reducing the initial high irradiation without changing the total delivered dose can be achieved by fractionation at appropriate time intervals. They also show that during the 100-day period the Sr^{90} level in the animals that received the total dose in either 5 or in 20 fractions was much the same. Thus any variation in tumor incidence between groups of animals receiving 5 or 20 fractionated injections would more likely be due to differences in uniformity of distribution than to differences in dose-rate.

TABLE 5

Average daily body burden

Number of fractions	Per cent of total injected dose		
	0-5 days	0-60 days	0-1000 days
1	64	31	13-14
5*	13	27	13-14
20**	9	25	13-14

*One per week for 5 weeks.

**Five per week for 4 weeks.

As previously mentioned, each point in Figure 6 represents the average value of 10 animals. It seemed worth while to estimate what proportion of the variations observed among each group of 10 was due to inequalities in the amount of material injected, to retention differences among the individual animals, and to physical sources of error such as the positioning of the animal for counting or crystal and scaler performance. In Figure 7 it can be seen that the average coefficient of variation ($\sigma_{\overline{M}}/\overline{M}$) after a single injection increased from 10% at one day to 25% at 100 days. The value for the 3 survivors at 992 days is not unduly far from a straight, semilogarithmic extension of this curve. The averages for the combined data are presented also, but it is felt that the single-injection curve is more useful for the present considerations since any complications associated with repeated injections need not be considered. For instance, the dashed line in Figure 7 represents the sharp increase in the coefficient of variation among the animals that received 20 injections. This increase occurred after the 15th injection, and it was associated with difficulty in administering an accurate, intravenous dose into some animals whose tails were scarred from previous injections.

Since approximately 24 hr elapsed between injection and the first bremsstrahlung measurements, during which time biological differences could contribute to the observed coefficient of variation of 10%, another method for estimating injection error was devised. This involved adding, by tuberculin syringe, 0.1 ml of a Sr^{90} solution to each of 10 gelatin-containing test tubes of the same size as those used for housing the living mice during counting. This volume was the minimum injected into mice; the average volume of solution injected was approximately 0.15 ml. Bremsstrahlung counts of the tubes showed the injections to have a coefficient of variation of 6%. They also served to demonstrate that the

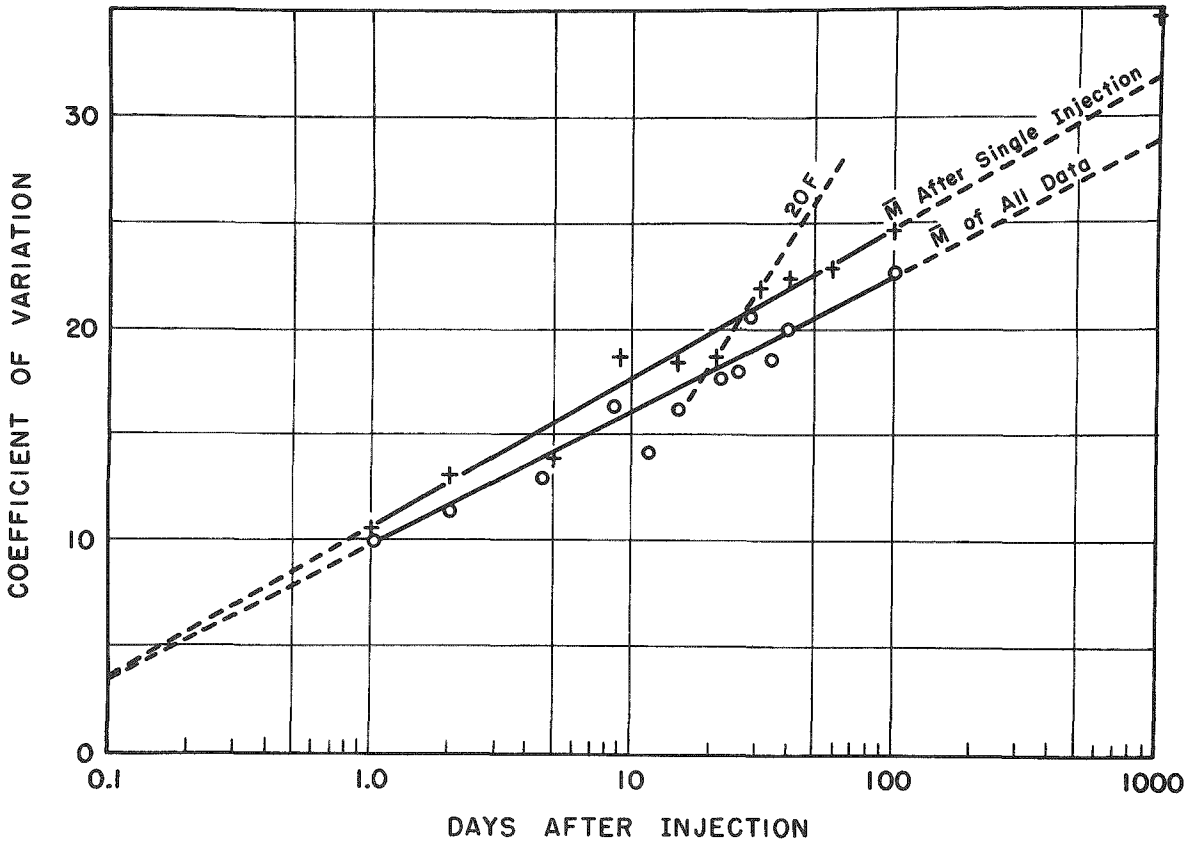

Figure 7. Variability of body burden among similar animals.

counting errors on successive days due to the physical factors involved were negligible as long as fluctuations in background and in scaler performance were negated by the usual corrections. During the course of this experiment the average coefficient of variation for the "standards," which were several mice that had been killed immediately after the injection of known amounts of Sr^{90}, was 4.4%.

The reliability of bremsstrahlung counting for estimating body burden was checked by comparing the measurements made on 19 animals just before sacrifice with the Sr^{90} determinations based on ash analyses. The coefficient of variation of the ratios of radioactivity as determined by these two methods was 1.4%.

Distribution. The preparation of representative bones for autoradiography has not been completed. However, the few specimens now available illustrate the type of distribution found in the mouse. An autoradiograph of a longitudinal section of the lumbar spine of a mouse that received 0.5 $\mu c/g$ in a single dose 30 days earlier appears in Figure 8A. There is greater contrast between the darker and lighter areas of this

section than are seen in Figure 8B, which is a section of spine from a mouse that received the same total dose but in 20 fractions. An autograph of the femur of the latter mouse appears in Figure 8C. This can be contrasted with the autograph in Figure 9A, which demonstrates the distribution of Sr^{90} in a femur when the same total dose is given in 5 fractions. The small area of Sr^{90} concentration seen in the shaft is typical of the "hot spots" found in the bones of larger mammals A microradiograph of this section (Figure 9B) discloses that this point of concentration is located adjacent to a blood vessel in an area of very dense bone that is not unlike an haversian system in its general appearance.

212-Day Survey of the Long-Term Study

Survival. The survival curves of the animals of the long-term toxicity experiment are presented in Figure 10. At 212 days there was no apparent difference attributable to dose fractionation when the total dose was 0.25 or 0.5 μc/g. However, dividing 1.0 μc/g into 5 or 20 fractions decreased mortality markedly. Shifting the curve by 28 days in order to correct for the delay in administering the total dose when it was fractionated does not reduce the discrepancy appreciably. Therefore, it appears that some protection against early mortality is afforded by fractionating a total dose of 1.0 μc/g, which is 1/6 of the 30-day LD_{50}.[3] Whether this represents a threshold effect or a recovery phenomenon, or both, can only be speculated upon at this point.

Carcinogenicity. The incidences of neoplasms of bone and of the reticular tissues at 212 days are summarized in Figure 11. The animals still alive at that time that had gross evidence of either disease were included.

The percentage of animals with bone tumors was based upon the population alive at 150 days, this correction is necessary because of the latent period involved in the appearance of bone tumors. An additional correction to compensate for the fact that the final injection in the case of fractionation was not administered until the 28th day after the beginning of the experiment was considered, but it was rejected in view of the fact that the minimum time between the first injection and death with a malignant bone tumor was 199 days among the animals that received a single injection, 178 days among those that received 5 divided doses, and 157 days among those that received 20 divided doses. By 212 days bone tumors had appeared in 80% of the animals that had received 1.0 μc/g. The incidence was 27.3% and 34.5% in the groups that had received 5 or 20 injections, respectively.

The lymphoid tumor data at 212 days suggest that the incidence may decrease both with decreasing dose and with increasing fractionation. However, the low levels among the animals that received 0.25 μc/g in a single

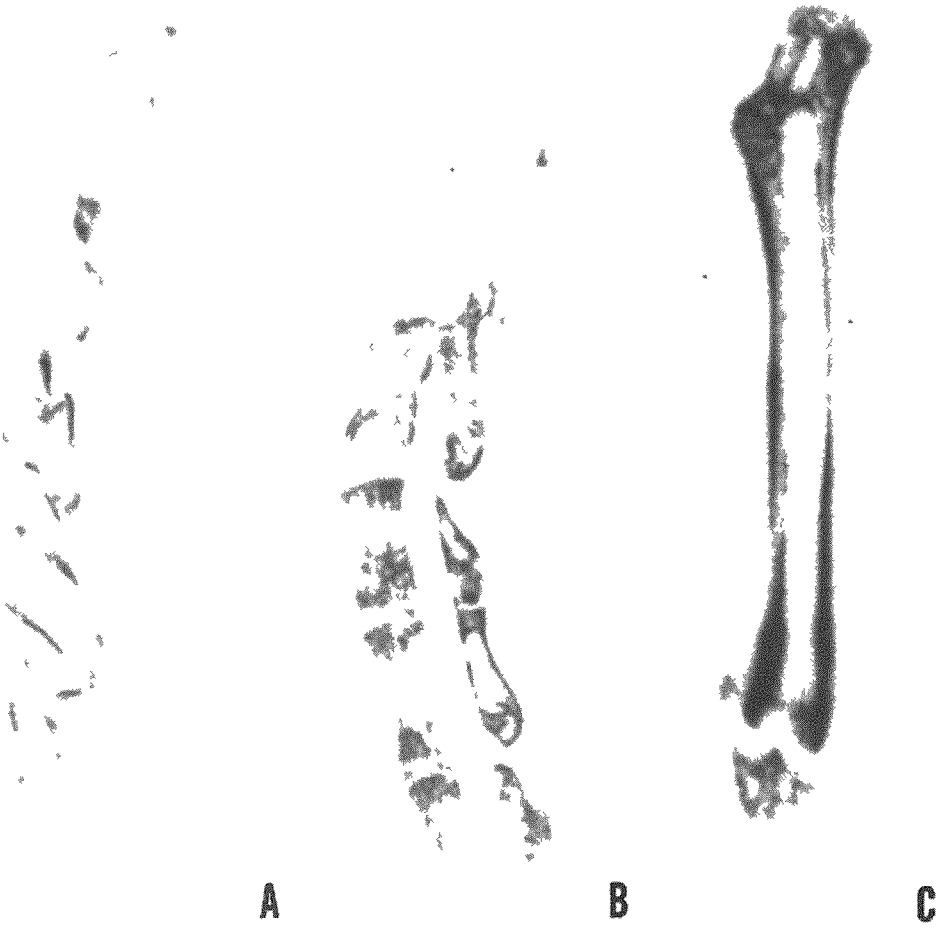

Figure 8.

Autoradiographs of bones from mice that received 0.5 μc/g. A, longitudinal section of lumbar spine 30 days after the total dose had been given in a single injection. B, similar section 33 days after the last of 20 fractionated doses had been given. C, longitudinal section of femur of mouse whose spine appears in B.

Figure 9.

Longitudinal section of femur of mouse 32 days after the last of 5 fractionated doses (total dose = 0.5 μc/g) had been given. A, autoradiograph. B, microradiograph (prepared by R. Rowland of the Radiological Physics Division).

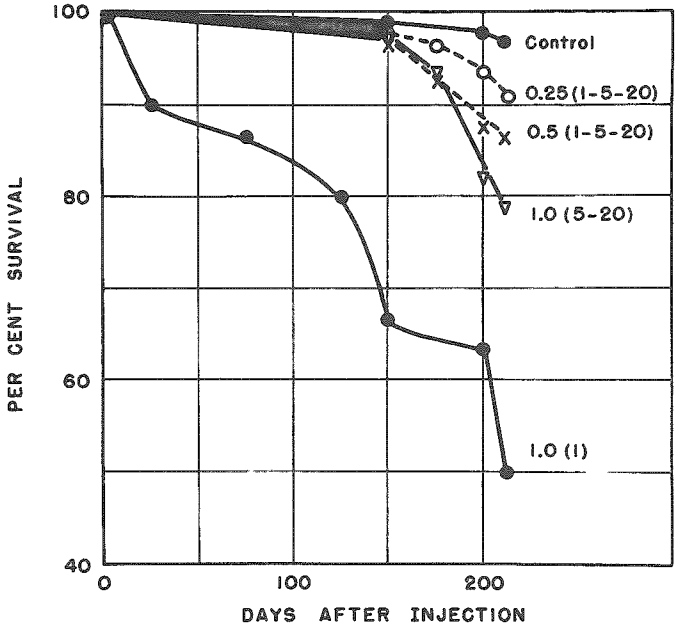

Figure 10.

Survival during the acute and subacute stage as influenced by size of dose and by dosage pattern. Number of fractions stated in parenthesis after dose, which is given in μc/g.

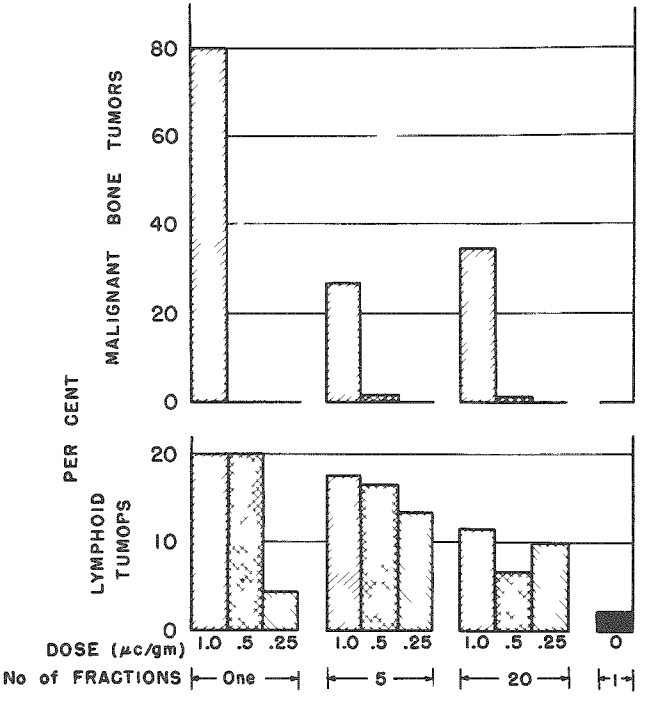

Figure 11.

The incidences of tumors of bone and of reticular tissues 212 days after the beginning of the experiment.

injection and those that received 0.5 $\mu c/g$ in 20 injections are not consistent with this trend. All the experimental groups had a higher incidence of lymphoid tumors than the control population.

Summary

1. CF No. 1 female mice received total intravenous injections of 1.0 $\mu c/g$, 0 5 $\mu c/g$, or 0.25 $\mu c/g$ of Sr^{90} (in equilibrium with Y^{90}) in a single injection or in 5 or 20 doses. The five fractions were given at the rate of one per week for 5 weeks and the 20 fractions at the rate of 5 per week for 4 weeks.

2 After a single injection retention decreased from approximately 75% at one day to 18% at 100 days and 9% at 1000 days.

3. The maximum body content after five fractions was 47.5% of the total dose, after 20 fractions it was 35% of the total dose.

4. The differences in total body content noted among comparable animals were found to be due to injection error and to individual variability. The coefficient of variation of the injection of 0.1 ml of solution was estimated to be 6%; dissimilarities among the animals increased this measure of variability to 10% at one day and to 25% at 100 days after injection.

5. The autoradiographs that have been completed support the expectation that uniformity of distribution increases with increasing fractionation. There is evidence that localization in "hot spots" similar to that found in larger mammals occurs in the mouse.

6. Early mortality was decreased when 1.0 $\mu c/g$ was given in 5 or 20 divided doses rather than in a single injection.

7. Two hundred and twelve days after 1 0 $\mu c/g$ had been given in a single injection, 80% of the 150-day survivors had malignant bone tumors. Only 27 3% of those that received the dose in 5 fractions and 34.5% of those that received it in 20 fractions had similar lesions.

8. At 212 days all the experimental groups had a higher incidence of lymphoid tumors than the control group. These early data suggest that the incidence may decrease with decreasing dose and with increasing fractionation.

21

References

1. Finkel, M., and G. Scribner. Toxicity of strontium-90 and of calcium-45 in mice. II. Status of experiments 625 days after injection. Quarterly Report of Biological and Medical Research Division, Argonne National Laboratory. ANL-5597, pp. 16-20 (1956).

2. Norris, W. P., and L. W. Speckman. Embedding of large bone specimens. Quarterly Report of Biological and Medical Research Division, Argonne National Laboratory. ANL-5486, p. 82 (1955).

3. Finkel, M. and G. Scribner. Toxicity of strontium-90 and of calcium-45 in mice. I. Status of experiments 200-300 days after injection. Quarterly Report of Biological and Medical Research Division, Argonne National Laboratory. ANL-5456, pp. 36-37 (1955).

EFFECT OF WHOLE-BODY X-IRRADIATION ON AUTOLYTIC DESTRUCTION OF LIVER CATALASE

Robert N. Feinstein

It has been shown[1,2] that radiation-labile inhibitors of certain of the intracellular proteolytic enzymes (cathepsins) exist in a variety of mammalian tissues. The cathepsins themselves are much more resistant than the inhibitors to the effect of whole-body X-irradiation,[1] and so it follows that the effect of such irradiation will be an apparent activation of certain catheptic activities. Since other tissue enzymes are proteins and thus subject to catheptic destruction, and since their destruction is readily susceptible to quantitative determination, the measurement of autolytic decrease in enzyme activity should afford a convenient means of observing radiation effects on catheptic systems. It is, of course, known that many enzymes, too numerous to cite here, do decrease in activity in the tissues after whole-body X-irradiation, a phenomenon which may conceivably be due to the mechanism described. One such enzyme is catalase;[3] since its determination[4] is simple and rapid, it has been used in preliminary studies of this hypothesis.

Experimental and Results

Animals used were CF No. 1 female mice and Sprague-Dawley male rats. X-irradiation for both was to the whole body and the dose of 850 r was given at a rate of about 40 r/min. The treated animals, together with unirradiated controls, were starved but given free access to water until they were killed 24-78 hr later. The livers were excised, homogenized with cold water, and brought to pH 3.5. Catalase activity was assayed immediately and again after a period of incubation at 37° C, the pH being returned to 6.8 immediately before assay.

Results to date (Table 6) are not striking. The occasional marked effects in certain X-irradiated animals (e.g., experiments 3 and 9 in Table 6) are not reproducible, and no explanation is immediately apparent.

Discussion

Lack of a demonstrable X-radiation effect on what we may term "catalase-cathepsin" must not be permitted to invalidate the general hypothesis described above. It should, for example, be recalled that while whole-body X-irradiation has very significant "activation" effects (actually inhibitor destruction) on certain specific cathepsins in certain specific tissues, no effect of the irradiation can be detected on any tissue cathepsin using Anson's method[5] of undefined, over-all degradation of hemoglobin.[1] Other tissues and other enzymes must be tested.

The concept of determining catheptic activity by measuring a given enzyme activity of a tissue before and after incubation has been used before. Bach and Zubkowa in 1921 considered the decrease in blood catalase activity upon 30 min incubation at 37°C as a measure of blood protease activity.[6] They apparently incubated the blood solutions at unaltered and unmeasured pH. We have found that incubating liver homogenates at pH 5.5 or 7.0 for up to 2 hr brings about only extremely small changes in catalase activity.

TABLE 6

Decrease in catalase activity of liver of normal and X-irradiated mice and rats

Expt.	Species	Time until sacrifice, hr	Time homogenate incubated at 37°C, min	Catalase activity, perborate units/g					
				Control			X-irradiated		
				Initial	Final	Decrease	Initial	Final	Decrease
1	Mouse	24	105	577	168	409	546	121	425
2	Mouse	24	30	848	363	485	721	312	409
			120	848	147	701	721	120	601
3	Mouse	48	105	613	246	367	526	2	524
4	Mouse	48	30	852	238	614	746	58	688
5	Mouse	48	30	862	355	507	781	20	761
6	Mouse	48	15	1013	539	474	818	454	364
			30	1013	444	569	818	409	409
			60	1013	295	718	818	290	528
			120	1013	113	900	818	219	599
7	Mouse	48	30	1015	502	513	930	566	364
			30	1084	632	452	797	448	349
			30	881	545	336	768	450	318
			30	947	523	424	781	401	380
8	Mouse	48	30	742	18	724	659	13	646
9	Mouse	72	30	756	267	489	787	7	780
			120	756	36	720	787	0	787
10	Rat	72	30	1145	586	559	842	186	656
			60	1145	437	708	842	116	726
				Average		562			543

References

1. Feinstein, R. N., and J. C. Ballin. Effect of whole body X-irradiation on a natural inhibitor of carboxypeptidase. Proc. Soc. Exptl. Biol. Med. 83: 6-10 (1953).

2. Feinstein, R. N., and J. C. Ballin. Carboxypeptidase in mammalian tissues. Proc. Soc. Exptl. Biol. Med. 83: 10-14 (1953).

3. Feinstein, R. N., C. L. Butler, and D. D. Hendley. Effect of whole body X-radiation and of intraperitoneal hydrogen peroxide on mouse liver catalase Science 111: 149-150 (1950).

4. Feinstein, R. N. Perborate as substrate in a new assay of catalase. J. Biol. Chem. 180: 1197-1202 (1949).

5. Anson, M. L. The estimation of cathepsin with hemoglobin and the partial purification of cathepsin. J. Gen. Physiol. 20: 565-571 (1937).

6. Bach, A., and S. Zubkowa. Uber die Fermentzahlen des Blutes. I. Quantitative Bestimmung der Katalase, der Protease, der Peroxydase und der Esterase in einem Bluttropfen. Biochem. Z. 125: 283-291 (1921).

PROGRESS REPORT: THE BIOSYNTHESIS OF METHIONINE IN BACTERIA

The Production of Biochemical Mutants

Stanley K. Shapiro

Ultraviolet light was used to produce biochemical mutants of Aerobacter aerogenes and Escherichia coli. Cells from 4-hr-old cultures were suspended in 0.85% NaCl and irradiated for 90 sec at a distance of 18 cm from a 20-watt G.E. germicidal lamp. This treatment was found empirically to produce the desired killing of 99.99%. The survivors were screened for the specific biochemical mutants desired with the aid of the penicillin method of Lederberg(1) and the replica plating method of Lederberg and Lederberg.(2)

A number of mutants of E. coli K_{12} were isolated which require methionine or vitamin B_{12} for growth. These cultures will be used in an attempt to determine the role of vitamin B_{12} in transmethylation reactions. E. coli K_{12} was selected because previous studies have demonstrated the presence of an active transmethylase in cell free extracts of this organism.(3)

Two mutants of A. aerogenes have been reported previously that utilize S-adenosyl-L-methionine as efficiently as methionine for growth.(3) Recently, however, a mutant of A. aerogenes (designated here as AM-1) was isolated that grows well when supplemented with S-adenosyl-L-methionine, but shows no growth when supplemented with any of the individual breakdown products of the molecule. However, the culture grows when supplied with certain combinations of the constituents of S-adenosyl-L-methionine. A typical series of results is shown in Table 7. Only the combinations which support growth are shown here, as well as the necessary control cultures. The concentrations of the supplements shown in the table supported the maximum growth response that could be obtained.

It is interesting that adenosine would not support growth, but that thiomethyladenosine supports about 30% of the maximum growth response obtained. It is also important to note that adenine plus ribosylmethionine supports growth to an extent that is exactly comparable to that of S-adenosyl-L-methionine.

This problem will be further investigated with whole cells as well as cell-free extracts in the hope that the metabolic function of S-adenosylmethionine will be uncovered.

TABLE 7

Growth responses of culture AM-1 to various compounds after incubation for 18 hr at 35° C in minimal medium(3)

Supplement, 0.2 μ M/ml	Growth response*
None	0
S-Adenosyl-L-methionine	130
Adenine	0
Adenosine	0
Methylthioadenosine	72
Homoserine	0
Homoserine + Methylthioadenosine	71
Methionine	0
Ribosylmethionine	8
Ribosylmethionine + adenine	130

*Average Klett readings measured in Klett-Summerson Colorimeter with #62 filter.

References

1. Lederberg, J., and N. N. Zinder. Concentration of biochemical mutants of bacteria with penicillin. J. Am. Chem. Soc. 70:4267 (1948).

2. Lederberg, J., and E. M. Lederberg. Replica plating and indirect selection of bacterial mutants. J. Bacteriol. 63:399-406 (1952).

3. Shapiro, S. K. Biosynthesis of methionine from homocysteine and S-methylmethionine in bacteria. J. Bacteriol. 72:730-735 (1956).

THE EFFECT OF X-IRRADIATION ON THE INCREASE IN RAT LIVER TRYPTOPHAN PEROXIDASE PRODUCED BY ADRENAL STEROIDS

John F. Thomson and Florence J. Klipfel

Abstract

On the basis of glycogen deposition in X-irradiated adrenalectomized rats maintained on cortisone, it has been recently claimed that the irradiated rat uses cortisone more efficiently than does an unirradiated animal. Since the adrenal glucosteroids have been shown to elicit a dose-dependent increase in the tryptophan peroxidase activity of the livers of adrenalectomized rats, it was of interest to see whether this effect of cortisome or hydrocortisone was augmented by radiation. Our data showed, however, that there was certainly no evidence of increased utilization of cortisone or hydrocortisone by X-irradiated rats insofar as the effect on tryptophan peroxidase activity was concerned; if anything, there was a slight decrease in efficiency.

THE DISSOCIATION OF INSULIN IN PYRIDINE-WATER AND ACETIC ACID-WATER SOLUTIONS

David A. Yphantis*

Molecular weights approaching 5750, the combined weight of an A and a B chain of insulin, have been found for insulin under a number of conditions, for example at extremes of pH,[1-3] in solvents of low dielectric constant,[4-6] in concentrated guanidine chloride solutions,[7] and on surface monolayers.[8] Studies of the dinitrophenyl derivatives of insulin by counter-current distribution[9] and of the dinitrophenyl and acetyl derivatives by paper electrophoresis[10] indicate a molecular weight of ∿6000 for the derivatives in solvents such as dichloroacetic acid-water saturated with butanol and 33% acetic acid. It was felt worth while to investigate whether unmodified insulin itself is dissociated to monomers in mixed organic-aqueous solvents. If this is the case, there would be an opportunity to study the various factors involved in a comparatively simple protein-protein interaction in a controlled system. One could, for example, measure quantitatively the effects of small changes in solvent composition and of chemical modification of the insulin molecules on the monomer-dimer equilibrium.

The systems that were chosen for investigation were aqueous pyridine near pH 7 and aqueous acetic acid. While this work was in progress, Fredericq[11] reported molecular weights close to 6000 for insulin in aqueous dioxane solutions near pH 3; however, no evidence of a monomer-dimer equilibrium in the dioxane-water solutions was presented.

The insulin used was of bovine origin; it was recrystallized and electrodialyzed to remove salts and zinc of crystallization. The pyridine-water solvents contained 0.1 M NaCl to suppress charge effects and 0.06-0.095% acetic acid; their pH ranged from 6.9 to 7.4 as measured directly with the glass electrode. Acetic acid-water solvents contained 0.15 M NaCl to suppress charge effects; their pH ranged from 2.3 to 1.7. Sedimentation runs were performed in Spinco ultracentrifuges equipped with Wolter phaseplates.[12] Sedimentation coefficients, s, were calculated from the rate of motion of the schlieren maxima using the equation

$$s = \frac{dr}{dt}\Big/\omega^2 r$$

*A portion of this work was performed while the author was a Fellow of the American Cancer Society at the Biology Department of the Massachusetts Institute of Technology, in collaboration with Professor David F. Waugh.

where $\underline{r}$ is the radius from the center of rotation, $\underline{t}$ is the time, and $\underline{\omega}$ is the angular velocity. The coefficients were corrected to water at 20°C using the measured or calculated densities and viscosities of the solvents. The diffusion coefficient was obtained in the ultracentrifuge in a synthetic boundary cell at low speeds using the area-height method of calculation. Molecular weights were obtained through the Archibald method as outlined by Klainer and Kegeles,[13,14] and by Ginsburg, Appel, and Schachman.[15] To conserve insulin some of the molecular weights in 20% acetic acid were determined using a modification of the Archibald technique in which the synthetic boundary run is combined with the sedimentation run. No significant differences were observed between the results obtained by the two techniques. The value of the partial specific volume was taken as 0.707[11] throughout.

The sedimentation coefficients of insulin in various concentrations of pyridine are given in Table 8. These coefficients were obtained in the commercially available metal synthetic boundary cells.[16] The data indicate a progressive dissociation of insulin with increasing pyridine concentration. The diffusion coefficient obtained for 1% insulin in 40% pyridine, when corrected to water at 20°C., was $1.23_9 \pm 0.06_6 \times 10^{-6}$ cm^2 sec^{-1}. With a partial specific volume of 0.707 and the sedimentation coefficient of $0.83_3 \pm 0.01_6 \times 10^{-3}$ sec one obtains a frictional coefficient of 1.48 and a molecular weight of 5570 ± 310.

TABLE 8

Sedimentation coefficients of insulin in pyridine-water solutions containing 0.1 M NaCl

Pyridine Concentration, % v/v	Insulin Concentration, % w/v	$S^{20,w} \times 10^{13}$ sec
5.0	<0.5*	$2.16 \pm 0.01_2$
10.0	0.59	1.68 ± 0.02
20.0	0.50	$0.93_1 \pm 0.01_1$
20.0	1.00	$1.07_0 \pm 0.01_1$
21.2**	0.50	$0.93_2 \pm 0.01_9$
40.0	0.50	$0.83_6 \pm 0.01_1$
40.0	0.50	$0.84_7 \pm 0.01_5$
40.0	1.00	$0.81_6 \pm 0.01_3$

*Limit of solubility less than 0.5%

**No NaCl added.

The values of the sedimentation coefficients obtained in various concentrations of acetic acid are shown in Figure 12 These sedimentation coefficients are not as reliable as those of the pyridine system since they were determined in Kel-F synthetic boundary cells,[17] which appeared to distort at the high centrifugal fields employed. It can be seen that insulin dissociates on increasing the concentration of acetic acid and is practically completely dissociated in 30% acetic acid, as shown by the small concentration dependence at that concentration.

The molecular weights determined for 0 59% insulin in 30% acetic acid using the Archibald technique are given in Table 9. Since the values of the molecular weight are essentially independent of time and equal at the base and at the meniscus of the cell, the system is monodisperse and fully dissociated [15] From the sedimentation coefficient of $0.95 \pm 0.02 \times 10^{-13}$ sec one can calculate a frictional coefficient of 1 35 for 0 59% insulin in 30% acetic acid.

TABLE 9

Molecular weight of insulin in 30% acetic acid containing 0.15 M NaCl as determined by the Archibald method at 20° C and at 23,150 rpm

Time, min	Molecular weight	
	at meniscus	at base
9	5860	--
17	5780	--
135	6130	5920
183	6030	5825
199	5890	5825

The molecular weight of insulin was determined as a function of concentration in 20% acetic acid by the Archibald technique at 20.0 ± 0 5°C and is shown in Figure 13. Concentrations indicated are those calculated from the schlieren diagrams for the base or the meniscus of the cell; they were corrected for ~5% moisture content of the insulin. The curve drawn is for an ideal monomer-dimer equilibrium of units of 5750 and 11500 molecular weight, with an association constant of 443 ± 98 liter $mole^{-1}$, the average of the association constants of all the determinations. The ΔF° calculated from this association constant is -3.55 kcal/mole at 20°C.

The molecular weights found for the fully dissociating conditions are not far from the chemically found molecular weight of 5750, thus the assumption of a partial specific volume of 0.707, a value found in purely

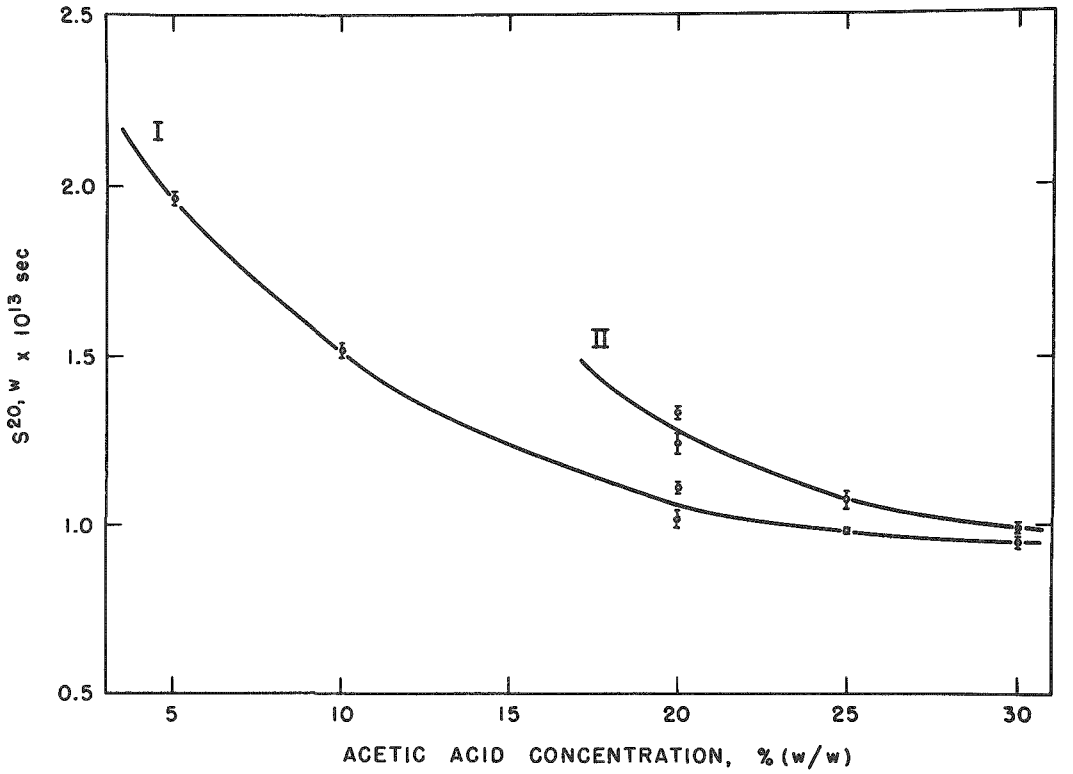

Figure 12.

Sedimentation coefficients, $S^{20,w}$ as a function of acetic acid concentration. I. 0.59% insulin; II. 1.2-% insulin.

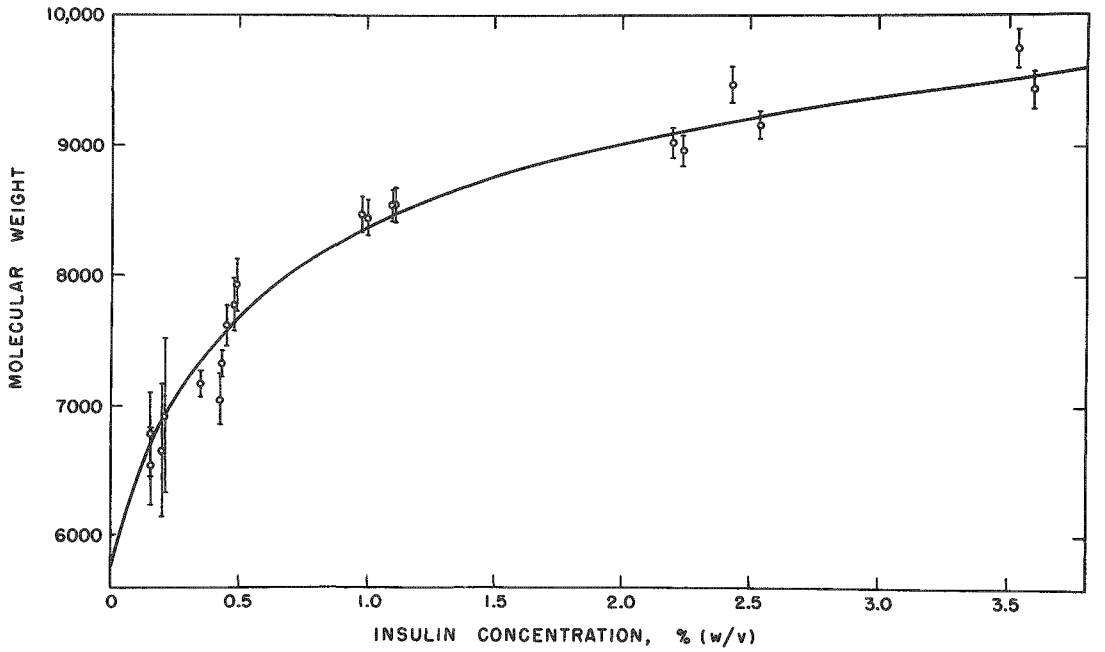

Figure 13.

Dissociation of insulin in 20% acetic acid (molecular weight vs insulin concentration).

aqueous solutions of insulin, appears reasonable. The values of the frictional coefficients indicate that there is considerable asymmetry or solvation or both for insulin under these conditions. One expects considerable solvation.

The mechanism of the dissociation in pyridine-water is probably twofold: First, there is a lowering of the dielectric constant of the solvent, thus increasing the electrostatic repulsion between insulin monomers. Second, pyridine is an excellent proton acceptor and as such should form strong hydrogen bonds with insulin in competition with insulin-insulin hydrogen bonds, thus lowering the attractive forces. Similar mechanisms should apply to the acetic acid-water system with an additional contribution to the electrostatic repulsion because of the repression of the carboxyl ionization at the low pH.

Preliminary experiments on the effects of nonpolar substances on the monomer-dimer equilibria are in progress. The results to date have shown that when the solutions are saturated with benzene (care being taken to minimize changes in the gross composition of the solvent) association is favored. For example, the sedimentation coefficient of an 0.59% insulin solution in 10% pryidine was found to be $1.68 \pm 0.02 \times 10^{-3}$ sec; on saturation with benzene the sedimentation coefficient was found to be $2.02 \pm 0.06 \times 10^{-13}$ sec. In 20% acetic acid and at 0.3-0.6% insulin concentration one finds apparent association constants roughly twice as large in the presence of benzene as in its absence.

These findings are not totally unexpected. There has been a report[18] of dimerization of serum albumin in the presence of benzene; however, this could not be satisfactorily confirmed, possibly because of different preparations of serum albumin.

If a completely nonpolar substance, such as a hydrocarbon or benzene interacts with a protein, the interaction would presumably be only with the nonpolar (lipophilic) side chains of the protein amino acids. In the presence of a nonpolar substance, nonpolar side chains that are suitably located on the protein molecule may coalesce with the nonpolar substance to form a small nonpolar region which presents less area to the (polar) solvent than do the side chains alone, thus allowing the solvent to form more hydrogen bonds with itself.[19] If nonpolar regions from two protein molecules coalesce in the presence of nonpolar substances and expose a smaller non-hydrogen bonding area to the solvent, one should observe a tendency towards association.

References

1. Fredericq, E., and H. Neurath. The interaction of insulin with thiocyanate and other anions. The minimum molecular weight of insulin. J. Am. Chem. Soc. 72: 2684-2691 (1954). (See however Tietze, F., and H. Neurath. The sedimentation constant of insulin in acid solution: A re-examination. J. Am. Chem. Soc. 75: 1758-1760 (1953).)

2. Fredericq, E. Reversible dissociation of insulin. Nature 171: 570-571 (1953).

3. Fredericq, E. The association of insulin molecular units in aqueous solutions. Arch. Biochem. and Biophys. 65: 218-227 (1956).

4. Rees, E. D., and S. J. Singer. Molecular weight of insulin in N,N-dimethylformamide. Nature 176: 1072-1073 (1955).

5. Ress, E. D., and S. J. Singer. A preliminary study of the properties of proteins in some nonaqueous solvents. Arch. Biochem. and Biophys. 63: 144-159 (1956).

6. Crespi, H. L., R. L. Uphaus, and J. J. Katz. The ultracentrifugal behavior of some proteins in non-aqueous solutions. J. Phys. Chem. 60: 1190-1192 (1956).

7. Kupke, D. W., and K. Linderstrøm-Lang. Size of the monomer of insulin. Biochim. et Biophys. Acta 13: 153-154 (1954).

8. Fredericq, E. L'état d'agrégation de l'insuline en couches monomolécularies superficielles. Biochim. et Biophys. Acta 9: 601-608 (1952).

9. Harfenist, E. J., and L. C. Craig. The molecular weight of insulin. J. Am. Chem. Soc. 74: 3087-3089 (1952).

10. Sluyterman, L. A. AE. Electrophoretic behaviour in filter paper and molecular weight of insulin. Biochim. et Biophys. Acta 17: 169-176 (1955).

11. Fredericq, E. The molecular weight of insulin in dioxane-water solutions. J. Am. Chem. Soc. 79: 599-601 (1957).

12. Trautman, R. Theory and test of commercially available Wolter phaseplate for use in schlieren optical systems employed in ultracentrifugation and electrophoresis. Biochim. et Biophys. Acta 14: 26-35 (1954).

13. Klainer, S. M., and G. Kegeles. Simultaneous determination of molecular weights and sedimentation constants. J. Phys. Chem. 59: 952-955 (1955).

14. Klainer, S. M., and G. Kegeles. The molecular weights of ribonuclease and bovine plasma albumin. Arch. Biochem. and Biophys. 63: 247-254 (1956).

15. Ginsburg, A., P. Appel, and H. K. Schachman. Molecular weight determinations during the approach to sedimentation equilibrium. Arch. Biochem. and Biophys. 65: 545-566 (1956).

16. Pickels, E. G., W. F. Harrington, and H. K. Schachman. An ultracentrifuge cell for producing boundaries synthetically by a layering technique. Proc. Natl. Acad. Sci. U.S. 38: 943-948 (1952).

17. Kegeles, G. A boundary-forming technique for the ultracentrifuge. J. Am. Chem. Soc. 74: 5532-5534 (1952).

18. Bresler, S. E. Structure of globulin proteins and their interaction with the external medium. Biokhimiya 14: 180-189 (1949).

19. Waugh, D. F. Protein-protein interactions, in Advances in Protein Chemistry, Vol. 9, pp. 325-437. Academic Press, New York (1954).

AUTOMATIC COUNTING OF INDIVIDUAL BACTERIA

H. E. Kubitschek

An important technological advance for bacteriology would be the automatic counting of single bacteria. Of several possible approaches to this problem the best seems to be to attempt to extend the Coulter Counter,* which counts red blood cells successfully, down to the region of sizes of bacteria. The advantage of the Coulter Counter appears to be that the ratio of signal to noise is theoretically greater than that obtainable with counters employing light absorption. Furthermore, it dispenses with the optical microscope in the detection circuit and is therefore simpler to operate.

Attempts have been made to count Escherichia coli with a counting aperture of 35 μ in diameter. The results indicate that an aperture of 10 to 25 μ may be successful. The problem of the construction of such apertures in glass and in a polymer of ethyl and butyl methacrylate is under study.

---

*Coulter Electronics, 5227 N. Kenmore, Chicago, Illinois.

A DEVICE FOR DISPENSING MICROBIAL CULTURES RAPIDLY

H. E. Kubitschek

A device for the rapid delivery of uniform volumes of fluid has been invented, primarily for its use in the production of large numbers of individual cultures of microorganisms distributed over a small area within a relatively short time. This device dispenses drops of liquid from a hypodermic needle onto a rotating Petri dish, in such a way that drops are laid down along a spiral trajectory. This technique takes advantage of the natural uniformity of drop volumes available with constant flow rates provided that the latter are below the critical velocity at which turbulence sets in. With a properly ground tip a 26-gauge hypodermic needle will deliver drops about 7.5 microliters in volume, constant to 1% at rates up to 5 drops per second.

This technique has three potential advantages.

1. Quantitative data can now be obtained with cultures in liquid almost as readily and accurately as are those obtained by the use of standard plate culture techniques upon agar.

2. Certain flagellated microorganisms which swarm, such as Proteus vulgaris, and some fungi that were not previously amenable to quantitative study upon agar plates, can now be localized and therefore counted.

3. Cultures with fastidious growth requirements and a high probability of contamination, such as, perhaps, some tissue cultures, can now be subcultured in large numbers of discrete cultures. This procedure should greatly reduce the chance of losing the culture as compared to classical culture techniques. Furthermore, the small culture volumes now available should make this method of culture less expensive.

PROGRESS REPORT: PROTEIN SYNTHESIS IN PANCREAS

IV. Changes in the intracellular distribution of amylase during the secretory cycle

Anna Kane Laird and A. D. Barton

In recent studies[1,2] of the intracellular distribution of amylase in rat pancreas, it was shown that a large part of the amylase activity is found in association with the microsome and supernatant fluid fractions, and that the distribution of activity between these two fractions in the actively secreting pancreas differs from that in the resting pancreas. The present report concerns a more detailed study of the changes observed both in the intracellular distribution of amylase and in the biochemical properties of the microsome and supernatant fluid fractions during one complete secretory cycle.

A single shipment of 24 rats was used for this study; they were all male rats of the Sprague-Dawley strain, weighing about 350 g. They were starved overnight in order to minimize secretion of digestive enzymes; under these conditions the acinar cells accumulate digestive enzymes and then become relatively quiescent with respect to synthesis of new enzyme protein.[3] On the morning of the experiment, 4 animals were chosen at random from each of 4 cages, to serve as the "starved controls." Each of the other animals received 10 mg of pilocarpine hydrochloride in 1 cc of isotonic saline by intraperitoneal injection. The first 4 animals injected constituted the first experimental group; these animals were killed 1 hr and 5 min later. Members of the subsequent experimental groups of 4 rats were picked at random for sacrifice at 2 hr and 15 min, 4 hr and 20 min, 6 hr and 25 min, and at 8 hr and 25 min after the injection of pilocarpine.

The pancreas tissue was rinsed in isotonic sucrose, dissected free from extraneous fat and connective tissue, pressed through a plastic mincer, and homogenized in 0.88 M sucrose, in a concentration of 12% by weight. The homogenate was strained through a fine stainless steel screen to remove as much as possible of the remaining masses of connective tissue and whole cells. The homogenate was centrifuged at 18,000 g for 15 min to sediment the whole cells, nuclei, mitochondria, and secretory granules. The supernatant fluid, which contained the microsome material and soluble proteins, was carefully removed with a pipette and the sediments were discarded. The supernatant fractions were diluted to reduce the concentration of sucrose to 0.25 M (thus facilitating the sedimentation of more microsome material than can be obtained from 0.88 M sucrose[2]), and were sedimented at 105,000 g for 60 min. Aliquots of the unfractionated homogenates, and of the 18,000 g

supernatant fractions, the microsome material sedimented at 105,000 g, and the final supernatant fluids, were assayed for amylase activity by the method of Meyer et al.,[4] and were analyzed for protein nitrogen, ribose nucleic acid (RNA), and phospholipid phosphorus.

The changes in the intracellular distribution of amylase activity that occurred during the secretory cycle are shown in Figure 14. The curve for the secretory granules was obtained by subtracting the sum of the activities recovered in the microsomes and supernatant fluid from the total activity of the unfractionated homogenate. The figures therefore include activity present in contaminating whole cells as well as in the secretory granules proper, but the curve probably gives a reliable though not precise indication of the changes occurring in the secretory granules. As shown in the figure, the most extensive early loss of amylase activity was in the secretory granules; the loss from the supernatant fluid was even more extensive, but the activity reached a minimum somewhat later than did that of the secretory granules. In proportion to the initial activity, the smallest relative loss was in the microsome fraction. Relatively low activities were observed in all three fractions between the first and fourth hours after the injection of pilocarpine. Return toward the values found in the starving pancreas was noted earliest in the microsome and supernatant fluid fractions, between the second and fourth hours, with rapid rises between the fourth and sixth hours. The secretory granule fraction lagged behind the other two in its return toward the resting condition. At 8 hr after injection of pilocarpine, the amylase activity of the microsome fraction was higher than that of the starving controls, while at this time the activities of the secretory granules and supernatant fluid were only approaching the initial values.

The ratios of amylase activity and of RNA and phospholipid phosphorus to protein nitrogen in the microsome and supernatant fluid fractions are given in Table 10. The ratios of RNA and phospholipid-P to protein-N showed only small (± 8%) and random variations. In contrast, the ratio of amylase to protein-N in the microsome fraction reached a single minimum, at 2 hr, which was less than 40% of the maximum observed at 8 hr, and the relative activity in the supernatant fluid reached a single minimum, also at 2 hr, which was only about 25% of the value observed at 8 hr.

In contrast to the stability of the structural components (protein, RNA, and phospholipid) of the microsome and supernatant fluid fractions during the secretory cycle, the quantity of the secretory granule material changed considerably during the cycle, as indicated by Figure 15. In this photograph are shown the sediments obtained at 18,000 g from closely similar amounts of pancreas; the white layer at the bottom of the pellet is the secretory granule material. The dark oval area visible at the bottom

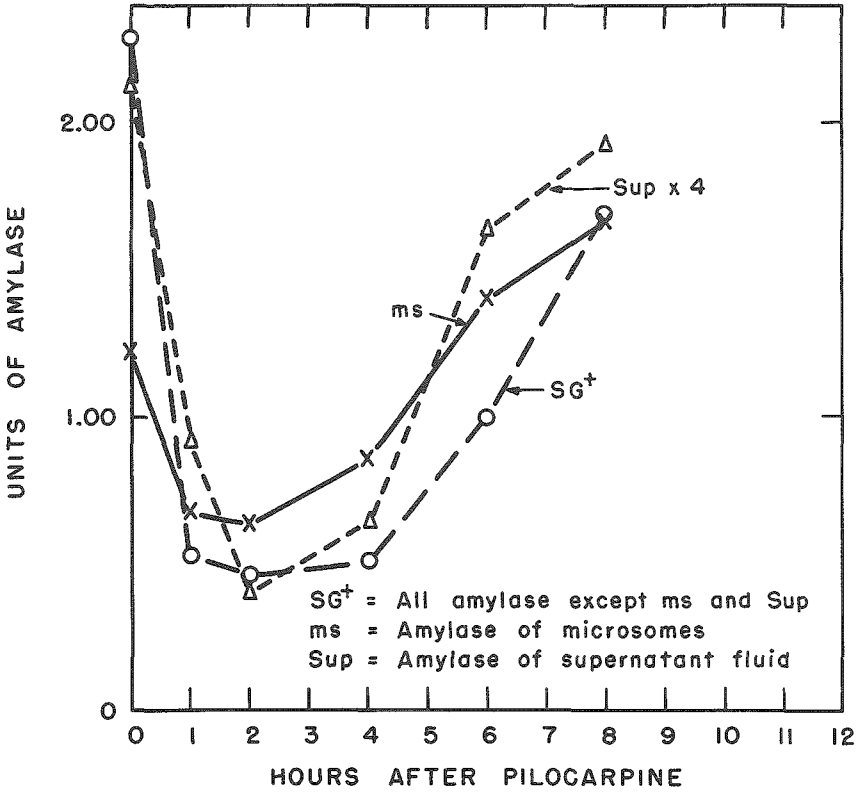

Figure 14.

Amylase distribution following administration of pilocarpine. Units of amylase for each fraction = mg maltose x 10^4 produced in 30 min per mg DNA in unfractionated homogenate. The values obtained for the supernatant fluid were multiplied by 4, to facilitate comparison with the other cell fractions.

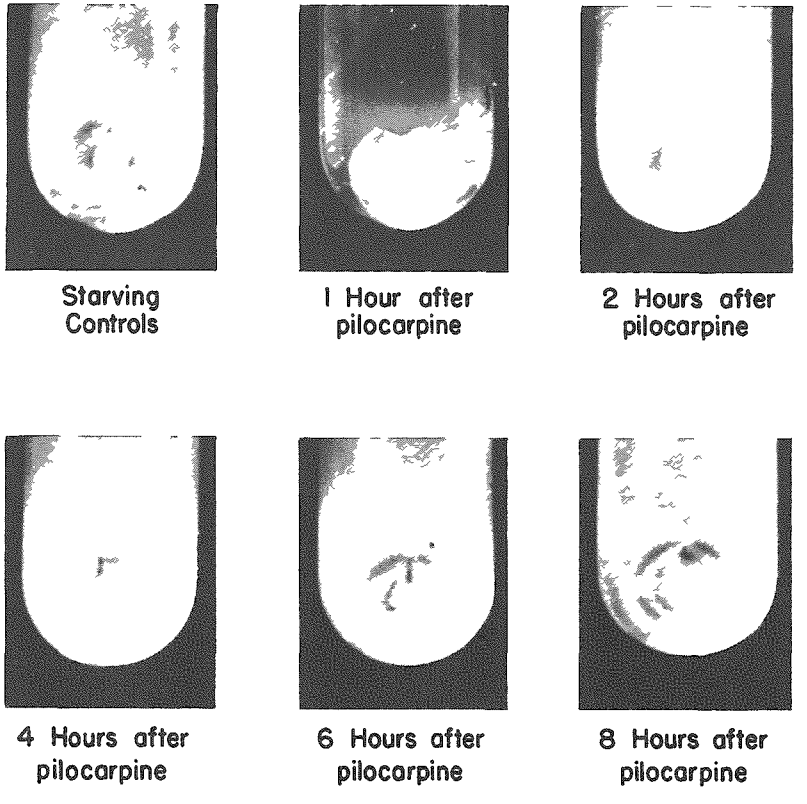

Figure 15.

Pellets obtained from pancreas homogenates by centrifugation at 18,000 g for 15 min, after removal of nuclei. The secretory granules form the compact white layer at the bottom of the pellet; the overlying sediments are mitochondrial components. The dark oval area visible at the bottom of several of the tubes is a reinforcing layer on the tube, and is not related to the sediments.

of several of the tubes is a reinforcement of the tubes and is not related to the sediments. The round white pellet of secretory granule material was rather large and easily seen when obtained from starving pancreas, but its relative size decreased rapidly after injection of pilocarpine, reaching a minimum at 2 hr, when it was reduced to a narrow white slit. Recovery was evident at 4 hr and continued through 6 hr; at 8 hr the pellet was distinctly larger than in the starving controls.

TABLE 10

Relative concentrations of constituents in microsome pellet and supernatant fluid during response to pilocarpine

All values represent ratios of given activity or constituent to protein nitrogen

Time after injection of pilocarpine, hr	Microsome pellet			Supernatant fluid		
	Amylase* / protein-N	RNA / protein-N	Phospholipid / protein-N	Amylase* / protein-N	RNA / protein-N	Phospholipid / protein-N
Starved control	5.7	1.9	0.13	3.3	0.59	0
1	3.9	2.3	0.15	1.9	0.76	0
2	3.8	2.1	0.13	0.97	0.67	0
4	4.8	1.9	0.15	1.3	0.56	0
6	9.3	2.2	0.14	4.3	0.58	0
8	9.9	1.9	0.13	3.9	0.59	0
Ave., ± mean deviation		2.0 ± .15	0.14 ± .01		0.63 ± .05	

*mg x 10^4 maltose produced in 30 min per mg protein-nitrogen.

These results taken together suggest that the amylase which is stored in the secretory granules is the first to be secreted after the injection of pilocarpine, as would be expected on the basis of the classical histological studies.(5) The "soluble" amylase of the supernatant fraction lags slightly behind that of the secretory granules in the order of secretion, but it is also rapidly lost from the cell. The activity associated with the microsomes is the best conserved, although the molecules of enzyme protein may be (and probably are) in a state of rapid metabolic turnover. The loss of amylase activity in the secretory granules is associated with a loss of the substance of the secretory granules, in contrast to the losses sustained by the microsomes and supernatant fluid, whose structural components are conserved throughout the cycle. The data reinforce the suggestion made

S1

earlier in these studies[1] that the new enzyme protein is being synthesized in association with the microsomes and released in soluble form into the cell sap (the supernatant fluid); the soluble enzyme protein is then organized, possibly by the Golgi apparatus,[6] into the secretory granules where it is stored awaiting secretion.

References

1. Laird, A. K., and A. D. Barton. Progress report: Protein synthesis in pancreas. Intracellular localization of a pancreatic digestive enzyme. Quarterly Report of Biological and Medical Research Division, Argonne National Laboratory. ANL-5518, pp. 131-133 (1956).

2. Laird, A. K., and A. D. Barton. Progress report: Protein synthesis in pancreas. Subfractionation of microsomes. Quarterly Report of Biological and Medical Research Division, Argonne National Laboratory. ANL-5655, pp. 65-68 (1956).

3. Daly, M. M., and A. E. Mirsky. Formation of protein in the pancreas. J. Gen. Physiol. 36: 243-254 (1952).

4. Meyer, K. H., E. H. Fischer, and P. Bernfeld. Sur les enzymes amylolytiques (I). L'isoelement de l'α-amylase de pancreas. Helv. Chim. Acta 30: 64-78 (1947).

5. Ries, E. Histophysiologie des Mausepancreas nach Lebendbeobachtung, vital Farbung und Stufenuntersuchung. Z. Zellforsch. u. mikroscop. Anat. 22: 523-585 (1935).

6. Junquiera, L. C. U., and G. C. Hirsch. Cell secretion: A study of pancreas and salivary glands. Internat. Rev. Cytol. 5: 323-364 (1956).

PROGRESS REPORT: DENSITY GRADIENT CENTRIFUGATION

Effect of 3-Amino-1,2,4-Triazole on Intracellular Distribution of Catalase and Uricase

John F Thomson and Florence J. Klipfel

The ability of 3-amino-1,2,4-triazole (AT) to inhibit liver catalase *in vivo* was first observed in rats by Heim *et al.*(1) Feinstein et al.(2) have subsequently shown that the inhibition also occurs in mice, a 95% decrease in liver catalase developing within 30 min after intraperitoneal injection. Since in mouse liver catalase and uricase are associated with the same size of cytoplasmic particulate, not identical with those particulates which contain cytochrome oxidase (i e., mitochondria),(3) we were interested in seeing (a) whether AT altered the size distribution of these catalase-containing particles, and (b) whether AT effected a diminution *in vivo* of uricase as well as of catalase.

Methods

CF No 1 female mice, 8 weeks old, were used in these experiments. Doses of 2 g/kg of AT were administered intraperitoneally as a 20% aqueous solution * At intervals of 1, 2½, 16, and 24 hr after injection, the mice were killed by cervical dislocation, and their livers promptly removed and chilled in cracked ice. The tissue was homogenized and subjected to gradient centrifugation.(3) Catalase, uricase, and total nitrogen were measured on the various fractions thus obtained, and distribution curves were constructed as previously described.

Results and Discussion

The effect of AT on concentration of catalase and uricase is given in Table 11. These findings essentially confirm those of Feinstein *et al.*(2) in respect to the effect on catalase. The data on uricase indicate that the concentration of this enzyme was not essentially reduced, actually there was an apparent increase in uricase 16 hr after injection, although the number of animals involved is too small to permit one to attach any significance to this effect.

Figures 16 and 17 show the distribution of catalase and uricase as a function of particle size. The most pronounced effect on catalase distribution was seen at 2½ hr after injection. The observation that such a high proportion of the activity was found associated with the smaller particles is

---

*Dr. R. N. Feinstein provided a generous sample of recrystallized AT.

probably attributable to the fact that most of the catalase activity of these livers was that of the blood entrapped in the organ, and hence was soluble.* Except for slightly diminished maximum values at 2½ and 16 hr, the distribution pattern of uricase was not greatly altered. There was no pronounced shift in the size associated with maximum activity such as we had seen in livers of hypoxic guinea pigs(5) or of rats treated with carbon tetrachloride.(6) There was some alteration, however, in the distribution of the uricase-containing particles, as shown by the considerable increase in the percentage of activity sedimentable in 2 hr in the mice killed 1 and 2½ hr after injection (Table 11). It is conceivable that this change may be the result of physical effects of AT, which is present in the homogenized liver in appreciable quantity (0.0024 M, if one assumes equal distribution) rather than to any in vivo effect.

TABLE 11

Activity and sedimentability of catalase and uricase in livers of rats injected with 2 g/kg 3-amino-1,2,4-triazole

Time after injection, hr	Homogenate activity			Percent sedimented in 2 hr		
	No. mice	Catalase*	Uricase**	No. mice	Catalase	Uricase
Control	9	29.8 ± 2.7†	61.9 ± 3.4†	5	5.8 (2.8 - 8.3)	8.3 (5.7 - 11.2)
1	5	1.74. (1.58 - 1.90)	65.7 (42.8 - 84.0)	2	20.9 (19.7 - 22.1)	13.6 (13.1 - 14.2)
2½	4	0.92 (0.68 - 1.61)	55.5 (38.6 - 74.6)	4	22.7 (17.6 - 38.8)	15.2 (13.6 - 17.9)
16	2	7.0 (6.5 - 7.6)	71.4 (68.6 - 73.2)	2	10.6 (7.7 - 13.4)	8.8 (7.5 - 10.1)
24	3	9.6 (9.0 - 10.0)	58.8 (52.8 - 72.0)		-	-

*M eq. perborate destroyed/5 min/mg N

** μM urate destroyed/min/mg N

† Averages and standard deviations; other values are averages and ranges.

*In view of our experiences with rat liver catalase,(4) which is dissolved out of the particles in sucrose media, it is possible that some of the soluble catalase arising from the blood may be adsorbed in vitro on liver microsomes.

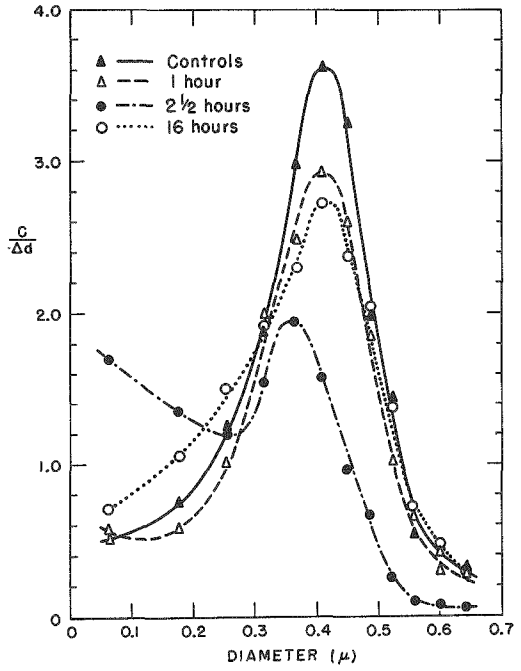

Figure 16

Distribution of catalase in livers of mice treated with 3-amino-1, 2, 4-triazole. Each point represents the fraction of total enzyme activity found in a given zone of the gradient tube divided by the increment of particle diameters within the zone ($C/\Delta d$), plotted against the mean diameter of the particles within the zone.

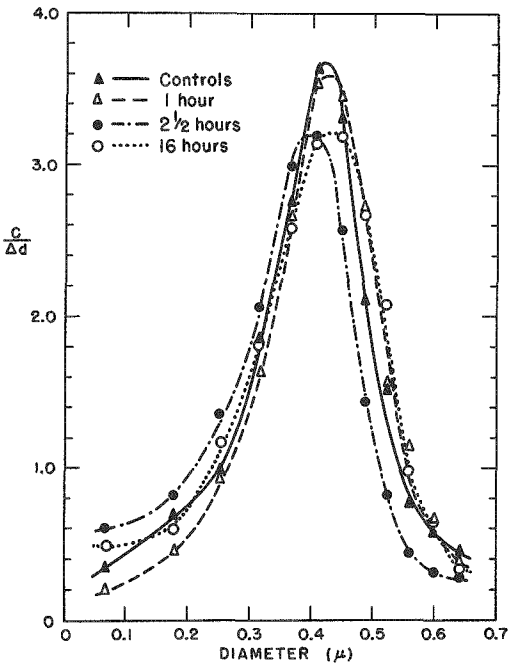

Figure 17

Distribution of uricase in livers of mice treated with 3-amino-1, 2, 4-triazole.

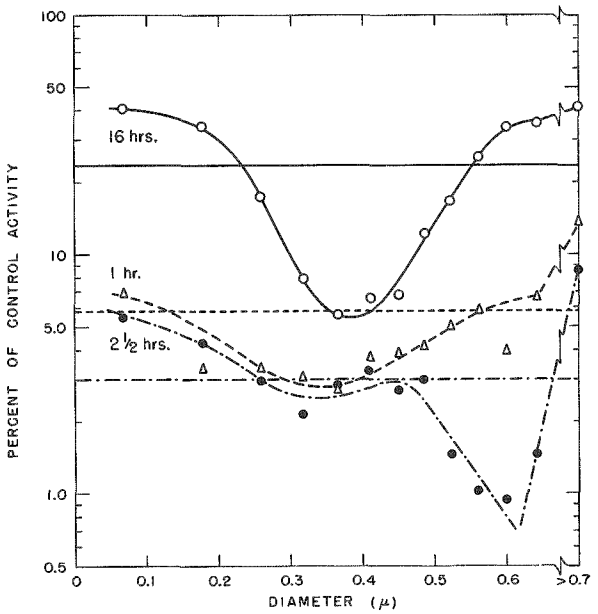

Figure 18

Effect of 3-amino-1, 2, 4-triazole on the catalase activity per unit nitrogen of the various zones. The "per cent control activity" is based not on the activity of the unfractionated control homogenate, but on the activity per unit nitrogen of the individual zones obtained after centrifugation of the homogenate. The horizontal lines represent the activity per unit nitrogen, as per cent of the controls, of the unfractionated homogenates of livers of the treated mice.

Figure 18 shows that the decrease in catalase activity was not manifested uniformly by all of the tissue fractions obtained. At 1 and 16 hr after injection, the greatest inhibition occurred roughly in those particles with the maximum total activity (ca. 0.4 μ). At $2\frac{1}{2}$ hr, however, the decrease in activity became progressively greater with increasing particle size, except for that associated with the largest particles, which had sedimented completely during this time.

Thus it appears that AT had essentially negligible effects on the catalase-containing particles themselves, as judged by the failure of the uricase distribution to be grossly altered. The effects on the distribution of catalase would seem to be due in large part to the presence of soluble catalase from the blood, which would be present in high enough concentration to contribute significantly to the activity of the liver. Blood catalase is not inhibited by AT.(1)

References

1. Heim, W. G., D. Appleman, and H. T. Pyfrom. Production of catalase changes in animals with 3-amino-1,2,4-triazole. Science 122: 693-694 (1955); Effects of 3-amino-1,2,4-triazole (AT) on catalase and other compounds. Am. J. Physiol. 186: 19-23 (1956).

2. Feinstein, R. N., S. Berliner, and F. O. Green. 3-Amino-1,2,4-triazole. II. Effects on tissue catalase: possible similarity to tumor growth. Quarterly Report of the Biological and Medical Research Division, Argonne National Laboratory. ANL-5655, pp. 110-117 (1956).

3. Thomson, J. F., and F. J. Klipfel. Further studies on cytoplasmic particulates isolated by gradient centrifugation. Arch. Biochem. and Biophys., in press.

4. Thomson, J. F., and E. T. Mikuta. Enzymatic activity of cytoplasmic particulates of rat liver isolated by gradient centrifugation. Arch. Biochem. and Biophys. 51: 487-498 (1954).

5. Klein, P. D., and J. F. Thomson. Comparison of enzyme distribution in liver of normal, fasted and hypoxic guinea pigs. Am. J. Physiol. 187: 259-262 (1956).

6. Thomson, J. F., and E. M. Moss. The effect of oral administration of carbon tetrachloride on the intracellular distribution of uricase and succinic dehydrogenase activity of rat liver. Cancer 8: 789-795 (1955).

BIOCHEMICAL AND MORPHOLOGICAL STUDIES OF NUCLEI FROM RAT LIVER

A. D. Barton and Anna Kane Laird

The present experiments represent an extension of earlier studies on the structure and biochemical properties of cell nuclei.[1,2] A recent report by Chaveau et al.,[3] giving a method for the isolation of rat liver nuclei in a medium containing 75% sucrose, has made it possible to prepare nuclei with much less cytoplasmic contamination than was possible previously. All of the nuclei used in the present experiments were isolated by this new method.

Biochemical studies. The behavior of the "soluble" protein of the nucleus has been studied by disrupting nuclei in the Waring Blendor and by exposing nuclei to various media.

Nuclei suspended in a sucrose medium to which no ionized salts had been added lost very little protein, even when they were disrupted in the Waring Blendor. For example, nuclei containing 12.5 mg protein nitrogen (protein-N) lost 0.92 mg protein-N when washed once in 30% sucrose. When the washed nuclei were resuspended in 30% sucrose, and chopped to pieces in an ice-jacketed Blendor by intermittent runs totalling 15 min at full voltage, only 0.25 mg protein-N was found in the supernatant fluid after the mixture was centrifuged.

When nuclei are washed repeatedly in sucrose media, the ionized salts are removed and the nuclei swell enormously.[4] Various media containing salts have been proposed in order to avoid the nuclear swelling.[4] However, other studies[5] have shown that certain enzymes found in nuclei isolated from a sucrose medium can be removed from the nuclei quite readily by extraction with dilute salt solutions. In the present experiments, nuclei isolated in 75% sucrose lost considerable quantities of "soluble" protein when washed with solutions containing salts. For example, nuclei containing 12.5 mg protein-N lost 3.4 mg protein-N in one wash with isotonic saline, and even more (4.7 mg) when washed with isotonic saline containing 0.1% sodium desoxycholate (DC).

An experiment was performed to test whether the nuclei can take up protein again after their "soluble" protein has been removed by washing in a salt medium. Nuclei isolated from the 75% sucrose medium were suspended in the medium (AW) of Anderson and Wilbur[4] (containing 0.0094 M KH_2PO_4; 0.0125 M K_2HPO_4; 0.0015 M $NaHCO_3$; 0.015 M sucrose), and the mixture was centrifuged at 1500 g for 10 min. Of the 4.51 mg protein-N present originally, 2.58 mg was recovered in the washed nuclei and 1.58 mg (35% of the total) was recovered in the supernatant fluid. Two

samples of these washed nuclei were resuspended, one in 30% sucrose (sample A) and one in a "soluble" protein fraction (sample B), which was obtained by centrifuging a homogenate of the same rat liver in 30% sucrose at 105,000 g for 60 min and discarding the sediment. After centrifugation, each nuclear sediment was washed once in 30% sucrose and then in the AW medium.

The data in Table 12 show that when the washed nuclei were suspended in the "soluble" protein fraction, they took up "soluble" protein once more, retained a considerable quantity of it through a wash in 30% sucrose and liberated it again when washed with the AW medium. Apparently the washed nuclei took up a quantity of protein equivalent to one-half the amount that was removed by the first washing in the AW medium. In similar experiments, comparable results were obtained when the nuclei were washed with isotonic saline rather than the AW medium.

TABLE 12

Uptake of "soluble" protein by washed nuclei

Sample A	Protein, mg	Sample B	Protein, mg
Nuclei in 30% sucrose	2.58	Nuclei in protein medium	13.9
Sucrose wash 1	0.40	Protein medium removed from nuclei	8.3
Sucrose wash 2	0.31	Sucrose wash	0.53
AW wash	0.29	AW wash	1.00
Nuclei after washing	1.55	Nuclei after washing	1.58

Washing nuclei in the AW medium, in isotonic saline, or in isotonic saline containing a low concentration of DC (up to about 0.03%) removed essentially no ribose nucleic acid or desoxyribose nucleic acid.

Morphological studies. When nuclei sedimented in 75% sucrose are resuspended in 30% sucrose, the osmotic shock weakens the nuclear membrane. The diluting of the ions in the mixture produces swelling of the nuclear matrix, which may become locally explosive, when the nuclear membrane ruptures, as shown in Figure 19.

When nuclei isolated in sucrose are exposed to ionic media, such as isotonic saline, they shrink and become granular in appearance, as seen in the phase contrast microscope.(4) Addition of sodium desoxycholate (DC) to the saline weakens the nuclear membrane and tends to cause the nuclear material to swell, thus offsetting the contractile effect of the saline.

Figure 19. Nuclei sedimented in 75% sucrose and resuspended in 30% sucrose. Note the swelling of the nuclear matrix that follows local rupture of the nuclear membrane. Phase contrast.

With a very low concentration of DC (0.01-0.03%) the nuclei become clear and the nucleoli are very prominent (Figure 20). In some cases a nucleolus may be seen to move to the nuclear membrane and then out into the medium through a small rupture in the membrane. Usually the rupture enlarges eventually and some of the matrix material of the nucleus also extrudes through the opening. Even though the nucleolus moves some distance from the nucleus, often it can be shown by manipulation of the coverglass that the nucleolus remains attached to the nucleus by an invisible connection.

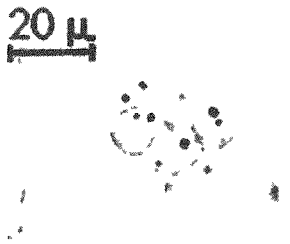

A. Shortly after mixing; two nucleoli have already been extruded from the nucleus whose remnant can be seen in the upper center of the group.

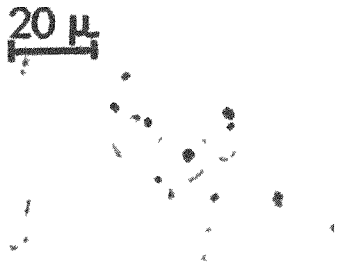

B. About 45 min after mixing. The first two nucleoli have moved farther out, but were found to be still attached to the central mass. Nucleoli have moved to the periphery in the two outer nuclei.

Figure 20. Nuclei suspended in isotonic saline containing 0.02% sodium desoxycholate (DC). Phase contrast.

When saline containing higher concentrations of DC (0.05-0.1%) is used, the nuclei swell, and many small dark bodies appear in the nuclear matrix. When in this condition, the nuclei can be drawn out into long fibrous structures, as shown in Figure 21. Isolated nuclei were homogenized in isotonic saline containing 0.1% DC, and a sample of this material, dried by the critical point method of Anderson(6) for examination in the electron microscope, is shown in Figure 22. This material consists primarily of a jumble of highly contorted strands, which have a rough, irregular outline. These contorted strands, whose minimum diameter appears to be approximately 250 A, have been seen under a variety of conditions. The slender fibrils, whose minimum diameter may be less than 50 A, have been seen under conditions in which some of the desoxyribose nucleic acid was beginning to be extracted. The two types of particulate matter in the background apparently represent material that was associated with the stranded structures.

Even after the "soluble" protein has been extracted and the nuclear membranes disrupted by homogenization in saline containing DC, the random clumps of material that remain will still expand and contract in response to changes in the salt concentration in the medium, in much the same way as intact nuclei do. They still are able to take up and liberate "soluble" protein.

Discussion. The present results suggest that the "soluble" protein of rat liver is associated with relatively insoluble material which is present in the form of highly contorted strands. The minimum diameter of these strands is approximately 250 A and they resemble the chromatin microfibrils postulated by Ris.(7) Apparently these structures are responsible for the ability of the nuclei to take up and release "soluble" protein, which in turn may well prove to be related to the function of the nucleus. Swelling or shrinking of nuclei in response to changes in the ion concentration of the medium is due to changes in the disposition of this strand material(7) and is not related to the presence or absence of the soluble protein in the nucleus.

The nucleoli seem to be attached to the stranded structures. Under some conditions, the stranded material associated with the nucleolus responds more vigorously to DC than the rest of the nuclear matrix, with the result that the nucleolus may be extruded a considerable distance into the medium through a rupture in the nuclear membrane. The nucleolus remains attached to the invisible structure that extrudes it, which in turn remains attached to the nucleus.

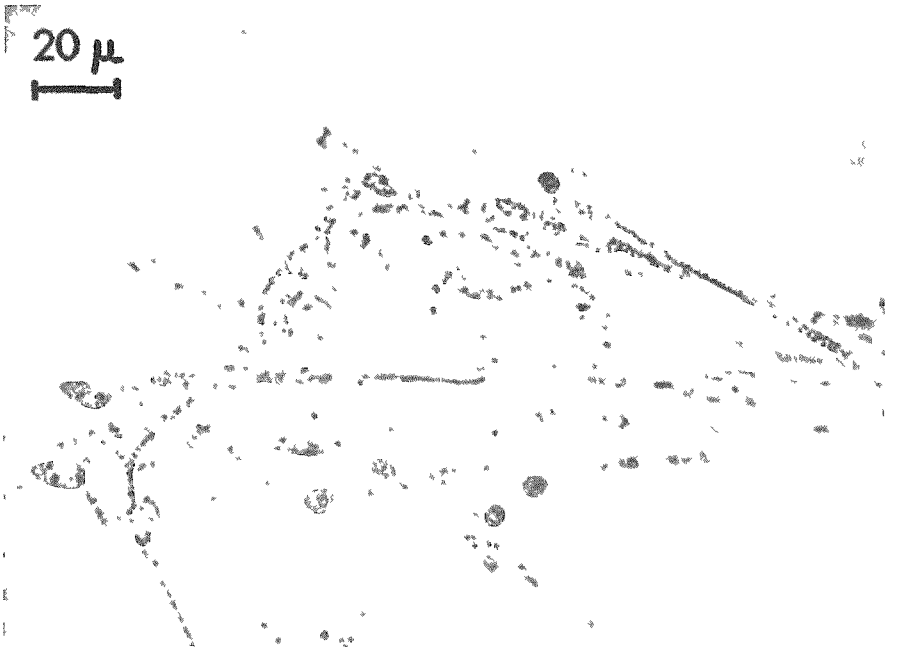

Figure 21. Nuclei suspended in isotonic saline containing 0.05% DC and drawn out to form long fibrous structures. Phase contrast.

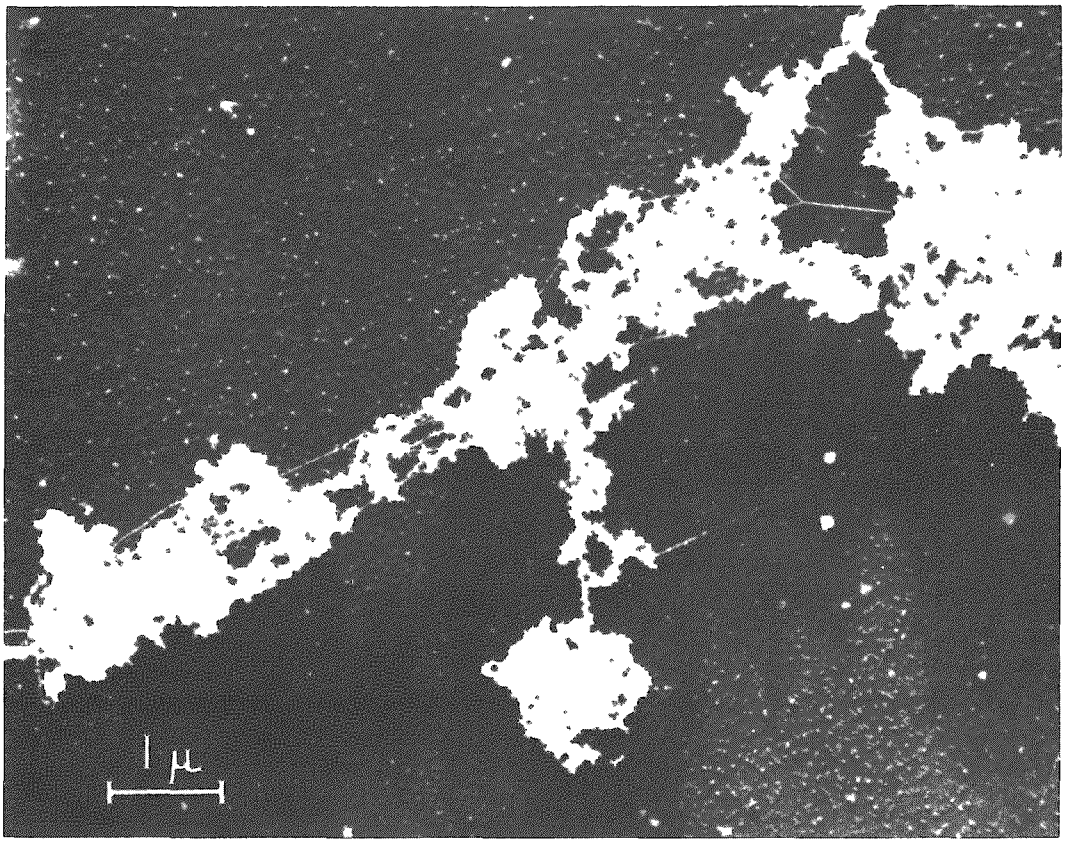

Figure 22. Nuclei disrupted by homogenization in isotonic saline containing 0.1% DC; sample dried by the critical point method. Electron micrograph.

References

1. Barton, A. D., and A. K. Laird. Studies of the role of the nucleus in protein synthesis. Quarterly Report, Division of Biological and Medical Research, Argonne National Laboratory. ANL-5378, p. 155 (1955).

2. Barton, A. D., and A. K. Laird. The role of the nucleus in protein synthesis. Quarterly Report, Division of Biological and Medical Research, Argonne National Laboratory. ANL-5456, pp. 70-72 (1955).

3. Chaveau, J., Y. Moule, and Ch. Rouiller. Isolation of pure and unaltered liver nuclei. Morphology and biochemical composition. Exptl. Cell Research 11: 317-321 (1956).

4. Anderson, N. G., and K. M. Wilbur. Studies on isolated cell components. IV. The effect of various solutions on the isolated rat liver nucleus. J. Gen. Physiol. 35: 781-795 (1952).

5. Rosenthal, O., E. Gottlieb, J. D. Gorry, and H. M. Vars. Influence of cations on the intracellular distribution of rat liver arginase. J. Biol. Chem. 223: 469-478 (1956).

6. Anderson, T. F. Electron microscopy of microorganisms, in Physical Techniques in Biological Research, ed. G. Oster and A. W. Pollister. Academic Press, New York (1956)

7. Ris, H. A study of chromosomes with the electron microscope. J. Biophys. and Biochem. Cytol. Suppl. 2: 385-390 (1956)

ELECTRON MICROSCOPIC OBSERVATIONS OF THE PROTOZOAN FLAGELLATE, PERANEMA TRICHOPHORUM

L. E. Roth

Study of this organism was begun because of its unique flagellar motion, in which only the far distal portion of the flagellum beats while the remainder is held rigid. A more general study has been undertaken, however, since other portions of the organism have shown structural features of cytological interest.

The organisms were fixed for one hour in 1% osmium tetroxide in 0.9% NaCl and buffered to pH 7.4 with MacIlvaine's buffer. After embedding in a mixture of butyl and ethyl methacrylate, sections were cut at 1/40 μ and examined in the RCA EMU-3A electron microscope using a 100-kv beam.

The two flagella are attached near the anterior end of the organism inside a pear-shaped reservoir (Figure 23). In cross section, both flagella have the nine peripheral and two central fibrils characteristic of the shafts of cilia and flagella; in addition, a dense, rod-shaped structure about 0.2 μ in diameter is included in the flagellar membrane (Figure 23). Near the basal region, the central two fibrils are absent and the flagellum is much thicker, about twice the usual diameter (Figure 24). The pellicular membrane is continuous with the flagellar membrane which has attached material ranging from fine, thread-like filaments (Figure 24) to a dense, striated, layered covering (Figure 25). This latter covering is in two separate pieces which are present only on the leading flagellum in the rigid shaft portion outside the reservoir. The trailing flagellum (Figure 23, TF) does not have this covering, but has filamentous material attached.

The basal portions of the flagella are composed only of extensions of the nine peripheral fibrils around which a small granule or two is present (Figure 24, B); the central fibrils are absent. A fibrillar connection has been observed near the basal ends which is either a connection between the two flagella or a rhizoplast extending to the nucleus.

In the cytoplasm close to the flagellar reservoir, two rods are present which measure about 0.5 μ in diameter and 30 μ long. In cross section, each rod is seen to be composed of a central group of longitudinal tubules, an outer homogeneous layer, and finally a double layered membrane surrounding the whole rod (Figure 23, P).

The mitochondria typically are short rods filled with small vesicles which are oval shaped in sections (Figure 23, M).

Figure 23. A section through the anterior end of Peranema including cross sections of the two flagella (F), the trailing flagellum (TF), a cross section of a pharyngeal rod (P), mitochondria (M), and a portion of the contractile vacuole (V). The line indicates 0.5 μ.

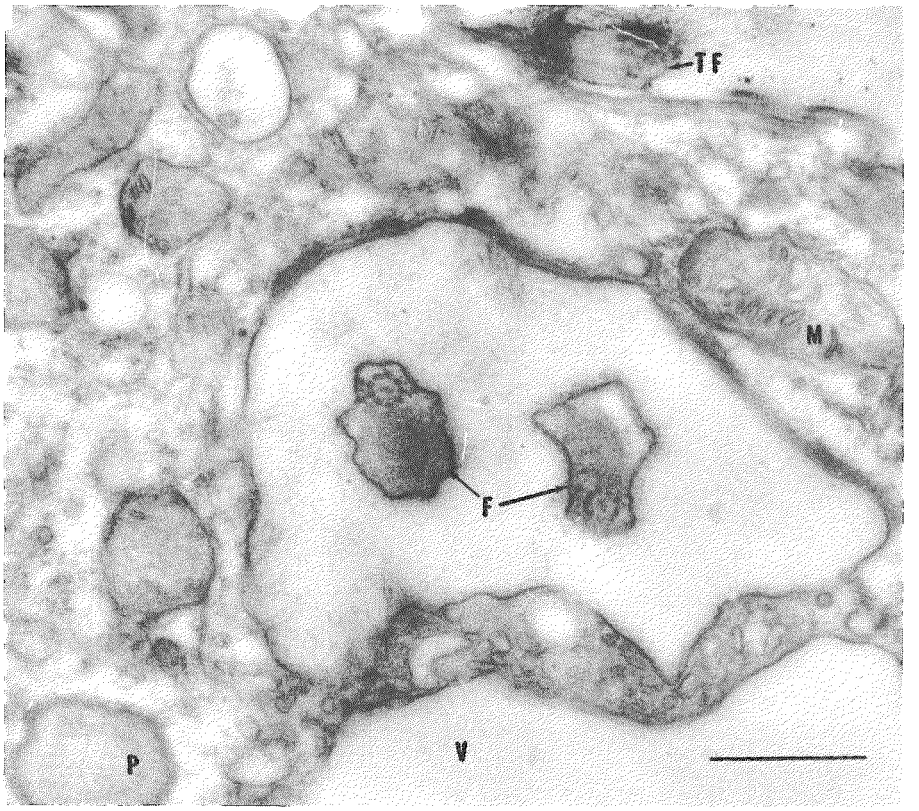

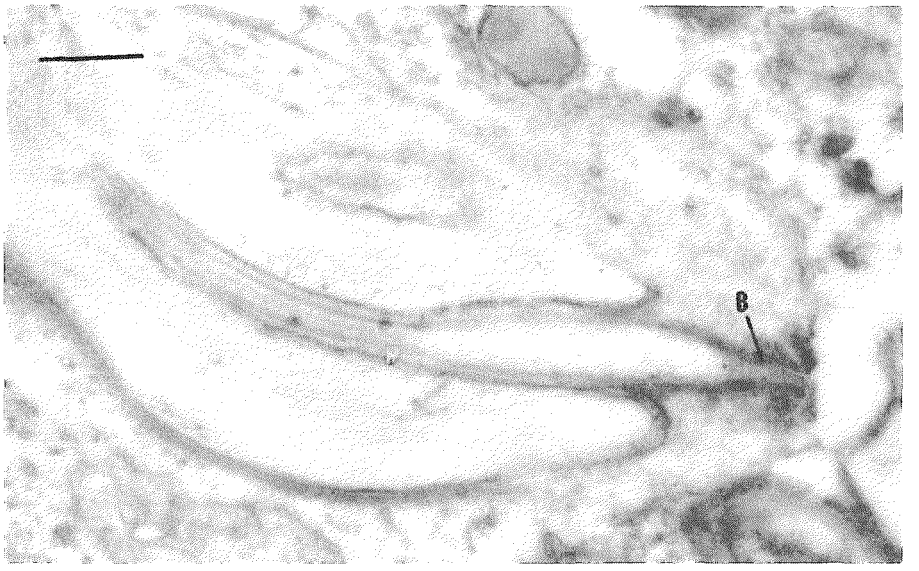

Figure 24. A longitudinal section through one flagellum showing the basal region (B) and the swelling in the near-basal portion of the shaft. The line indicates 0.5 μ.

The contractile vacuole is surrounded by a single layered membrane; no structures have been observed in the vacuole (Figure 23, V).

The nucleus is oval in section and contains several granular components. One or two large nucleoli are present (Figure 26, N) which have a finely granular structure. In addition, numerous rod-shaped structures measuring 0.2 μ in diameter, which have a light center and an outer membrane, are present (Figure 26). There are also two smaller components present, a rather dense one measuring 0.02 μ in diameter and a less dense, finer material.

Figure 25. A cross section and oblique section of the leading flagellum showing its attached, striated material present on the rigid portion of the flagellum. The flagellar fibrils (FF) are located centrally. The line indicates 0.5 μ.

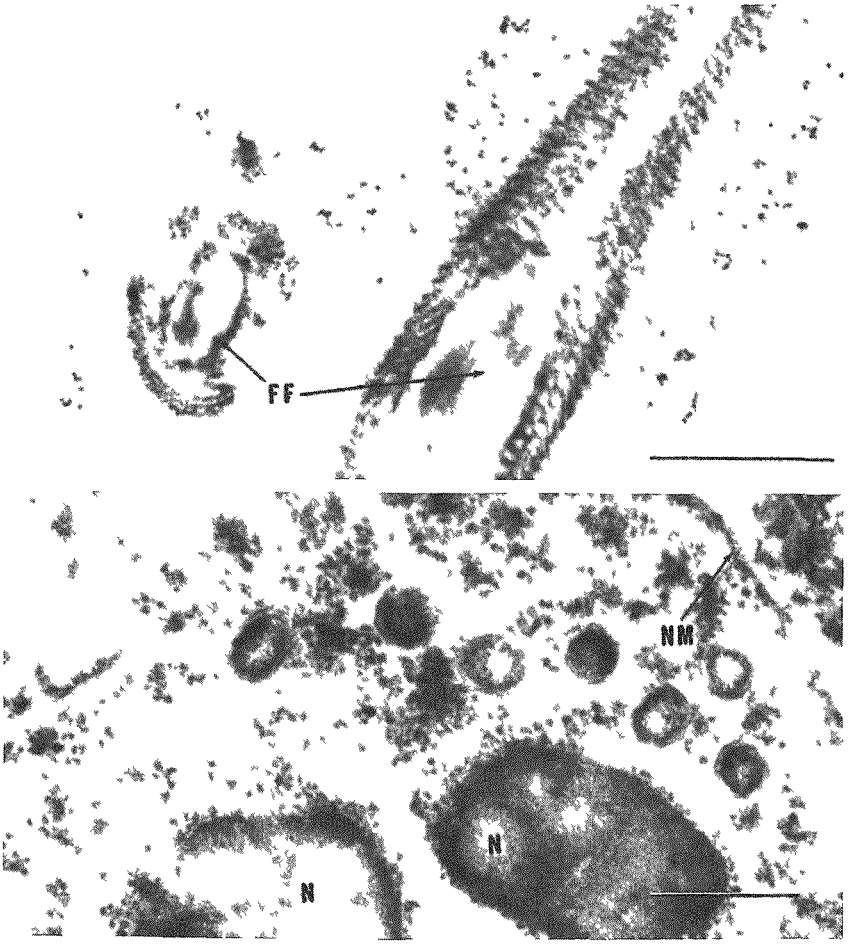

Figure 26. The nucleus contains one or two large nucleoli (N), numerous rod-shaped bodies surrounded by a membrane, a small, dense component, and some fine, less dense material all surrounded by a double layered nuclear membrane (NM). The line indicates 0.5 μ.

THE INITIAL POSTIRRADIATION PERIOD IN THE PIGEON

S. Phyllis Stearner, Margaret H. Sanderson,
and Emily J. Christian

Early mortality following lethal exposure to ionizing radiations does not occur in the pigeon as it does in the chicken and duck.[1] Mortality 3 to 30 days after exposure, however, shows a time dependence which may be similar to that occurring in chickens. This paper discusses the initial radiation syndrome of the pigeon and its effect on blood pressure and renal function. Comparison with early effects in chickens[2,3] will be made.

Male white Carneaux pigeons, 6-8 years old, which had been fasted for 16 hr before exposure, were exposed to 1800-2400 r total body X-rays at about 50 r/min. Cannulation of the femoral artery was performed under nembutal anaesthesia and mean arterial pressure was measured with a saline-mercury manometer hourly for 6 hr after exposure. The cannula was then removed, the incision sutured, and survival time recorded. Blood urate concentration and urate excretion rate were determined according to Brown's method[4] to estimate the effect of irradiation on renal function. The birds were fasted for 16 hr before exposure. Urate excretion was collected hourly for 6 hr after exposure. Blood samples were taken prior to and at 4 and 6 hr after X-ray. Similar blood pressure and urate determinations were made on control pigeons.

The 30-day LD_{50} for the pigeon was approximately 2200 r, and no deaths occurred earlier than 4 days after exposure. The mean arterial pressure showed no effect of irradiation during the observation period (Table 13).

TABLE 13

Mean arterial pressure (mm Hg) of control and X-irradiated pigeons in the initial postirradiation period

	No. of animals	Weight, g	Time after exposure, hr					
			1	2	3	4	5	6
Control	6	550	139	144	133	141	148	151
X-irradiated*	5	556	149	142	141	138	140	146

*2200-2400 r.

Blood urate concentration also showed no change during this period (Table 14A). Individual variation in rate of urate excretion was large but mean values were fairly constant (Table 14B). Excretion rates in the irradiated and control groups were similar, but a slight increase 4 to 6 hr after exposure is suggested.

TABLE 14

Effect of X-irradiation on blood urate and urate excretion rate

A. Blood urate concentration, mg %

	No. of animals	Time after exposure		
		Control	4 hr	6 hr
Control	7	4.9	4.7	5.0
X-irradiated*	12	4.3	4.6	5.2

B. Urate excretion rate, mg/hr

	No of animals	Weight, g	Time after exposure, hr						M
			0-1	1-2	2-3	3-4	4-5	5-6	
Control	7	522	18.4	18.3	18.0	22.6	19.9	19.7	19.5
X-irradiated*	12	524	18.9	15.3	19.7	22 7	25.1	25.9	21.2

*1800-2200 r.

Circulatory and renal failure were invariably associated with death in the initial postirradiation period in young chicks.[2] In the adult chicken only a moderate hypotension developed, the rate of urate synthesis increased, and there was no evidence of decreased renal function. Nevertheless, qualitative clinical evidence suggested that a circulatory insufficiency was important in the initial syndrome in the adult.[3] In the pigeon these effects were not seen in the initial postirradiation period: there was no evidence of a circulatory response and no hypotension. The normal rate of urate synthesis for several hours after exposure suggests that cellular breakdown may not be as severe and/or rapid as it is in the chicken. The slight increase in rate of urate excretion 4 to 6 hr after exposure indicates that urate synthesis may increase later, perhaps after 24 to 48 hr. This point is now under investigation.

The available evidence suggests that the development of circulatory insufficiency may be a critical factor in the initial radiation mortality in the bird. The pigeon apparently is able to maintain an adequate circulation during the initial postirradiation period and no early mortality occurs. It has

been suggested that radiation results in the accumulation of toxic products of cell destruction,[5,6] and such substances may contribute to a circulatory collapse. If rate of urate synthesis can be considered an indicator of the extent of cellular destruction, cell breakdown may proceed more slowly in the pigeon. It is possible that in this way the amount of tissue breakdown may influence circulatory dynamics and so indirectly affect mortality in the initial postirradiation period.

References

1. Stearner, S. P. The effect of variation in dose rate of roentgen rays on survival in young birds. Am. J. Roentgenol. 65: 265-271 (1951).

2. Stearner, S. P., A. M. Brues, M. H. Sanderson, and E. J. Christian. Role of hypotension in the initial response of X-irradiated chicks. Am. J. Physiol. 182: 407-410 (1955).

3. Stearner, S. P., M. H. Sanderson, E. J. Christian, and A. M. Brues. Initial radiation syndrome in the adult chicken. Am. J. Physiol. 184: 134-140 (1956).

4. Brown, H. The determination of uric acid in human blood. J. Biol. Chem. 158: 601-608 (1945).

5. Moon, V. H., K. Kornblum, and D. R. Morgan. Pathology of irradiation sickness: a new method for inducing shock. Proc. Soc. Exptl. Biol. Med. 43: 305-306 (1940).

6. Rugh, R., J. Suess, and J. Scudder. Shock, toxemia in radiation lethality. Nucleonics 11: 52-54 (1953).

AMYLOID DISEASE IN NONIRRADIATED AND IRRADIATED MICE

Samuel Lesher, Douglas Grahn, and Anthony Sallese

Although the liver and kidney are considered relatively resistant to acute irradiation,[1-3] it was noted that in two groups of LAF_1 mice exposed to daily gamma irradiation at the 6 and 12 r levels, lesions indicative of degenerative changes developed. Similar lesions were also observed in the nonirradiated controls. The most pronounced grossly detectible lesion occurs in the kidneys which in a high percentage of mice are polycystic. On the other hand the liver changes are less obvious and require microscopic examination to establish. A study of the liver, kidney, and spleen following the periodic acid-Schiff reaction (PAS) and methyl violet and congo red staining revealed amyloid deposits in the tissues of all three organs. Amyloid involvement is not confined to the liver, kidney, and spleen but in advanced stages, deposits are found in a wide variety of organs including adrenal glands, walls of the intestine, heart, lungs, and tongue.[4-6]

In a high percentage of irradiated and nonirradiated mice dying within a certain age period (Figure 27) the liver, kidney, and spleen contained amyloid. The peak incidence is higher and is reached earlier in the irradiated animals. Following start of irradiation at 100 days of age the peak occurs at the 376- to 475-day period in mice receiving 12 r/day, and in the 476- to 575-day period in those receiving 6 r/day, whereas in the nonirradiated controls it is reached between 576 and 675 days (Figure 28). At 24 r/day the incidence of amyloid disease is negligible (3 in 210), and above this dose the animals apparently do not live long enough to reach the susceptible period.

The incidence of amyloid disease in irradiated and nonirradiated animals, as summarized in Figures 27 and 28, indicates a definite dose dependency. During the peak period the percentage of animals which have amyloid disease is quite high; e.g., in the 376- to 475-day period (Figure 27), approximately 50% of the 12 r/day mice have amyloid deposits in their liver, kidneys, and spleen. Irradiation apparently accelerates the course of the disease, but does not appreciably shorten the induction or so-called latent period, since amyloid appears at approximately 276 days in all three groups. It is of particular interest that amyloid disease in mice is predominantly a disease of the mid-life span. Late in life, regardless of the radiation history, the incidence of the disease falls back to very low levels, possibly not occurring at all among the last 10% of the deaths.

Heston has shown that in certain strains of mice there is a genetic predisposition for primary amyloidosis.[7] He found that the incidence was approximately 100% in strain A and 18.2% in strain L, whereas in the LAF_1 hybrid it was 27.5%. The incidence in the three LAF_1 series (6 r/day, 12 r/day, and controls) used in this investigation is in close agreement with

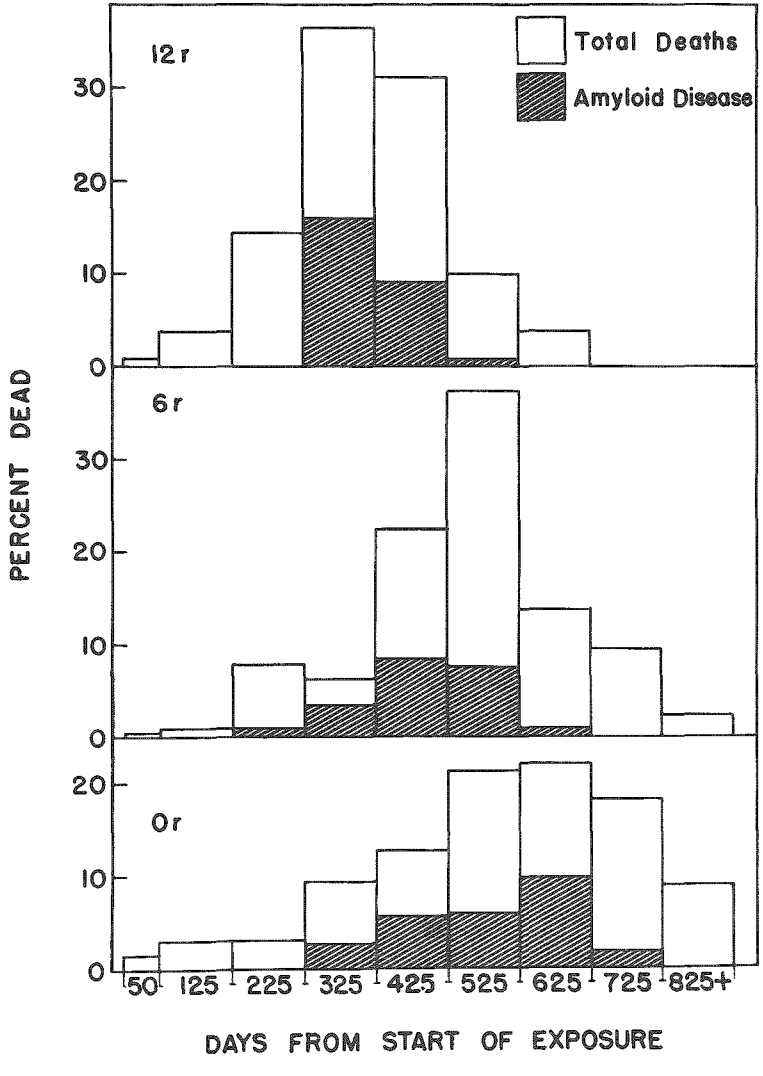

Figure 27. Frequency distribution of mice dying during 100-day intervals after the start of irradiation. All mice were 100 days of age at start of mortality experience.

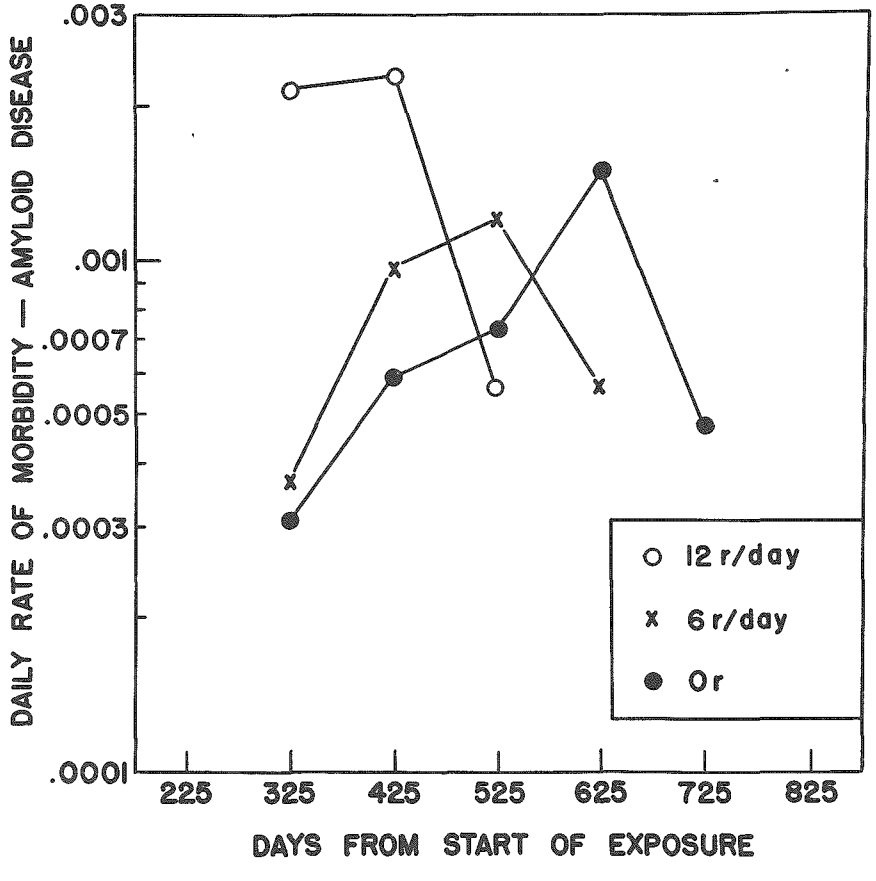

Figure 28. Rates of morbidity of amyloid disease calculated on the basis of 100-day interval lengths; morbidity rates on log scale. All mice were 100 days of age at start of exposure.

Heston's data. It would appear that the genetic susceptibility of amyloid disease is an important factor in establishing the incidence regardless of the evocator; hence, irradiation increases the morbidity rate in the early periods without increasing the total incidence.

References

1. Bloom, W. The kidney, in Histopathology of Irradiation from External and Internal Sources, W. Bloom, editor, McGraw-Hill Book Company, New York (National Nuclear Energy Series, Div. IV, Vol. 22I, Chap. 14.), pp. 674-703 (1948).

2. Rhoades, R. P. Structures accessory to the gastrointestinal tract, in Histopathology of Irradiation from External and Internal Sources, W. Bloom, ed., New York, McGraw-Hill Book Company (National Nuclear Energy Series, Div. IV, Vol. 22I, Chap. 17), pp. 541-549 (1948).

3. Warren, S. Effects of irradiation on normal tissues. VII. Effects of radiation on the urinary system. The kidneys and ureters. Arch. Pathol. 34:1079-1084 (1942).

4. Dunn, T. B. Relationship of amyloid infiltration and renal disease in mice. J. Natl. Cancer Inst. 5:17-28 (1944).

5. Heston, W. E., and C. D. Larsen. Variation in occurrence of pathologic calcification, nephritis and amyloidosis in mice fed control and modified diets. J. Natl. Cancer Inst. 6:41-57 (1945).

6. Rukavina, J. G., W. D. Black, C. E. Jackson, H. F. Falls, J. H. Carey, and A. C. Curtis. Primary systemic amyloidosis: A review and an experimental, genetic, and clinical study of 29 cases with particular emphasis on the familial form. Medicine 35:239-334 (1956).

7. Heston, W. E., and M. K. Deringer. Hereditary renal disease and amyloidosis in mice. Arch. Pathol. 46:49-58 (1948).

PROGRESS REPORT: GAMMA-RAY TOXICITY PROGRAM

Genetic Variation in the Survival Time of Mice under Daily Exposure to Co^{60} Gamma Radiation

Douglas Grahn, George A. Sacher and Katherine F. Hamilton

The first report of this series[1] presented preliminary survival data for inbred strains BALB/c, A/Jax, $C3H_f$/He and C57BL/6 exposed to daily doses of Co^{60} γ-radiation between the levels of 220 r and 24 r/day. The present report gives more complete survival data at the lowest dose levels, 32 r, 24 r and 12 r/day, where a significant number of tumors is observed.

The mean aftersurvival (MAS) data are based on essentially equal numbers of the two sexes. An approximation of the control MAS is also given. Control estimates for strains BALB, A, and C57BL are probably accurate within ± 25 days. The $C3H_f$ estimate is uncertain at this time.

In Table 15 the survival statistics are presented in two ways: the MAS and the per cent reduction of control aftersurvival. Considerable strain variation is evident in both statistics. At 32 r and 24 r/day, the per cent reduction values show less variation than the MAS values. This is also true at doses greater than 32 r/day. These findings indicate that a positive relationship exists between control survival and survival following irradiation at the acute and subacute levels of response.

At 12 r/day, where the chronic radiation syndrome is becoming evident, the above-noted relationship begins to break down. The BALB strain diverges from the others by showing a markedly lower reduction of aftersurvival. As a result, there is an actual increase in variation between strains BALB and C57BL when the data are expressed as per cent reduction of aftersurvival. The BALB strain has the shortest control survival and is the most radiosensitive in terms of acute lethality. The data thus suggest that an animal with a poor normal life expectation may be relatively less affected by the chronic radiation. This can be interpreted as a function of the long time period required for the lethal expression of irreparable injury, which is the predominant cause of death at low exposure intensities. The poor genotype may not have a life span long enough to permit full expression of the late radiation injury.

The above hypothesis is presently under test at 6 r/day, the lowest available dose rate in the existing radiation facilities. Strains BALB and C57BL are being studied with the expectation that 6 r/day should cause very little reduction of aftersurvival in the BALB as compared to C57BL.

TABLE 15

Response of four inbred mouse strains to 32, 24 and 12 r/day of Co^{60} γ-radiation, beginning at 100 days of age

Strain	n	MAS, days	Reduction of control MAS, %	Leukemia incidence, %
		32 r/day		
BALB/c	48	153	59	4.5
A/Jax	48	175	63	15.2
$C3H_f$/He	54	186	63	7.5
C57BL/6	48	208	67	47.8
		24 r/day		
BALB/c	42	188	50	7.5
A/Jax	42	222	53	17.5
$C3H_f$/He	45	251	50	6.7
C57BL/6	48	265	58	56.3
		12 r/day		
BALB/c	33	307	18	6.7
A/Jax	27	323	32	4.2
$C3H_f$/He	30	359	28	13.3
C57BL/6	30	430	31	25.0
		Control: Estimated MAS from 100 days of age		
BALB/c		375		
A/Jax		475		
$C3H_f$/He		500		
C57BL/6		625		

The single-dose 30-day LD_{50} is positively related to the control aftersurvival (see Table 16) as is the survival under daily irradiation at the higher doses. Consequently, at acute and subacute levels of response, the LD_{50} is positively related to the MAS. This relationship has been developed by Blair[2] into a general hypothesis regarding the late effects of radiation exposure. This hypothesis states that a given per cent reduction of life expectation is brought about by an accumulated dose that is, for all mammalian species, a constant multiple of the LD_{50}. For example, a mean accumulated dose (MAD) three times the LD_{50} will cause a 20% reduction of life. However, the existing data at 12 r/day do not support Blair's hypothesis.

TABLE 16

Relation between single-dose 30-day LD_{50} and the mean accumulated dose (MAD) and reduction of aftersurvival at 12 r/day

Strain	Co^{60} 30-day LD_{50},* r	MAD 12 r/day, r	MAD ÷ LD_{50}	% reduction of MAS
BALB/c	800	3684	4.6	18
A/Jax	880	3876	4.4	32
C57BL/6	1000	5160	5.2	31

*Co^{60} LD_{50} = 200 kvp X-ray LD_{50} x 1.6

In Table 16, the Co^{60} γ-ray LD_{50} values are given for strains BALB, A, and C57BL, along with the MAD values expressed as multiples of these LD_{50}'s. It may be seen that strains A and C57BL, with a similar reduction of aftersurvival, have quite different MAD:LD_{50} ratios. Strains A and BALB have similar MAD:LD_{50} ratios, but dissimilar reductions of aftersurvival. Thus, no simple relationship exists between the LD_{50} and the per cent reduction of aftersurvival at low daily doses of radiation.

The four strains also show considerable variation in the leukemia incidence. Excepting strain $C3H_f$, all strains have a maximum incidence at 24 r/day. The extreme sensitivity of the C57BL strain to the leukemogenic effect of irradiation is notable. In addition, preliminary analysis shows that nonleukemic C57BL mice at 24 r/day have a 10% greater MAS than leukemic mice and also tend to come from older dams (or later parities). Mice of all strains will continue to be entered at these lower doses to provide a detailed analysis of leukemia induction.

Small numbers of pulmonary, mammary, and ovarian tumors have also been detected at these doses. Strain $C3H_f$ females show the greatest susceptibility to radiogenic ovarian tumors with an incidence of 33% in the 12 r/day group.

References

1. Grahn, D., K. F. Hamilton, and G. A. Sacher. Progress report: Gamma-ray toxicity program. Genetic radiation in the survival time of mice under daily exposure to Co^{60} γ-radiation. I. Quarterly Report of the Biological and Medical Research Division, Argonne National Laboratory. ANL-5597, pp. 36-38 (1956).

2. Blair, H. A. Data pertaining to shortening of life span by ionizing radiation. University of Rochester Atomic Energy Project Report. UR-442.

A TENTATIVE MODEL OF THE 0-2 DAY ACUTE RADIATION RESPONSE IN THE CHICK

Sylvanus A. Tyler and S. Phyllis Stearner

In previous reports,[1,2] evidence is presented which suggests that the 0-2 day mortality following γ-irradiation of young chicks can be ascribed to some chain of events separable from that governing later mortality. The basic experiment consisted of exposing 2500 3- and 4-day-old, male white leghorn chicks in groups of approximately 36 to Co^{60} γ-radiation. Dosages used ranged from 600 r to 2400 r, and exposure times ranged from 30 min to 8 hr. A total of 72 groups of animals was employed.

In Figure 29 are given plots of the dose-mortality pattern by exposure time groups up to 4 hr. Next, we attempt a reduction of the data, by exhibiting whatever empirical relationships exist between this set of exposure-time patterns, and by computing the characterizing parameters. At least two questions come to mind. What assumptions should be accepted as to the underlying form of the individual exposure-time curves? Then, after adopting a form, can the extracted parameters be expressed in dimensions that permit a meaningful interpretation? For example, suppose we assume that these curves are members of some "S"-shaped family and are suitably approximated by a set of cumulative normals. We thus could compute the empirical relationships between the pairs of estimates (mean and standard deviation), the parameters of which completely describe each member of the family of normals. But unless some method of handling the resulting relationship is set up beforehand, our description will yield very little usable information. To avoid such a situation the 72 groups of animals were divided into 6 categories according to the mortality experienced during the first 2 days; Figure 30 shows the dosage versus exposure-time patterns for groups that experienced approximately equal mortality.

If a reversal of radiation effects is postulated, the slopes (b_m) of the equimortality lines (Figure 30) could then be considered as measures of the rates at which a reversal is taking place, and the intercepts (a_m) would estimate the amount of radiation without reversal necessary to produce, on the average, m% mortality. The intercept to slope ratios (a_m/b_m) are approximately equal and average 138 min. This suggests that at all mortality levels there is a time constant (not a half-time) that characterizes the relation between radiosensitivity and reversal rate for at least one mechanism governing mortality in this period. To check the linearity of this family of equimortality relationships, a second population of chicks was exposed at dosages up to 7000 r and for exposure times as long as 16 hr. Similar dose-exposure-time dependence was observed and the intercept to slope ratio remained unchanged. The intercepts (instantaneous dosages) and slopes (reversal rates)

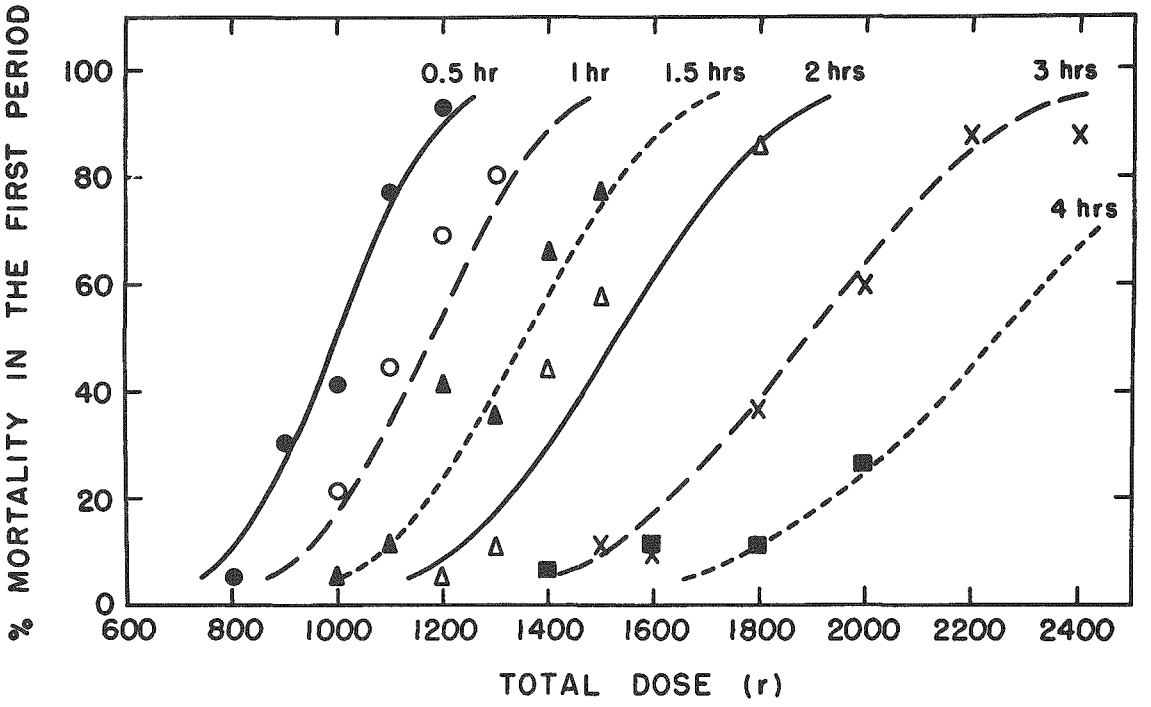

Figure 29. Dose-mortality data for the 0-2 day period by exposure time groups. (Method used in drawing curves is described in text.)

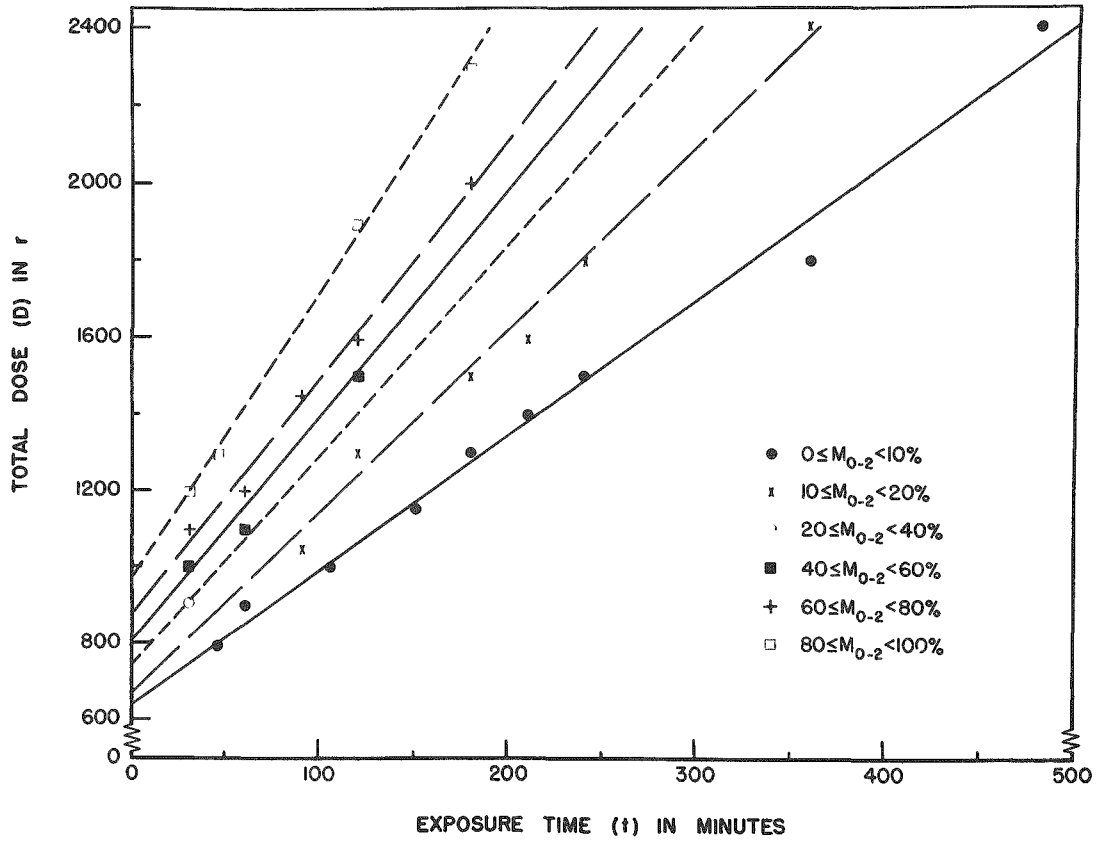

Figure 30. Relation between total dose and exposure time in the 0-2 day period by equimortality groups.

of the equimortality curves are each approximately normally distributed with respect to mortality; and the ratios of corresponding estimates of the distribution parameters are approximately equal.

$$\frac{\hat{a}_{50}}{\hat{b}_{50}} = \frac{816 \text{ r}}{5.93 \text{ r/min}} = 138 \text{ min}; \frac{\hat{\sigma}_a}{\hat{\sigma}_b} = \frac{127 \text{ r}}{0.95 \text{ r/min}} = 134 \text{ min} \qquad (1)$$

Thus the distribution of instantaneous dosages is some constant (K) times the distribution of reversal rates. By assuming linearity of the equimortality relationships and using the distributional values for a_m and b_m determined by Equation 1, the curves of constant exposure time (Figure 29) were drawn.

Proposed Model*

We propose the following model of radiation effects during exposure that may lead to mortality in the chick within the first 2 postirradiation days:

(a) Exposure produces an effect (Y) that accrues at a rate which is proportional to the dosage rate, i.e. $\frac{d}{dt} Y = \mu \frac{dD}{dt}$ where D is the delivered dosage and $\mu > 0$ is a constant scale factor relating dose to effect.

(b) The effect (Y) is reversed during exposure by chick i at a rate which is equal to a constant B_i or to the rate of accrual, whichever is smaller. The net effect (Y) present at any time t during exposure is represented by $Y_i'(t)$.

(c) Death within 2 days following irradiation occurs if the net amount $Y_i'(t)$ of effect (Y) accumulated reaches, in chick i, the value Y_{oi}.

(d) In a given population of chicks, $\frac{B_i}{\mu}$ and $\frac{Y_{oi}}{\mu}$ are normally distributed with ratios of corresponding parameters equal to a constant K.

By (a) and (b)

$$\frac{d}{dt} Y_i'(t) = \begin{cases} \mu \frac{dD}{dt} - B_i & \text{for } \mu \frac{dD}{dt} > B_i \\ 0 \text{ otherwise} \end{cases}, \qquad (2)$$

Thus, if $Y_i'(0) = 0$ at the start of irradiation (t = 0), then when a dose D has been delivered in time t

*The formal presentation of this model was influenced greatly by Dr. Henry Quastler of Brookhaven National Laboratory.

$$Y_i'(t) = \begin{cases} \mu D - B_i t & \\ & \text{for } \mu D - B_i t > 0 \quad , \\ 0 \text{ otherwise} & \end{cases} \tag{3}$$

By (c), death occurs within 2 days after irradiation if

$$Y_{oi} \leq \mu D - B_i t \quad . \tag{4}$$

Let $D_o(i,t)$ designate the smallest dose which is fatal to chick $\underline{i}$ if delivered in time t. We have by expression(4)

$$D_o(i,t) = \frac{Y_{oi}}{\mu} + \frac{B_i t}{\mu} \quad . \tag{5}$$

Thus by (d), the dose $D_o(i,t)$ will also be fatal within the 0-2 day period to all chicks $\underline{j}$ of the same population with $B_j \leq B_i$ $(\underline{i} \neq \underline{j})$ and not fatal in this period to all chicks $\underline{p}$ with $B_p > B_i$ $(\underline{i} \neq \underline{p})$. If m is the percentage of chicks with constant reversal rates equal to or less than β_m, then $D_o(t) \equiv D_{m,t}$, the dose which is fatal to a percentage m of the chicks when delivered in time t, and the equation of the proposed process becomes

$$D_{m,t} = \frac{K \beta_m}{\mu} + \frac{\beta_m}{\mu} t \tag{6}$$

Equation 6 is thus equivalent to the empirical relationships exhibited in Figure 30

$$D_{m,t} = a_m + b_m t \tag{7}$$

where $b_m = \frac{\beta_m}{\mu}$, $a_m = K b_m$ and $K \doteq 138$ min. It is important to note that the linear model proposed implies the existence of a one-parameter system as the mechanism controlling mortality in this period.

An Alternative Model*

Although the linear reversal hypothesis, as set forth above, is tenable over the entire range of dosage and exposure times investigated, we mention the exponential reversal hypothesis because of its frequent acceptance and use in more comprehensive investigations of the recovery phenomenon. An extension of this hypothesis, the exponential reversal hypothesis with additive irreversible component,(3,4) has been tested using the chick mortality data for the 0-2 day period. It yields satisfactory predictions for exposure times less than 8 hr.

*Description of this hypothesis was suggested by Dr. H. D. Landahl of the University of Chicago.

Let

Y_r = measure of the effect-reversible component

Y_n = measure of the effect-nonreversible component

α = nonreversible fraction of the total radiation-induced effect

b = a reversal constant.

In this case, the reversal rate is proportional to Y_r so that

$$\begin{cases} \dfrac{dY_r}{dt} = \mu \dfrac{dD}{dt} - b\, Y_r \\ \\ Y_n = \alpha\, \mu\, D. \end{cases} \tag{8}$$

Hence, at the end of an exposure of duration t,

$$Y_i = Y_r + Y_n = \alpha\, \mu\, D + \frac{\mu D}{bt}(1 - \epsilon^{-bt}) \quad . \tag{9}$$

At $t = 0$, a dose $D_o = D(0)$ is required for $Y_i' = Y_{io}'$; thus

$$D_o = \frac{Y_{io}'}{\mu(1 + \alpha)} \quad . \tag{10}$$

By (d), the reversal constant b is proportional to Y_{io}'. Let $\frac{\gamma}{\mu(1 + \alpha)}$ equal the proportionality constant (γ a constant), then

$$b = \frac{\gamma Y_{io}'}{\mu(1 + \alpha)} = \gamma D_o \quad . \tag{11}$$

Solving (9) for $\frac{D}{D_o}$ where $Y_i' = Y_{io}'$, we have for the group of animals with thresholds near Y_{io},

$$\frac{D}{D_o} = \frac{(1 + \alpha)\ \gamma D_o t}{1 - \epsilon^{-\gamma D_o t} + \alpha\ \gamma\ D_o t} \tag{12}$$

If we take $\alpha = 0.1$ (10%) and $\gamma^{-1} = 6 \times 10^4$ r-sec, a good fit of the equimortality curves (Figure 30) for exposure times less than 8 hr is achieved. For a typical animal having a threshold of say 800 r, the time constant $\frac{1}{\gamma D_o} = \frac{6 \times 10^4}{800} = 75$ min, roughly compares with the half-value of the time constant found under the linear hypothesis $\left(\frac{138}{2} = 69 \text{ min}\right)$. The irreversible component adds considerable breadth to the possible descriptions of the dosage-exposure time relations, for since α ranges from 0 to 1, each equimortality curve ranges from concavity to convexity.

References

1. Stearner, S. P., and S. A. Tyler. An analysis of the dependence of the radiation response in the chick on dose and exposure time. Quarterly Report of Biological and Medical Research Division, Argonne National Laboratory. ANL-5576, pp. 61-63 (1956).

2. Stearner, S. P., and S. A. Tyler. An analysis of the role of dose and dosage rate in the early radiation mortality of the chick. Radiation Research, in press.

3. Blair, H. A. A formulation of the injury, life span, dose relations for ionizing radiations. I. Application to the mouse. University of Rochester Atomic Energy Project Report UR-206 (1952).

4. Blair, H. A. A formulation of the injury, life span, dose relations for ionizing radiations. II. Application to the guinea pig, rat and dog. University of Rochester Atomic Energy Project Report UR-207 (1952).

PROGRESS REPORT: DEUTERIUM OXIDE INTOXICATION IN RATS

Effect of Deuteration on Urea Formation

John F. Thomson and Florence J. Klipfel

In the first communication of this series[1] we reported an increased level of urea nitrogen in the blood of rats treated with D_2O. Although the kidneys of rats dying from deuterium intoxication showed considerable histologic changes, we were not convinced that this elevation of blood urea was due solely to kidney damage. Since the concentration of blood glucose was concomitantly decreased, we believed that the increased concentration of urea reflected at least to some extent an accelerated destruction of protein. The increase in size of the adrenals is in keeping with this supposition. It was thus of interest to study the rate of urea formation in D_2O-treated rats.

Methods

Male rats of the Sprague-Dawley strain, 3 months old and weighing 315 to 365 g at the start of the experiment, were given 50% D_2O as drinking water ad libitum for 21 days. The concentration of D_2O was then reduced to 30% for the next 7 days to maintain a urinary D_2O level of about 21 atom-per cent deuterium.* A group of control rats of the same age and body weight was studied at the same time.

Urea formation was studied by the technique of Engel,[2] slightly modified.[3] Blood urea levels were measured at varying intervals after bilateral nephrectomy; the rate of increase in blood urea was virtually linear over the entire period of time until the death of the animal (54 hr in one rat, 30 to 48 hr in most of the others).

The rate of ureagenesis was calculated for each animal, and the average for the group was then obtained by weighting the individual rates according to the number of analyses carried out on each rat.**

Results and Discussion

At the level of deuteration employed (21 atom-per cent), the rats appeared to be fairly healthy, although their average body weight was about 70 g below that of the control group. The principal symptoms of deuteration

*Deuterium analyses were carried out by Dolores Symon of the Chemistry Division.

**We wish to thank S. A. Tyler for his advice in the statistical treatment of these data.

were marked hyperirritability and increased aggressiveness, necessitating separation of the rats into individual cages during the last days of the experiment.

Table 17 shows the initial levels of urea nitrogen and the rate of urea formation in the control and D_2O-treated rats. The average rate of the control animals was about 50% higher than that previously reported.[4] The fact that the rats used in these experiments were considerably heavier than those previously used may account for the difference.

TABLE 17

Body weight, blood urea, and rate of urea formation in rats treated with deuterium oxide

	Controls	D_2O-treated
No. of rats	7	6
Body weight, final, g		
Average	384	311
Range	(337-410)	(268-337)
Blood urea N, initial level		
Average (mg/100 ml)	9.7	26.5
Standard error	0.72	0.26
Rate of urea formation (mg urea N/hr/100 g rat)		
Average	3.22	3.98
Standard error	0.063	0.245

It is evident that the D_2O-treated rats were producing urea at a significantly higher rate than were the controls ($p = 0.02$). It seems unlikely, however, that this 25% increase in rate is sufficient to account for a nearly threefold increase in the concentration of blood urea unless there was also a diminished rate of urea excretion.

References

1. Thomson, J. F., F. J. Klipfel, and J. J. Katz. Deuterium oxide intoxication in rats. Quarterly Report of Biological and Medical Research Division, Argonne National Laboratory. ANL-5597, pp. 41-43 (1956).

2. Engel, F. L. On the nature of the interdependence of the adrenal cortex, nonspecific stress and nutrition in the regulation of nitrogen metabolism. Endocrinology, 50: 462-477 (1952).

3. Thomson, J. F., and E. T. Mikuta. Urea formation in irradiated nephrectomized rats. Quarterly Report of Biological and Medical Research Division, Argonne National Laboratory, ANL-4948, pp. 99-101 (1953).

4. Thomson, J. F., and E. M. Moss. Urea formation is irradiated nephrectomized rats. II. Quarterly Report of Biological and Medical Research Division, Argonne National Laboratory. ANL-5378, pp. 79-80 (1955).

PROGRESS REPORT: DEUTERIUM OXIDE INTOXICATION IN RATS

Effect of Deuteration on Renal Function

John F. Thomson and Florence J. Klipfel

In previous experiments we have shown that the blood levels of non-protein nitrogen and urea are greatly increased in rats drinking heavy water.[1] Part of the increase in blood urea could be attributed to an increased rate of urea formation,[2] although as pointed out earlier[2] the increase in ureagenesis did not seem to be great enough to account for the degree of elevation of blood urea which we observed.

We have attempted to study various aspects of kidney function in rats. The principal difficulty has been the quantitative collection of urine. Catheterization of the rat bladder has not been uniformly successful, and we have relied on manual compression of the lower abdomen to obtain urine samples. By inducing diuresis with large amounts of water given orally, the errors involved in collection of urine are considerably reduced.

Experimental

Creatinine clearance. The procedure followed was essentially that of Smith and Boss.[3] Rats were given two 10-ml doses of water orally, 60 min apart. Immediately after the second dose, 250 mg/kg of creatinine was injected subcutaneously as a 5% solution. Urine was then collected over a 50-min period; the bladders were emptied as completely as possible by suprapubic compression. A sample of blood was taken by heart puncture, and creatinine was measured in plasma and urine.

Creatinine clearance was measured in the same group of rats twice in the course of deuteration and again 8 days after removal from D_2O. A group of control rats was studied at the same time. The data (Table 18) show that there was a marked depression of the glomerular filtration rate. However, there was a prompt reversal of this depression after the rats were given H_2O instead of D_2O.

Table 18 also shows the urine flow. These values tend to be low, since some urine was left on the surface of the collection funnels. The creatinine determinations, of course, were carried out on the combined urine and washings.

Some indication of the reproducibility of successive determinations of the creatinine clearance on the same rat may be gained from this table. The average value for the average deviations of the individual control rats was 9.43%, with a maximum (No. 1) of 19.2% and a minimum (No. 7) of 3.0%.

p-Aminohippurate (PAH) clearance. At the same time that the creatinine clearances were carried out, PAH clearances were also studied in the same animals. The data are summarized in Table 19, which shows a depression of PAH clearance (renal plasma flow) which also seemed readily reversible. However, the clearance values for normal rats are much lower than those reported in the literature (e.g., 3,4) and it is likely that maximal clearance values have not been established. A single subcutaneous injection of PAH has been used throughout, and while this procedure gave reproducible results for creatinine, it may not have been adequate for PAH, which is much more readily cleared. Additional work is being carried out to attempt to maintain a reasonably constant plasma level of PAH below that which saturates the tubules.

TABLE 18

Creatinine clearance in D_2O-treated rats

	D_2O-treated			Control		
	Date			Date		
	5/9	5/21	5/29	5/10	5/23	5/29
Days on 50% D_2O	17	29	H_{20} for 8 days	-	-	-
Plasma D_2O, %	28.5	26.7	<5	-	-	-
Average weight, g	230	205	222	248	250	264
Urine flow (ml/min/100 cm^2 surface)*	0.016** ±0.0027	0.014 ±0.0013	0.028 ±0.0050	0.027 ±0.0027	0.029 ±0.0050	0.030 ±0.0021
Creatinine clearance (ml/min/100 cm^2 surface)*						
1	0.500	0.185	0.672	0.424	0.640	0.454
2	0.338	0.061	Dead	0.832	0.608	0.524
3	0.410	0.254	0.570	0.660	0.535	0.514
4	0.526	Dead	-	0.584	-	0.624
5	0.477	0.365	0.512	0.720	0.826	0.780
6	0.445	0.385	0.651	0.677	0.775	0.642
7	0.438	Dead	-	0.613	0.670	0.644
8	-	0.500	0.651	0.738	-	-
Average	0.448	0.292	0.611	0.656	0.675	0.597
±S.E.	±0.023	±0.064	±0.030	±0.036	±0.044	±0.041

*Surface area estimated from body weight: $SA = 11.23\ W^{2/3}$.

**Average with standard error.

TABLE 19

PAH clearance in D_2O-treated rats

D_2O-treated					Control		
Date	Days on D_2O	Plasma D_2O, %	No. rats	C_{PAH}*	Date	No. rats	C_{PAH}*
5/9	17	28.5	8	0.445 ±0.068	5/10	8	0.880 ±0.035
5/21	29	26.7	6	0.520 ±0.107	5/23	6	0.726 ±0.047
5/29	H_2O for 8 days	<5	5	0.989 ±0.161	5/29	7	0.732 ±0.044

*Clearance values in ml/min/100 cm^2 body surface, with standard errors.

Urea clearance. Four rats which had been drinking 50% D_2O for 35 days (average plasma D_2O of 23.4%) and four control rats were given 10 ml of saline intraperitoneally. Urine was collected for two consecutive periods of one hour; a sample of blood was taken between the two collection periods. Table 20 shows that the average urea clearance of the deuterated rats was only one fifth as high as that of the controls, although the variation in both groups was very large.

TABLE 20

Urea clearance in D_2O-treated rats

	Average and range	
	D_2O-treated	Control
Body weight, g	234 (199-279)	267 (242-289)
Plasma urea, mg/100 ml	47.3 (35.8-60.9)	18.1 (14.3-27.0)
Urea clearance, ml/min/100 cm^2	0.044 (0.023-0.065)	0.236 (0.108-0.360)

Phenolsulfonphthalein disappearance. Rats were anesthetized with ether, a dose of 5 mg/kg of phenolsulfonphthalein in saline was injected either intravenously or intracardially, and 0.5-ml blood samples were taken by heart puncture at 30 sec, 1 min, and 2 min after injection. A plot of log plasma concentration against log time gave a reasonably straight line. The average slope for 8 determinations on 5 deuterated rats (plasma D_2O 22.5%) was -0.539, standard error 0.082; for 9 determinations on 6 control rats the average was -0.536 ± 0.075. At the levels of phenol red used in these studies, after the first minute after injection most of the removal was presumably accomplished by tubular excretion, so that one might be led to believe that there was no impairment of this function in deuterated rats. However, these experiments are open to criticism, since animals were under anesthesia during the experiment, and renal function may have been greatly depressed.

Discussion

The impairment in glomerular filtration in deuterated rats is shown conclusively by the decrease in creatinine clearance, and is confirmed by the diminished urea clearance. As far as renal plasma flow is concerned, the values are appreciably lower in the deuterated rats, although the low values for the normal rats make these findings open to some question. It is interesting to point out that although microscopically the tubular epithelium appears considerably damaged in rats dying of deuteration, the glomeruli seem essentially normal, despite the impairment in function.

As we have shown previously,[5] despite evidence of both morphologic and functional change, none of the enzyme systems of rat kidney for which we have assayed (including the oxidative phosphorylation system of kidney mitochondria) has shown any striking alterations.

The changes in kidney function can be reversed by replacing D_2O with H_2O as drinking water, provided the rats are not obviously moribund; after the change in drinking water, the rats gain weight, the symptoms of hyperirritability subside, and the animals appear normal.

References

1. Thomson, J. F., F. J. Klipfel, and J. J. Katz. Deuterium oxide intoxication in rats. Quarterly Report of Biological and Medical Research Division, Argonne National Laboratory. ANL-5597, pp. 41-43 (1956).

2. Thomson, J. F., and F. J. Klipfel. Progress report: Deuterium oxide intoxication in rats. Effect of deuteration on urea formation. This report, p. 81.

3. Smith, L. H., and W. R. Boss. Effects of X-irradiation on renal function of rats. Am. J. Physiol. 188:367-370 (1957).

4. Friedman, S. M., J. R. Polley, and C. L. Friedman. The clearance of inulin and sodium p-aminohippurate in the rat. Am. J. Physiol. 150:340-352 (1947).

5. Thomson, J. F., and F. J. Klipfel. Deuterium oxide intoxication in rats. Quarterly Report of Biological and Medical Research Division, Argonne National Laboratory. ANL-5696, pp. 64-67 (1956).

DEPOSITION OF LIVER GLYCOGEN IN X-IRRADIATED GUINEA PIGS

John F. Thomson and Florence J. Klipfel

It is well known that guinea pigs are much more susceptible than other rodent species to a variety of noxious stimuli, e.g., plant and bacterial toxins, cardiac glycosides, histamine, and of course, ionizing radiation. Our experiences with the effect of total-body irradiation on the tryptophan peroxidase activity of the liver suggested that the guinea pig might be deficient in certain heteropoietic mechanisms, since, unlike rat liver, guinea pig liver failed to show an increase in activity of this enzyme following exposure to X-irradiation.[1] Furthermore, although injection of hydrocortisone acetate was also capable of eliciting an appreciable increase in tryptophan peroxidase in rats, this compound had no effect in guinea pigs.

Since rats which have been irradiated are capable of synthesizing glycogen to a much greater extent than a similarly fasted control animal,[2,3] and since this deposition can be prevented by hypophysectomy,[3] it was of interest to see whether the irradiated guinea pigs could also deposit glycogen after exposure to X-rays. Lourau[4] reported that after X-irradiation extensive deposition of glycogen occurred in both mice and guinea pigs after administration of glucose; however, the data which she actually presented were obtained solely in mice, and the question of gluconeogenesis in guinea pigs has not been unequivocally answered.

Methods

Young female albino guinea pigs, weighing between 250 and 300 g, were used in these experiments. Total-body X-irradiation at a dose of 500 r, delivered at a rate of 200 r/min, was used throughout.

All animals were fasted 48 hr before sacrifice. The irradiated guinea pigs were fasted 24 hr before exposure and for 24 hr afterward. Prior to sacrifice, the animals were given 50 mg/kg sodium pentobarbital intraperitoneally, and samples of heart blood and of liver were then obtained from the anesthetized guinea pigs. Glycogen was measured by the method of Blatherwick et al.,[5] glucose by the method of Nelson.[6]

Results

It is apparent from Table 21 that the fasted guinea pig is as capable as the rat of synthesizing glycogen after irradiation. There was a rather large degree of variation among the controls, probably attributable to the presence of unabsorbed foodstuffs still remaining in the gastrointestinal

tract, and it seems likely that longer fasting times might have improved the experiment as far as precision among the controls was concerned. Nevertheless the results clearly indicate that there is no deficiency in the guinea pig as far as gluconeogenesis is concerned.

TABLE 21

Effect of total body X-irradiation on body weight, liver glycogen, blood glucose, and NPN of fasted guinea pigs

	Averages and standard deviations*	
	Control	Irradiated
Weight loss, second 24-hr period, g	24.2 ± 6.31	42.8 ± 5.52
Liver glycogen (as glucose) (mg/g fresh weight)	0.89 ± 0.68	11.05 ± 5.88
Blood glucose (mg/100 ml)	129 ± 9.4	137 ± 8.8
Blood NPN (mg/100 ml)	44.8 ± 4.4	52.4 ± 4.7

*6 animals in each group.

Discussion

Mole[7] has recently suggested that glycogen deposition after irradiation is simply the result of increased conversion of protein to carbohydrate, for which the role of adrenal hormones is merely a permissive one; and that there is no evidence of stimulation of adrenal activity by radiation. On the basis of his experimental observations this latter conclusion seems shakily grounded; it would seem that he is justified in saying only that glycogen deposition in the fasted irradiated rat requires the presence of certain adrenocortical hormones, probably in minimal amounts, sufficient to maintain blood glucose levels above the threshold for glycogen synthesis. The question of adrenal stimulation may not even be relevant in connection with glycogen deposition.

Thus it is perhaps not surprising that fasted guinea pigs also can synthesize glycogen after irradiation, and it is still possible that the sensitivity of the guinea pig is due to its relatively poor capacity for adaptation to an unfavorable environment.

References

1. Thomson, J. F., and E. T. Mikuta. Effect of total body X-irradiation on the tryptophan peroxidase activity of rat liver. Proc. Soc. Exptl. Biol. Med. 85: 29-32 (1954).

2. Denson, J. R., E. J. Gray, J. L. Gray, F. J. Herbert, J. T. Tew, and H. Jensen. Effects of total body X-irradiation on some constituents of liver and kidney of the rat. Proc. Soc. Exptl. Biol. Med. 82: 707-711 (1953).

3. Nims, L. F., and E. Sutton. Adrenal cholesterol, liver glycogen and water consumption of fasting and X-irradiated rats. Am. J. Physiol. 177: 51-54 (1954).

4. Lourau, M. Modification, due á une irradiation générale par les rayons X, de l'utilisation du glycogéne du foie pendant le jeûne. Academie des Sciences Compt. rend. 236: 422-424 (1953).

5. Blatherwick, N. R., P. J. Bradshaw, M. E. Ewing, H. W. Larson, and S. D. Sawyer. The determination of tissue carbohydrates. J. Biol. Chem. 111: 537-547 (1935).

6. Nelson, N. Photometric adaptation of the Somogyi method for glucose. J. Biol. Chem. 153: 375-380 (1944).

7. Mole, R. H. Whole body irradiation and the idea of stress. Brit. J. Exptl. Path. 37: 528-530 (1956).

HISTOLOGICAL OBSERVATIONS ON THE SILVERING PROCESS IN THE CHAMPAGNE D'ARGENT RABBIT

Walter C. Quevedo, Jr.* and Herman B. Chase**

Abstract

In the Champagne d'Argent rabbit, the hair of the first growth cycle is fully pigmented. During the second hair cycle, the secondary guard hairs are generally unpigmented whereas the primary guard hairs and wool hairs are for the most part pigmented from tip to base. In older Champagne d'Argent rabbits the coat is lightened further and many of the primary guard hairs and wool hairs lack pigment. "Mosaic" or partially pigmented hairs have not been observed. Histologically, the progressive silvering involves a disappearance of mature melanocytes from the hair follicles with the consequent production of entirely unpigmented hairs. The unpigmented hair follicles of the Champagne d'Argent, unlike those of albinos, show no trace of "pigmentless" melanocytes or clear cells. Instead, the follicles are identical in appearance with the unpigmented follicles of white-spotted rabbits which have been demonstrated to lack clear cells. The pigmented Champagne d'Argent hair follicles contain apparently normal complements of mature melanocytes. "Mosaic" hair follicles containing reduced numbers of mature melanocytes have not been observed. Thus gene action during silvering in the Champagne d'Argent rabbit is postpartum, involves an "all or none" effect on the hair follicles, and occurs at different intervals in the life of the individual.

---

*Postdoctoral Resident Research Associate.

**Biology Department, Brown University, Providence, Rhode Island.
Work supported in part by grants-in-aid C-592 from U. S. Public Health Service and ENV-3 from American Cancer Society.

HYPERPIGMENTATION IN MICE

II. Influence of Ultraviolet Radiation and Further Observations on the Effect of Chronic X- and Gamma Radiation

Walter C. Quevedo, Jr.* and Douglas Grahn

Previously, it was reported that chronic exposure to X- and γ-radiation may cause a darkening of the extremities of pigmented mice.(1) This hyperpigmentation results from an increase in the amount of melanin pigment within the epidermis, apparently arising from an increase in the melanogenic activity of epidermal melanocytes.(1)

Preliminary observations indicate that hyperpigmentation may also be induced by exposure to ultraviolet (UV) radiation. The hind feet of C57BL mice were exposed at two day intervals to UV rays emitted by a commercially available G. E. Sunlamp (110-125V, 275W, 60 cycle, A.C.). Each exposure was made at a distance of approximately one foot from the source and lasted for 3 min. A darkening of the plantar surfaces of the hind feet was apparent by the 7th day and became quite definite by the 12th day. No hyperpigmentation was observed in the plantar surfaces of the forelimbs which had been shielded during the radiation process. Histologically, the hyperpigmented feet displayed a marked increase in the amount of melanin pigment within the epidermis. The distribution of pigment granules was quite similar to that found in cases of hyperpigmentation induced by X- or γ-radiation. Fitzpatrick et al.(2) have shown that when human skin is exposed to UV radiation the epidermal melanocytes are stimulated to begin the synthesis of melanin pigment. Presumably, UV radiation acts to oxidize sulfhydryl groups which normally inhibit the melanogenic activity of melanocytes.(3) The hyperpigmentation observed in the present study is also apparently due to an increased activity of epidermal melanocytes, although the mechanism for the activation of these cells remains to be elucidated.

It would appear that continued exposure to X- and γ-radiation is necessary for the persistence of hyperpigmentation in the extremities. As reported previously, C57BL mice X-irradiated with 200 r at weekly intervals exhibit darkening of the plantar surfaces of the feet 8-10 days from the beginning of the radiation exposure.(1) When X-irradiation was discontinued after 4 weekly exposures, it was found that the plantar surfaces gradually faded in color to a very pale grey by 4-6 weeks.** Weekly X-irradiation was then resumed and 8-10 days later definite hyperpigmentation was again observable in the irradiated feet. These results are in agreement with the concept of a radiation-sensitive inhibitor of melanogenesis(3) although no statement can be made as to its nature. Following

*Postdoctoral Resident Research Associate.

**Similar changes occur in chronically γ-irradiated mice when exposure is discontinued.

the termination of chronic irradiation the concentration of inhibitor might be expected to increase causing a reduction of melanogenic activity. Consequently, when chronic irradiation is terminated, the gradual loss of pigment-bearing epithelial cells through normal desquamation, coupled with the failure of melanocytes to elaborate the requisite number of pigment granules, would result in a slow depigmentation of the area.

At present, to determine the role that temperature may play in the hyperpigmentary process, both LAF_1 and C57BL mice maintained at either 26°C or 10°C are being exposed to UV radiation. In addition, it is planned to test several chemical sulfhydryl oxidants for ability to produce radiomimetic hyperpigmentation.

References

1. Quevedo, W. C. Jr., and D. Grahn. Hyperpigmentation in mice. Effect of chronic γ-irradiation. Quarterly Report of Biological and Medical Research Division, Argonne National Laboratory. ANL-5696, pp. 57-63 (1957).

2. Fitzpatrick, T. B., S. W. Becker, A. B. Lerner, and H. Montgomery. Tyrosinase in human skin: demonstration of its presence and its role in human melanin formation. Science 112: 223-225 (1950).

3. Flesch, P., and S. Rothman. Role of sulfhydryl compounds in pigmentation. Science 108: 505-506 (1948).

HYPERPIGMENTATION IN MICE

III. Effect of Chronic γ-irradiation on the Follicular Melanocytes of Mice

Walter C. Quevedo, Jr., and Douglas Grahn

When pigmented mice are chronically exposed to γ-radiation (6 r/day to 410 r/day the skin of the extremities becomes darkened.[1,2] Radiation-induced hyperpigmentation has been demonstrated to result from an increased epidermal melanization due to the enhanced melanogenic activity of melanocytes within the basal layer of the epidermis.[1-3]

Recent observations indicate that greying of the hair coat may occur in markedly hyperpigmented γ-irradiated mice (Figure 31). Greying is especially evident among the 43 r/day and 32 r/day LAF_1 mice by 4-5 months and in the 24 r/day mice by approximately 7 months of exposure. When hair growth cycles are repeatedly induced by periodic plucking of the body hairs[4] significant greying is observed in mice receiving the minimal dose of 6 r/day.

It would appear that radiation-induced greying results from the loss of mature melanocytes from the hair follicles.[4,5] Nonirradiated hair follicles contain numerous melanocytes in the upper hair bulb (Figure 32); however, partially greyed hair follicles contain reduced numbers of mature melanocytes and completely greyed hair follicles lack them entirely (Figure 33).

In chronically γ-irradiated mice, melanocytes within hair follicles apparently have a lower survival value than those situated in the basal layer of the epidermis. Since all melanocytes are thought to be derived from the embryonic neural crest,[6] the demonstration of enhanced activity of epidermal melanocytes and apparent destruction of follicular melanocytes under identical conditions of γ-radiation suggests an important influence of the cellular environment on melanocyte survival. This view is supported by evidence from acute radiation studies. Follicular melanocytes have been demonstrated to be destroyed by X- and γ-ray doses of 400 r.[5,7] Preliminary observations on LAF_1 mice have shown no evidence of a depigmentation of pigmented extremities at this dose of X- or γ-radiation.

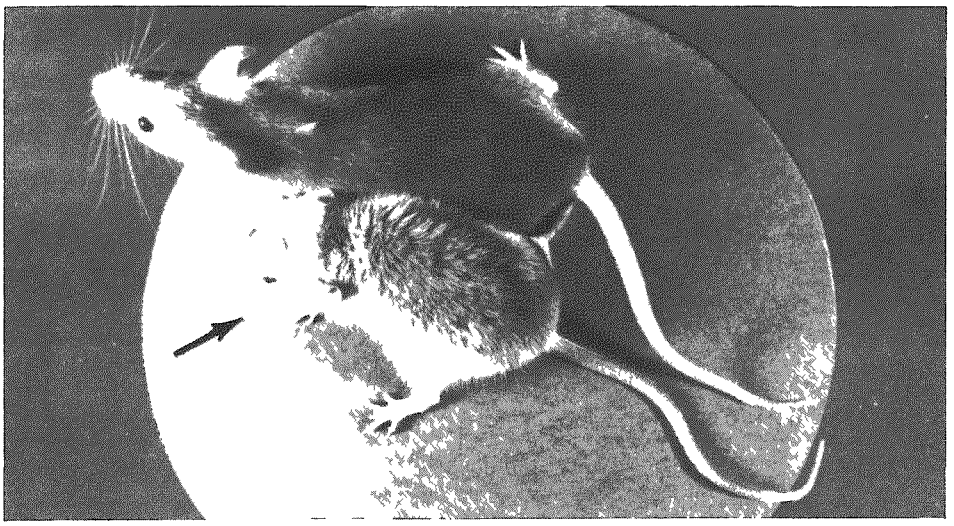

Figure 31

LAF_1 mouse (arrow) following 7 months exposure to 24 r/day of γ-radiation. A marked greying is evident in contrast to the darkly pigmented hair coat of the nonirradiated control.

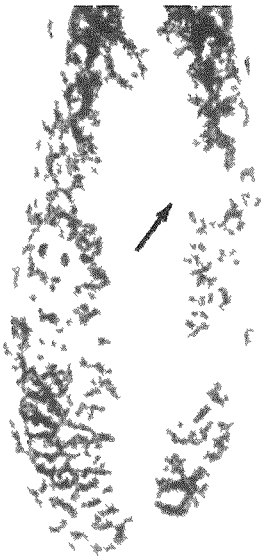

Figure 32

Hair follicle of a nonirradiated LAF_1 mouse. Several melanocytes (arrow) are evident in the upper hair bulb.

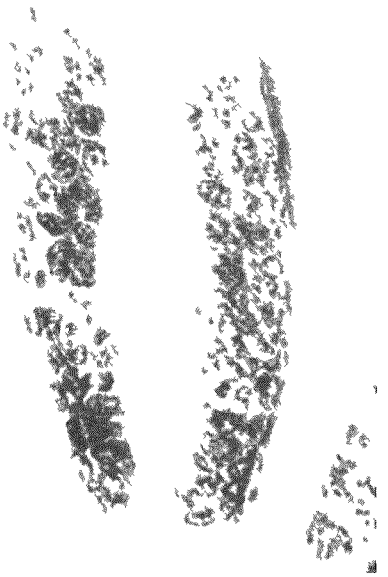

Figure 33

Hair follicle of a γ-irradiated LAF_1 mouse (24 r/day for 7 months). The border of the papilla cavity is uniform throughout with no trace of melanocytes in the upper hair bulb.

References

1. Quevedo, W. C., Jr., and D. Grahn. Hyperpigmentation in mice. I. Effect of chronic γ-irradiation. Quarterly Report of Biological and Medical Research Division, Argonne National Laboratory. ANL-5696, pp. 57-63 (1957).

2. Quevedo, W. C., Jr., and D. Grahn. Hyperpigmentation in mice. II. Influence of ultraviolet radiation and further observations on the effect of chronic X- and gamma-radiation. This report, p. 93.

3. Ellinger, F. The Biologic Fundamentals of Radiation Therapy. Elsevier Publishing Company, New York (1941).

4. Chase, H. B. Greying of hair. I. Effects produced by single doses of X-rays on mice. J. Morphol. 84: 57-80 (1949).

5. Chase, H. B., and H. Rauch. Greying of hair. II. Response of individual hairs in mice to variations in X-radiation. J. Morphol. 87: 381-391 (1950).

6. Rawles, M. E. Origin of melanophores and their role in development of color patterns in vertebrates. Physiol. Revs. 28: 383-408 (1948).

7. Moshman, J., and A. C. Upton. Depigmentation of hair as a biological radiation dosimeter. Science 119: 186-187 (1954).

RECOGNITION OF MODES OF DEATH IN THE ANALYSIS OF ACUTE RADIATION MORTALITY

S. Phyllis Stearner and Sylvanus A. Tyler

Many attempts have been made to discover and describe the mechanisms of radiation damage in a wide variety of biological materials. Because of the complexity of the chain of events activated by radiation and the absence of easily observable indicators of injury specific to each of the many systems involved, the establishment of a general theory of radiation effects compatible with even a small part of our empirical knowledge has yet to be realized. In order to effect some separation of the multiple factors that contribute to the acute radiation syndrome, two mechanistic approaches are available. The integral point of view considers the test organism as a unit. Then, under very general hypotheses a characterizing function is educed by inference from an analysis of the interrelationships, in time, between selected factors that are known to influence the physiological state of the organism. This approach requires a few assumptions and will yield models general enough to admit a variety of component processes.

An alternative is the differential approach. The organism is viewed as a network of systems or compartments and a description of the influence of each system on the radiation and result is attempted. Intra- and intercompartmental hypotheses are required. The difficulty inherent in this approach is its susceptibility to erroneous inferences and deductions incapable of experimental verification. Nevertheless, by this method it may be possible to obtain greater detailed knowledge of the individual processes involved.

Acute radiation damage in mammals is commonly expressed in terms of the 30-day mortality. This period provides a convenient end point, although it is generally recognized that multiple factors operate to produce the observed mortality. Many mechanisms are indistinct with overlapping times of occurrence, and even the most clearly described modes of acute radiation death cannot always be appraised in individual animals. Undoubtedly there are other mechanisms operating that as yet are unknown. The best described modes of death in this period are intestinal damage and hematopoietic failure. These have fairly characteristic syndromes and the mortality periods are sufficiently separated in time to be distinct in most cases. Two other modes of acute radiation death in mammals have been described recently by Quastler.[1,2] One mechanism may account for deaths occurring in the interval between intestinal and marrow deaths. Another, characterized by damage to the oral region, may produce deaths during the period of hematopoietic deaths. As yet, however, no early radiation effect has been found that could serve as a reliable indicator of injury at a more primary level.

The radiation response of the chicken is of special interest because in this animal there is a well-defined early indicator of radiation injury. This effect, manifest as mortality within 2 days after exposure at appropriate rates, is distinct both in time range of expression and in pathological nature. The daily death rate for the 12-day period following irradiation (Figure 34) showed a bimodal distribution, indicating that a separate mechanism is operating in the first 2 days. This mechanism is characterized by circulatory collapse and renal failure. The time distribution of fatal circulatory insufficiency, shown in Figure 35, corresponds almost completely with the first mortality peak so that time of death can be disregarded and the first mechanism considered not as "2-day deaths" but as "circulatory failure."

Preliminary mortality data are now available for approximately 2000 6-day chick embryos exposed to Co^{60} γ-rays at different doses and exposure times. The graph of daily mortality rate for all groups combined (Figure 36) appears to be bimodal and similar to the corresponding description for irradiated chicks. Although peak rates occur at 1 and 8 days, the high mortality rate observed on days 2-7 suggests that at least one additional factor is operating. To accomplish a finer partitioning, the pathology of the irradiated embryos after death was noted at gross autopsy and categorized according to the presence of all combinations of the following frequently appearing and readily discernible syndromes:

A. Circulatory failure
B. Generalized edema
C. Necrotic and hemorrhagic lesions of liver and kidneys

The observed frequencies are presented in Table 22. As a first approximation, it is assumed first that death of the organism results from a single syndrome although more than one may be manifest in a single individual, and second that these appear in combinations in the same proportion as they appear singly. Under these assumptions, Figure 37 illustrates the time distribution of the three syndromes appearing within 12 days after irradiation.

By means of such a method the acute radiation mortality in the chick embryo may be partitioned on the basis of pathology rather than time after exposure. This approach may yield a more detailed analysis of systems than has been possible so far. In mammals, identification of some early indicator of injury might make possible the correlation of early radiation injury with later effects. Some factor such as early weight loss or degree of lymphopenia might provide such an indicator. But perhaps the most useful indicators of early change will ultimately be provided by the biochemist. Early radiation effects in mammals probably differ from those in chickens only in that the chain of events initiated by exposure to ionizing radiations leads to some event critical for survival in the chicken and not in most

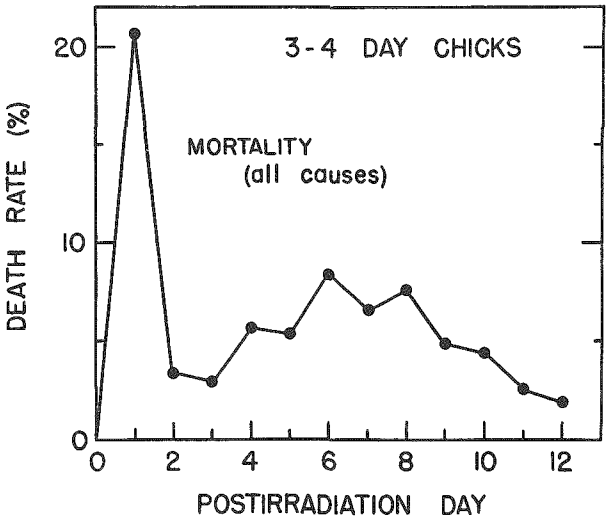

Figure 34

Daily death rate of 2500 chicks exposed to Co^{60} γ-rays (all time-dose groups combined).

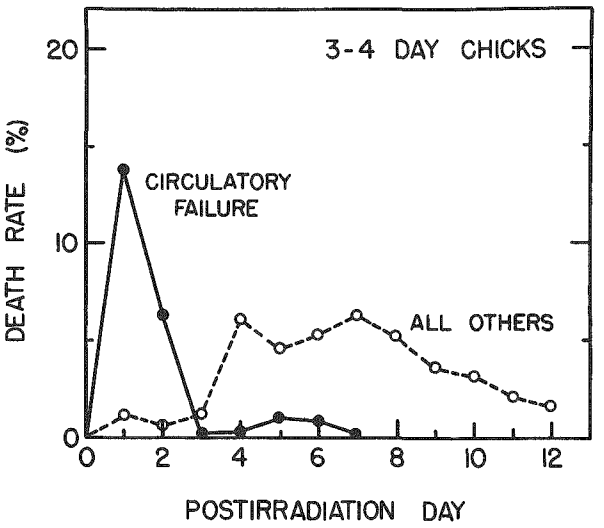

Figure 35

Time distribution of circulatory failure and of all other modes of death in the 3-4 day chick following Co^{60} γ-irradiation.

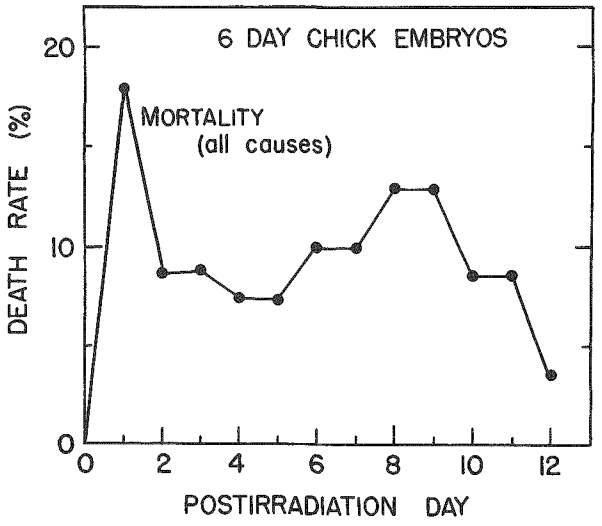

Figure 36

Daily death rate of 2000 6-day chick embryos exposed to Co^{60} γ-rays (all time-dose groups combined).

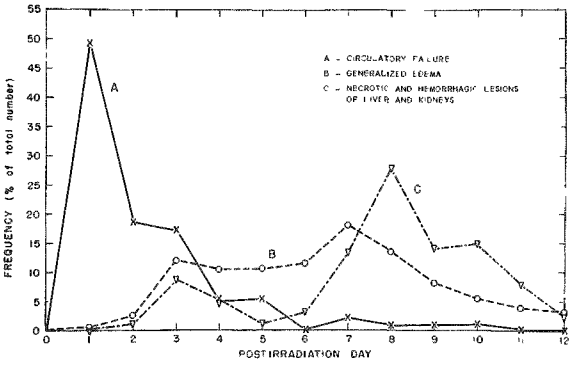

Figure 37

Frequency distribution of 3 major syndromes observed in the 12-day period following γ-irradiation of 6-day chick embryos, as per cent of total number showing each syndrome.

TABLE 22

Observed frequencies of 3 major syndromes in irradiated chick embryos

Syndrome*	Postirradiation day											
	1	2	3	4	5	6	7	8	9	10	11	12
A	381	82	57	16	24	0	10	4	4	4	1	0
B	2	7	26	24	26	16	43	29	20	11	10	13
C	0	3	13	7	2	2	15	24	15	14	10	4
A,B	3	33	62	17	22	8	8	7	3	6	2	1
A,C	1	21	13	8	1	1	3	17	7	6	3	1
B,C	0	1	13	13	13	27	39	47	22	23	12	4
A,B,C	0	14	35	21	13	15	27	21	14	10	3	0

*A = Circulatory failure (severe hemorrhages and/or venous pooling).
B = Generalized edema (usually severe).
C = Necrotic and/or hemorrhagic lesions of liver and kidneys.

mammals. Many similarities in the early response have been observed. For example, there are early circulatory changes following irradiation which resemble the circulatory insufficiency seen in chickens, but the effect is usually not severe enough to result in death.

Better understanding of the multiple factors involved in the acute radiation response would make possible a more rational approach in the determination of relative effectiveness of various qualities of ionizing radiations. Comparisons could then be based on a specific effect rather than the total response involved in the 30-day mortality.

References

1. Austin, M. K., M. Miller, and H. Quastler. Five to 8 day radiation death in mice. Radiation Research 5:303-307 (1956).

2. Quastler, H., M. K. Austin and M. Miller. Oral radiation death. Radiation Research 5:338-353 (1956).

DEMONSTRATION OF A BORON REQUIREMENT BY CHLORELLA*

Wayne J. McIlrath and John Skok

Boron is normally added to the medium for culturing algae although relatively few workers have demonstrated a need for this element. Eyster[1] reported a boron requirement by Nostoc, and Henkel[2] reported this requirement for optimal growth of Bangia and Porphyra; while Herzinger[3] indicated that 10 p.p.m. boron was optimal for the growth of Chlorella and Chlorococcum, Gerretson and de Hoop[4] failed to observe a favorable influence of boron on Chlorella and found that 10 p.p.m. markedly reduced growth.

Experiments were undertaken to determine whether a boron requirement could be demonstrated for Chlorella. Cells from a bacteria-free, plus-boron culture of Chlorella vulgaris Beijerinck (Columbia strain) obtained from Dr. Lawrence Bogorad were used. They were prepared by washing three times by centrifugation and resuspending in minus-boron nutrient solutions to remove traces of boron contained in the original culture media. An aliquot of the washed and resuspended cells was inoculated into 100 ml of sterile boron-free medium contained in a 250-ml Corning alkali-resistant (boron-free) glass Erlenmeyer flask. After one week this preparation was subcultured, and after an additional week the resulting culture was subcultured. Each subculture inoculum consisted of a 0.5-ml aliquot transferred into 100 ml of nutrient solution. The last culture was maintained for four weeks to permit the boron content of the cells to reach a low level. At the end of this period solutions with five levels of boron (minus-boron grown in boron-free glass vessels; minus-boron maintained in Pyrex flasks; and 0.5, 1.0 and 5.0 p.p.m. boron) were prepared and inoculated. All cultures were grown on a shaker at 750° F and under constant light conditions (16-hr photoperiod at approximately 1500 foot-candles). After a 24-day growth period, cell counts and total dry weights were determined on all cultures.

It appeared that boron is essential for normal and optimal growth of Chlorella. The cultures grown in a medium containing no boron but maintained in Pyrex flasks exhibited a greater concentration of cells than those grown in vessel of boron-free glass, suggesting a leaching of boron from Pyrex glass. The cultures receiving 0.5 p.p.m. boron made greatest growth;

---

*This work was aided in part by a grant from the Dr. Wallace C. and Clara A. Abbott Memorial Fund of the University of Chicago. It was completed while Dr. McIlrath was a Resident Research Associate at Argonne National Laboratory.

they produced a 60% increase in cell number, and a 137% increase in dry weight per cell, over the cultures grown in boron-free flasks receiving no boron. The 1 and 5 p.p.m. boron cultures made more growth than the minus-boron ones but less than that produced by the addition of only 0.5 p.p.m. boron.

References

1. Eyster, C. Necessity of boron for Nostoc muscorum. Nature 170:755 (1952).

2. Henkel, R. Ernährungsphysiologishe Untersuchungen an Meeresalgen, insbesondere an Bangia pumila. Kieler Meeresforchungen 8:192-211 (1951).

3. Herzinger, F. Beiträge zum Wirkungskreislauf des Bors. Bodenk. Pflanzenernähr. 16:141-168 (1940).

4. Gerretsen, F. C., and H. de Hoop. Boron, an essential micro-nutrient for Azotobacter chlorococcum. Plant and Soil 5:349-367 (1954).

PHOTOPERIODISM STUDIES: FACTORS INFLUENCING THE FLOWERING RESPONSE TO NIGHT INTERRUPTIONS IN XANTHIUM

William Chorney

Xanthium is a photoperiodic plant whose flowering is controlled primarily by the length of the dark period. Plants grown on relatively long light periods normally remain vegetative, but when placed on a photoinductive cycle that includes a dark period of 9 hr or more, they will promptly initiate floral primordia.

Hamner and Bonner[1] reported in 1938 that a night interruption of 1 min with 150 foot-candles of light given in the middle of a 9-hr dark period prevented floral initiation in intact Xanthium plants. They also reported that a 30-min light interruption near the middle of a 15-hr dark period did not prevent floral initiation in intact plants. Parker et al.[2] reported that brief periods of weak light given in the middle of 12-hr dark periods prevented floral initiation in single-leaf Xanthium plants.

Recently, in the course of attempts to induce flowering in Xanthium by infiltration of various materials, it was noted that interrupting a 16-hr dark period with a 15-min light period (1500 foot-candles, in the middle of the dark period) did not prevent floral initiations in intact Xanthium plants.

In order to test further the hypothesis that night interruption prevents floral initiation in Xanthium, experiments were designed using intact and single-leaf plants subjected to two different night periods, and also using two different light intensities for the night interruptions.

Experimental Procedure

Xanthium plants were grown in the greenhouse under an 18-hr daylight schedule. Before use, a number of the plants of the group were dissected to ascertain that they were in the vegetative condition.

Experiment 1. Plants of uniform size were selected and transferred to a controlled environment room where they were given the following treatment: 8 hr of light, followed by 8 hr of darkness, followed by 15 min of light (1500 foot-candles), followed by 7.75 hr of darkness. Nine lots of 10 plants each were exposed to this cycle for 1, 2, 3, 4, 5, 7, 10, 14, or 21 times respectively. After the last cycle, each lot was returned to the original 18-hr schedule in the greenhouse, where the plants remained until they were dissected 21 days after the first night interruption.

Experiment 2. This experiment was conducted in the greenhouse using photoperiod chambers for the night interruptions. Night periods of 12 hr and 16 hr were interrupted in the middle for 15 min with light from incandescent filament lamps providing intensities of about 40 foot-candles at the leaf surface. Both intact and single-leaf plants were used. Table 23 shows the number of night interruptions to which plants were subjected.

TABLE 23

Effect of night interruption of flowering of Xanthium

No. of night interruptions	16-hr night				12-hr night			
	Intact plants		Single-leaf plants		Intact plants		Single-leaf plants	
	V*	F*	V	F	V	F	V	F
1	0	5	5	0	5	0	5	0
3	0	5	4	1	0	5	5	0
5	0	5	5	0	0	5	5	0
7	0	5	4	1	0	5	3	2
14	0	5	0	5	0	5	0	5
21	0	5	0	5	0	5	0	5

*V, vegetative; F, flowering.

Results

All the plants in Experiment 1 flowered except those that received only a single night interruption. The results of Experiment 2 are shown in Table 23.

A 15-min light period using 40 foot-candles of incandescent light in the middle of a 16-hr dark period will not prevent floral initiation in intact Xanthium plants. In single-leaf plants on a 16-hr night period, floral initiation can be prevented by 7 consecutive night interruptions. However, new leaves had emerged and developed after 7 days, and, since these were not removed on emergence, the plants were no longer single-leaf plants, but behaved like intact plants.

In intact plants on a 12-hr night period, a single night interruption was effective in preventing floral initiation, but repeated night interruptions were ineffective. For single-leaf plants on a 12-hr night period, the interruptions were effective for 7 cycles, as in the 16-hr plants.

Discussion

The results substantiate the findings of Hamner and Bonner[1] and Parker,[2] and clarify the hypothesis of prevention of floral initiation in Xanthium by interruption of the dark period. The critical night length for Xanthium is 9 hr.[1] It appears that if the night period is near the critical duration for flowering in Xanthium, a short light interruption in the middle of night will prevent flowering. Flowering can also be prevented on single-leaf Xanthium plants by interruption of night periods even when these are for longer than the critical period. However, night interruptions are not effective in preventing floral initiation in intact plants when the night period exceeds the critical period by a few hours.

References

1. Hamner, K. C., and J. Bonner. Photoperiodism in relation to hormones as factors in floral initiation and development. Botan. Gaz. 100: 388-431 (1938).

2. Parker, M. W., S. P. Hendricks, H. A. Borthwick, and N. J. Scully. Action spectrum for the photoperiodic control of floral initiation of short day plants. Botan. Gaz. 108: 1-26 (1946).

PROGRESS REPORT: THE GIBBERELLINS

II. The Effect of Gibberellic Acid and Photoperiod on Indoleacetic Acid Oxidase in Lupinus albus L.

Robert E. Stutz and Ronald Watanabe

Increases in length of plant stems produced by the gibberellins, and similar promotive effects of long photoperiods, have been reported for many plant species.[1,2,3] The exact mechanism for these growth responses is not known. It has been speculated that the enhancement of growth may be associated with indoleacetic acid (IAA). An attempt to correlate the IAA oxidase in Lupinus albus L. with photoperiod has been previously reported.[4] It was thought to be of interest to investigate a possible interaction between gibberellin, photoperiod, and IAA oxidase in lupines.

Two lots of 60 plants each of Lupinus albus L. seedlings were grown under 8-hr and 16-hr photoperiods, respectively. When the plants were 30 days old, one-half of each lot was given 5 μg of gibberellic acid per plant by application to the terminal bud. The treatment was continued at intervals of 2-3 days until a total of 50 μg had been applied. Ten days after the final treatment, all the plants were harvested and measured individually for main axis length and for node number. They were then sectioned into stems, hypocotyls, buds and leaves; like tissues for each treatment were combined and frozen. Crude enzyme preparation was prepared from each tissue lot by the method reported previously.[5]

Table 24 shows a typical response of the main axis to photoperiod and gibberellic acid treatments. Plants treated with gibberellic acid had a significant increase in growth of the main axis and in the number of nodes under both photoperiods. The longer photoperiod increased the growth of the main axis but did not affect the rate of organ differentiation. Since it seems evident that gibberellic acid and long photoperiod act synergistically on stem elongation, it is possible that the two factors do not compete for the same growth centers but influence growth by independent pathways.

The effect of gibberellic acid and photoperiod on IAA oxidase is shown in Table 25. Increasing the length of the photoperiod had no effect on the total O_2 consumption, but it increased the time lag for activation of crude enzyme preparations in stems and decreased it in buds. Similar results were reported previously.[4] The significance of these differences is not apparent. The effect of gibberellic acid on the IAA-oxidase preparations from buds was very striking. This reduction in O_2 uptake produced by gibberellic acid suggests either a lower enzyme level or an increased concentration of inhibitor. In either case the physiological level of IAA would be shifted toward a higher concentration.

TABLE 24

Effect of photoperiod and gibberellic acid on growth of Lupinus albus L. Each datum represents the average from 28-30 plants 71 days after planting and 41 days after initial treatment.

	Photoperiod 8 hr		Photoperiod 16 hr	
	Control	Gibberellin-treated	Control	Gibberellin-treated
Growth of stem (cm)**	11.8 ± 0.5	21.2 ± 0.6*	22.9 ± 1.0	30.7 ± 1.2*
Number of nodes	13.9 ± 0.2	17.1 ± 0.4*	14.7 ± 0.4	17.6 ± 0.5*

*Significant difference between treated and control at the 1% level.
**Significant difference between photoperiod treatment: growth of stem: 8-hr treated versus 16-hr treated, at 1% level; 8-hr control versus 16-hr control, at 1% level.

TABLE 25

Effect of gibberellic acid and photoperiod on idoleacetic acid oxidase in Lupinus albus L.

Tissue	Gibberellin, total 50 μg	Total O_2 uptake, μl			
		Photoperiod 8 hr		Photoperiod 16 hr	
		Expt. 1* 300 min	Expt. 2 310 min	Expt. 1 320 min	Expt. 2 310 min
Buds	Control	333 (150)**	367 (100)	421 (70)	394 (40)
	Treated	46	39	42	37
Leaves	Control	17		24	
	Treated	28		28	
Stems	Control	301 (30)	398 (20)	258 (170)	281 (100)
	Treated	-	412 (40)	275 (170)	153 (120)
Hypocotyl	Control	0		0	
	Treated	7		5	

*Experiments were run for periods of 300-320 minutes in order to demonstrate activity of the tissues having different lag periods as affected by photoperiod (see text).
**Values in parentheses represent time lag (min) in O_2 uptake.

The results of these experiments suggest that gibberellic acid exerts its influence in stem elongation indirectly by lowering the IAA-oxidase activity. The effect of the long photoperiod on growth is apparently not mediated by an IAA system but by still another (unknown) pathway. Further experiments are contemplated to confirm these results.

References

1. Marth, P. C., W. V. Audia, and J. W. Mitchell. Effect of gibberellic acid on growth and development of various species of plants. Plant Physiol. (Suppl.) 31:43 (1956).

2. Skok, J., and N. J. Scully. Nature of the photoperiodic responses of buckwheat. Botan. Gaz. 117: 134-141 (1955).

3. Arthur, J. M. Some effects of radiant energy on plants. Boyce Thompson Inst. Plant Research, Professional Paper 12, (April, 1926).

4. Stutz, R. E. Indoleacetic acid oxidase and photoperiod. Quarterly Report of Biological and Medical Research Division, Argonne National Laboratory. ANL-5486, pp. 59-60 (1955).

5. Stutz, R. E. Indoleacetic acid oxidase. Quarterly Report of Biological and Medical Research Division, Argonne National Laboratory. ANL-5426, pp. 48-59 (1955).

110

NEUTRON SPECTRUM WITHIN THE BIOLOGICAL RADIATION CHAMBER AT CP-5

Howard H. Vogel, Jr., Donn L. Jordan, G. Kohler,*
Eugene Tochilin,* and Bruce W. Shumway*

This study was undertaken as a collaborative project between the Neutron Radiobiology group at Argonne and the Nuclear Radiation Branch of U. S. Naval Radiological Defense Laboratory. Its purpose is to determine the spectrum of neutrons at the animal exposure position within the gamma-neutron radiation chamber[1] at Argonne's research reactor, CP-5.

Ilford, type C-2, 200-micron nuclear track plates were exposed to the neutron field within the biological facility at CP-5. The reactor was operating at approximately 1000 kw, but its power level has since been increased to 2000 kw. After development of the plates by standard procedures,[2] the lengths of proton tracks in the emulsion were measured according to a method in which the track plate is used both as radiator and detector.[3] The number of neutrons in four overlapping energy regions was determined in order to obtain accurate estimates of flux in regions of low neutron population. The results were adjusted to bring overlapping flux values into agreement, so that smooth curves could be drawn. The spectrum is illustrated in Figure 38; each mean flux ± its standard error is given.

The spectrum reaches its maximum value at about 0.5 Mev and falls to 10% of this peak value by 2 Mev. Beyond 3 Mev the slope of the curve is similar to that obtained by Watt for thermal fission neutrons from U^{235}.[4] In this figure, because of the limitations of the method, there are no experimental values for the neutron flux below 0.4 Mev.

A similar spectrum, also obtained by counting tracks in photographic emulsions, is illustrated for comparison in Figure 39. This exposure was made several years ago when the radiation chamber was in front of the thermal column of the CP-3' reactor.**

---

*U. S. Naval Radiological Defense Laboratory, San Francisco.

**Counts were made by P. Gustafson of this Division.

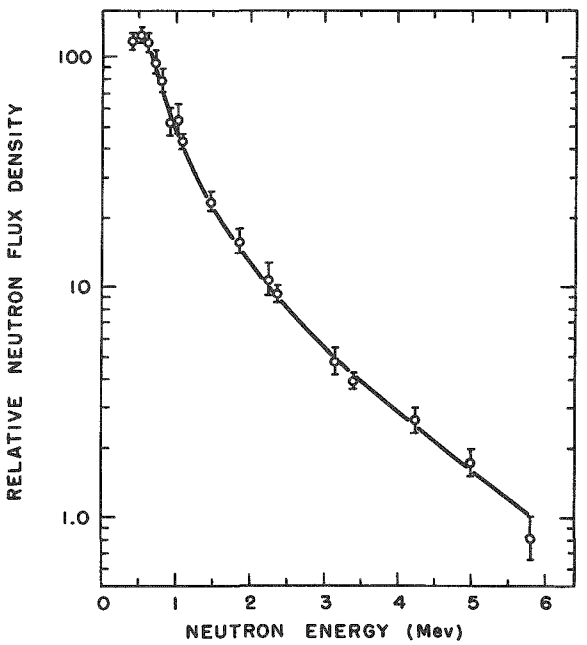

Figure 38

Neutron fission spectrum within the biological exposure facility at the Argonne CP-5 Reactor.

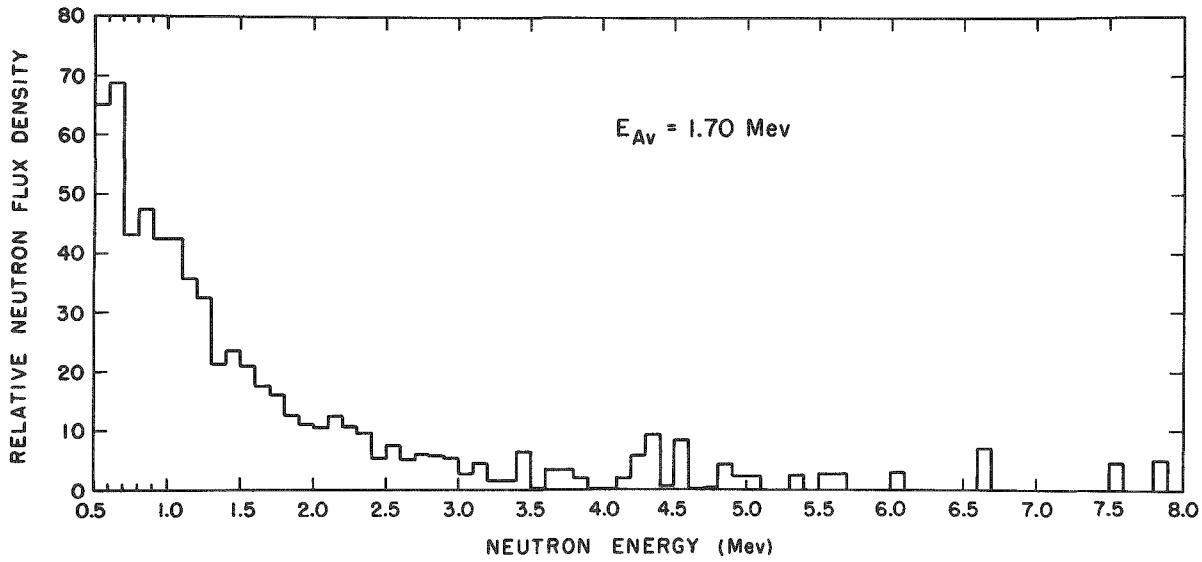

Figure 39. Similar neutron spectrum taken in the exposure facility at the former CP-3' Reactor.

Further work has been started to investigate the neutron spectrum at lower energies and to perform measurements of the LET (linear energy transfer) distribution. Harald Rossi and Walter Rosenzweig of the Radiation Research Laboratory at Columbia University are attempting such a study using a Rossi spherical tissue-equivalent chamber and a 256-channel analyzer at CP-5. This work should be of considerable interest for there is some evidence that the RBE of neutrons exhibit a maximum at some neutron energy as yet undetermined, which decreases again as the energy is lowered.

References

1. Vogel, H. H., Jr., R. Blomgren, and N. Bohlin. The gamma-neutron radiation chamber for radiobiological studies. Nucleonics 11:(3) 28-31 (1953).

2. Allred, J., and A. Armstrong. Laboratory Handbook of Nuclear Microscopy. LASL-1510 (1953).

3. Rosen, L. Nuclear emulsion techniques for the measurement of neutron energy spectra. Nucleonics 11: 32-38 and 38-44 (1953).

4. Watt, B. E. Energy spectrum of neutrons from thermal fission of U^{235}. Phys. Rev. 87: 1037-1041 (1952).

THE EFFECT OF SINGLE AND SPACED MULTIPLE DOSES OF Co^{60} GAMMA AND FISSION NEUTRON RADIATION ON THE INCORPORATION OF Fe^{59} INTO THE RAT ERYTHROPOIETIC SYSTEM

Howard H. Vogel, Jr., John W. Clark, Donn L. Jordan, Howard Alt,* John Cooper,* and Walter Rambach*

Sprague-Dawley female rats (average weight 170-180 g) were exposed either to fission neutrons or to Co^{60} γ-rays in the gamma-neutron radiation chamber[1] at the CP-5 research reactor. Irradiation cages (Figure 40) were designed and constructed so that 9 animals, exposed simultaneously, would be in one isodose group. The circular cage, constructed of Lucite, contained ten internal compartments, one for a Victoreen dosimeter and 9 for rats. The animals were loaded into the cage singly, through an opening in the top (toward the viewer in the illustration). After the animals were in position, the plastic top was fastened securely to the circular cage and the entire structure was then inserted into the square aluminum cage-holder (16 x 16 x 2 inches). In the upper left hand corner of the cage-holder can be seen a portion of a small motor which was connected by a rack-and-pinion device to the circumference of the cage. During irradiation the cage was thereby slowly rotated (1 rpm) through the field. The sensitive volume of the Victoreen thimble-chamber was held in the same standard position for all exposures, approximating the mid-body region of the rats. The animal compartments were designed to hold rats weighing up to 250 g. The animals shown in Figure 40 weighed only 100-150 g, and could turn around easily. When loaded for an exposure, the heads of all animals were placed toward the center of the cage.

Results and Discussion

Single acute exposures. Following irradiation the rats were transported to Northwestern Medical School, where they were injected intracardially with Fe^{59}, 24 hr after exposure. Six-hour Fe^{59} uptake studies were then carried out on the bone marrow of both irradiated and control rats, as a part of a hematological study of the effects of the two ionizing radiations.

The irradiation data and the Fe^{59} uptake by rat bone marrow are presented in Tables 26 and 27 and are illustrated graphically in Figures 41 and 42. It is clear from these graphs that (a) there is a linear relationship

*Departments of Medicine and Biochemistry, Northwestern University Medical School.

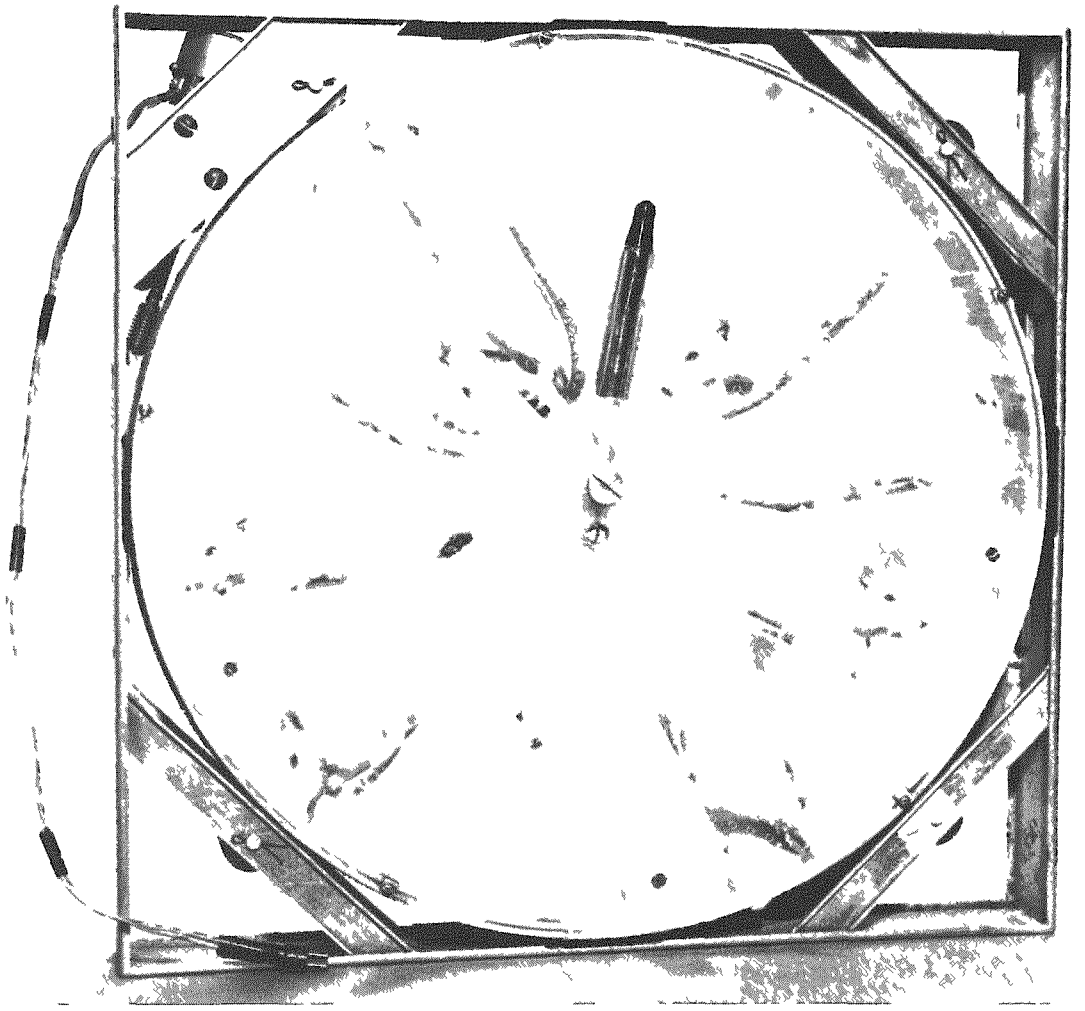

Figure 40. Rat irradiation cage.

between the total dose (at least up to 150 rads) and Fe^{59} uptake by the bone marrow, when these two are plotted on semi-log paper; (b) the RBE (γ/n) for this biological effect is probably 1.0; (c) a single exposure of 40 rads produces a significant depression on Fe^{59} uptake by the rat bone marrow; (d) a minimum absolute value (5-7%) for Fe^{59} uptake is obtained after a single dose of either γ-rays or fission neutrons exceeding 125 rads.

Chronic exposures. Five groups of rats were exposed once each week to Co^{60} γ-rays with dosages of 16 r weekly for 5 weeks, 16 r weekly for 10 weeks, 32 r weekly for 5 weeks, 32 r weekly for 10 weeks, or 150 r weekly for 5 weeks, respectively. Three similar groups were irradiated with fission neutrons at single dosages of 27 rads weekly for 5 and 10 weeks and 81 rads weekly for 5 weeks.

TABLE 26

Effect of single doses of Co^{60} γ-irradiation on Fe^{59} uptake by bone marrow

Date of irradiation	Dose rate, r/min	Time of exposure, min	Total dose		Fe^{59} uptake by bone marrow (av. absolute values), %	Fe^{59} uptake by bone marrow, % of controls
			r	rads*		
9/29/55	17.36	8.28	144	140	6.54	31.1
10/6/55	17.30	4.08	71	69	14.19	82.1
10/19/55	17.21	5.5	95	92	13.40	62.0
10/26/55	17.15	3.0	51	49	16.55	77.1
10/27/55	17.14	8.6	147	143	6.75	29.7
11/16/55	17.02	2.3	39	38	19.63	85.2
11/17/55	17.02	5.53	94	91	11.74	51.3
11/1/56	14.75	22.0	325	315	5.17	36.2

*For a conversion factor from roentgens to rads we have used a figure of 0.97, calculated by John S. Laughlin, Division of Biophysics, Memorial Center for Cancer and Allied Diseases. This absorbed dose (rads per roentgen) was calculated for Co^{60} γ-rays using a "whole mouse" of the following chemical composition: O - 69.8%, H - 9.8%, C - 13.9%, N - 4.4%, Ca - 0.75%, P - 1.3%, K - 0.3%, S - 0.2%.

TABLE 27

Effect of single doses of fission neutrons on Fe^{59} uptake by bone marrow

Date of irradiation	Pile power, kw	Total rads/ min	Time of exposure, min	Victoreen reading, η units	Total dose, rads*	Fe^{59} uptake by bone marrow (av. absolute values), %	Fe^{59} uptake by bone marrow, % of controls
11/30/55	1000	3-3.5	17	20.5	55.8	16.08	77.8
12/1/55	1000		26	33.0	86.5	10.69	45.9
12/8/55	1000		20	23.8	65.5	13.11	68.0
1/4/56	1000		39	42.0	115.3	5.78	28.4
1/5/56	1000		14	15.8	41.3	21.99	90.6
2/16/56	1000		14	25.5	65.8	10.8	47.5
2/23/56	1000		10	15.7	40.5	18.6	86.5
4/5/56	1000		37.5	62.8	163	7.22	34.0
10/25/56	1800	7	40	110	283.8	5.46	14.89

*A conversion factor of 2.62 (lithium geometry, first 5 neutron exposures) or 2.58 (boral geometry, all neutron exposures since 1/11/56) was used to convert readings on Victoreen dosimeters to total rads. This factor was obtained by calibrating at CP-5 a standard 25 Victoreen chamber with a Rossi-Failla tissue equivalent chamber. The total dose in rads, as listed in Table 27 for neutrons, includes the γ-ray contamination, which is estimated at 10-15% of the physical dose.

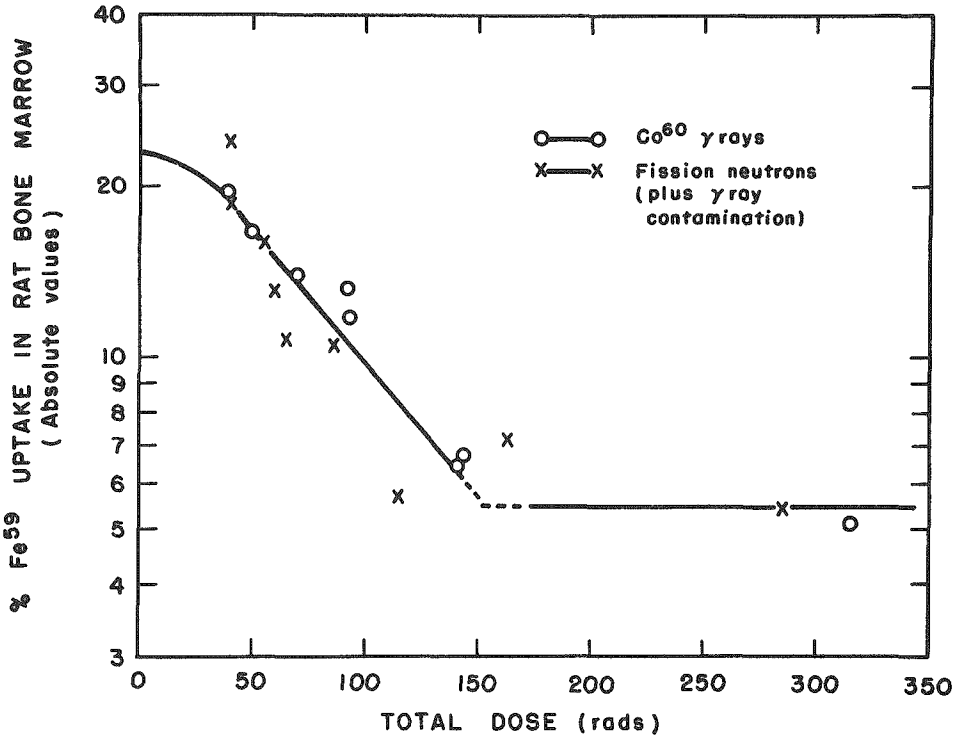

Figure 41. The relationship between total single doses of either fission neutrons or Co^{60} γ-rays and the absolute values (%) of 6-hr Fe^{59} uptake by the rat bone marrow.

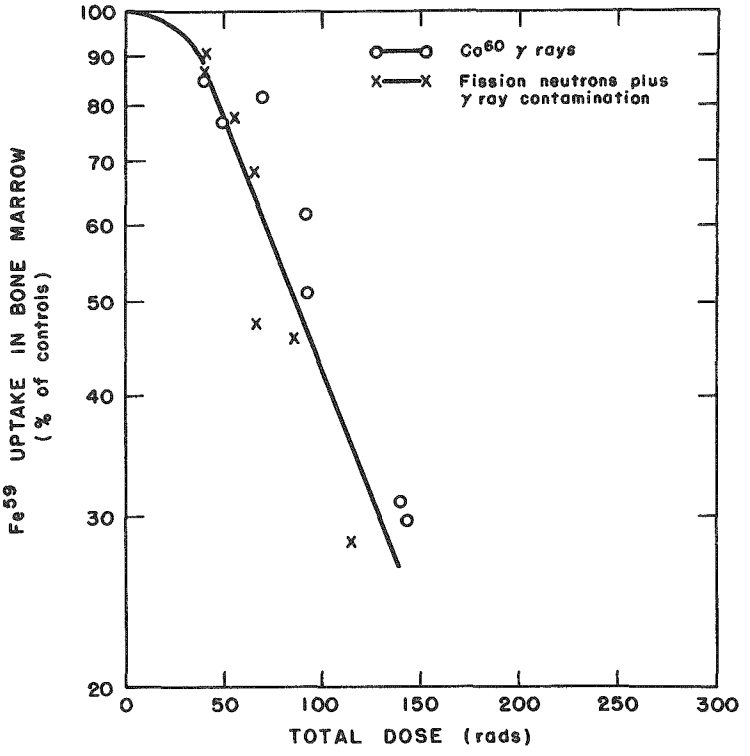

Figure 42. The relationship between total dose and Fe^{59} uptake by rat bone marrow, calculated as % of controls.

Following the last irradiation the rats were retained in cages for 10 or 11 days before injection in order to eliminate the acute effect of the single dose. They were then injected with Fe^{59} and 6-hr uptake studies were undertaken. The results are summarized in Tables 28 and 29.

TABLE 28

Uptake of Fe^{59} by rat cells after repeated weekly doses of γ-radiation

Group	Number of animals	Mean 6-hr Fe^{59} uptake (% injected dose Fe^{59}) and S.E.				
		Plasma	Red blood cells	Bone marrow	Spleen	Liver
16 r γ, 5 weeks						
Control	8	5.85 ± .98	4.70 ± 1.72	21.82 ± 2.58	1.66 ± 0.73	13.15 ± 2.14
Irradiated	8	5.80 ± 2.48	5.01 ± 1.48	23.38 ± 2.70	1.70 ± 0.41	13.77 ± 2.78
P		<0.50	<0.50	<0.95	<0.50	<0.50
16 r γ, 10 weeks						
Control	5	4.74 ± 3.90	9.45 ± 2.25	27.71 ± 4.09	3.64 ± 1.40	9.56 ± 1.19
Irradiated	9	2.81 ± 1.13	12.15 ± 2.47	27.33 ± 3.94	3.50 ± 0.74	9.27 ± 1.54
P		<0.80	<0.90	< .50	<0.50	<0.50
32 r γ, 5 weeks						
Control	8	3.83 ± 1.76	6.46 ± 2.89	29.78 ± 4.91	2.51 ± 1.05	10.55 ± 2.87
Irradiated	9	4.46 ± 1.59	7.90 ± 4.28	28.94 ± 3.82	2.27 ± 1.46	12.93 ± 1.52
P		<0.60	<0.60	<0.50	<0.50	<0.98
32 r γ, 10 weeks						
Control	9	7.68 ± 2.66	4.65 ± 2.55	24.57 ± 6.17	1.41 ± 0.64	9.77 ± 4.04
Irradiated	8	8.90 ± 2.26	2.83 ± 1.57	19.09 ± 6.78	1.19 ± 0.57	9.19 ± 3.18
P		<0.70	<0.90	<0.90	<0.60	<0.50
150 r γ, 5 weeks						
Control	9	6.32 ± 1.14	2.16 ± 0.61	12.93 ± 2.07	1.38 ± 0.21	41.22 ± 7.05
Irradiated	9	5.75 ± 0.84	3.30 ± 1.65	11.11 ± 2.47	2.06 ± 0.53	39.65 ± 8.96
P		<0.80	<0.95	<0.90	>0.99	<0.50

115

TABLE 29

Fe^{59} uptake by rat bone marrow after repeated weekly doses of fission neutrons

Group	Number of animals	Mean 6-hr Fe^{59} uptake (% injected dose Fe^{59}) and S.E.				
		Plasma	Red blood cells	Cells	Spleen	Liver
27 rads, 5 weeks						
Control	9	3.96 ± 2.30	8.09 ± 2.55	27.21 ± 3.52	2.78 ± 1.16	11.91 ± 2.29
Irradiated	9	4.39 ± 1.06	10.24 ± 3.62	26.74 ± 3.73	3.33 ± 1.05	14.50 ± 1.69
P		<0.50	<0.90	<0.50	<0.70	>0.99
27 rads, 10 weeks						
Control	5	8.05 ± 0.92	4.02 ± 1.08	23.42 ± 3.14	0.78 ± 0.13	13.85 ± 2.04
Irradiated	9*	6.22 ± 1.29	3.67 ± 1.46	24.41 ± 2.39	0.89 ± 0.33	13.95 ± 1.31
P		>0.99	<0.50	<0.50	<0.60	<0.50
81 rads, 5 weeks						
Control	9	6.58 ± 0.774	1.16 ± 0.641	12.02 ± 1.159	1.37 ± 0.327	39.69 ± 2.70
Irradiated	9	6.08 ± 0.967	6.16 ± 2.07	11.70 ± 1.463	3.08 ± 0.588	38.53 ± 3.43
P		<0.70	>0.99	<0.50	>0.99	<0.60

*Only 8 animals used for marrow and liver determinations.

With 6-hr Fe^{59} uptake by the bone marrow as a criterion, there were no significant differences between the irradiated rats and their controls. These data show clearly that the erythropoietic system of the rat is able to recover rapidly from repeated doses of Co^{60} γ-rays or fission neutrons within the dose range covered in these studies.

Complete hematological studies, including hemoglobin, red and white blood cell counts, differentials, cell pack, reticulocytes, platelets, and marrow counts, were also carried out on all irradiated and control rats. These will be summarized in later reports.

Reference

1. Vogel, H. H., Jr., R. Blomgren, and N. Bohlin. The gamma-neutron radiation chamber for radiobiological studies. Nucleonics 11:(3) 28-31 (1953).

CHRONIC RADIATION MORTALITY IN MICE FOLLOWING SINGLE WHOLE-BODY EXPOSURE TO 250, 135, AND 80 KVP X-RAYS

Douglas Grahn and George A. Sacher

The comparative effectiveness of several X-ray qualities has been established for the acute lethal response of mice.[1] RBE values, relative to 250-kvp X-rays and derived from the 30-day LD_{50} doses, were given as 1:.96:.78 for 250-kvp, 135-kvp, and 80-kvp X-rays, respectively. The survivors of fractionally lethal doses have been kept for the duration of life to compare the effectiveness of the three radiation qualities in terms of chronic radiation injury and mortality.

Male and female BA F_1 mice approximately 100 days of age were exposed to single whole-body doses of 250-, 135-, or 80-kvp X-rays. Dose ranges were 570-690 r at 250 kvp, 600-750 r at 135 kvp, and 725-875 r at 80 kvp. These doses produced an acute response that ranged from about 10% to 90% mortality in the first 30 days postirradiation. Details of the method of exposure and the X-ray characteristics were given in the previous report.[1]

Animals were autopsied when found dead, though some were sacrificed in an extreme moribund condition. Severely autolyzed and partially cannibalized mice were discarded and have been removed from any analyses relating to specific lesions observed at death. Tissue samples were taken from mice suspected of having a tumor or of any lesion not clearly definable by gross observation.

Results

The mean after-expectations of life are given in Table 30. No significant differences in after-survival exist among the several qualities in either sex. However, the irradiated groups have significantly shorter after-expectations than the controls. Although control females live longer than control males (75 ± 24 days, $P < .01$), no sex difference in survival is present among the irradiated mice. The per cent reduction of after-survival averages 29.2% in the males and 36.7% in the females. A greater sensitivity of the female to chronic injury has been noted previously by Sacher[2] in LA F_1 mice exposed to prompt fission radiation.

Acute injury was essentially the same for all mice, since about 40% to 49% mortality was observed in the first 30-day period in each quality group when averaging across all doses. A uniformity of injury is also manifest in the life expectancy data for survivors of the acute response. Consequently, the RBE values derived from the 30-day LD_{50} doses are valid for the expression of long-term radiation injury following single whole-body exposure.

TABLE 30

Mean after-survival for all mice surviving the first 30-day postirradiation period

Age at exposure averaged 100 days for all groups.

kvp	30-day LD_{50}, r	Mean after-survival, days			
		n	♂	n	♀
Control	-	74	578 ± 17	80	653 ± 16
250	634	77	421 ± 17	86	398 ± 19
135	663	73	402 ± 17	64	444 ± 24
80	816	88	405 ± 18	89	398 ± 20

A more detailed description of the data in terms of age-specific mortality rates is given in Figure 43 for non-leukemia deaths. The equivalence of chronic injury in the three radiation groups is evident. The mortality rate curve, or Gompertz function, is displaced upward to a similar degree for all qualities and is very nearly parallel to the control.

The post-mortem pathology in the three radiation groups was also very similar. Leukemia was the lesion most frequently observed. Figure 44 presents the age-specific mortality rates from this cause. Although a moderate amount of variation exists among the several qualities, no consistent differences can be noted, particularly when a comparison is made with the curve derived from the combined data of all qualities. In addition, no quality differences were observed in the incidence of ovarian tumors, pulmonary tumors, hepatomas, or chronic degenerative changes involving the kidneys, liver, and spleen.

Conclusions

Mice surviving fractionally lethal exposure to different X-ray qualities demonstrate a striking similarity in the magnitude of permanent injury. Within the limits of sampling error, mean after-survival and tumor incidence are the same for all qualities. Thus, for X-ray energies ranging from 80 kvp to 250 kvp, the RBE values for acute lethality are equally valid for measuring relative effectiveness in terms of chronic mortality following single whole-body exposure.

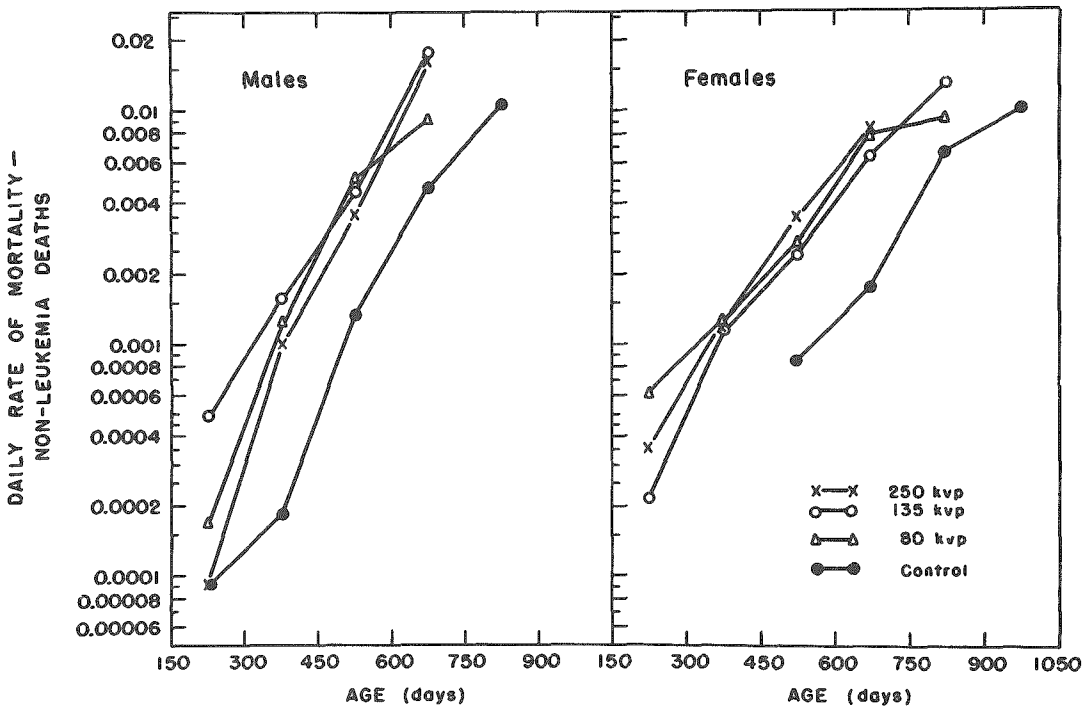

Figure 43. Age-specific rates of mortality for non-leukemia deaths. Mortality rates plotted on log scale. Age at exposure 100 days.

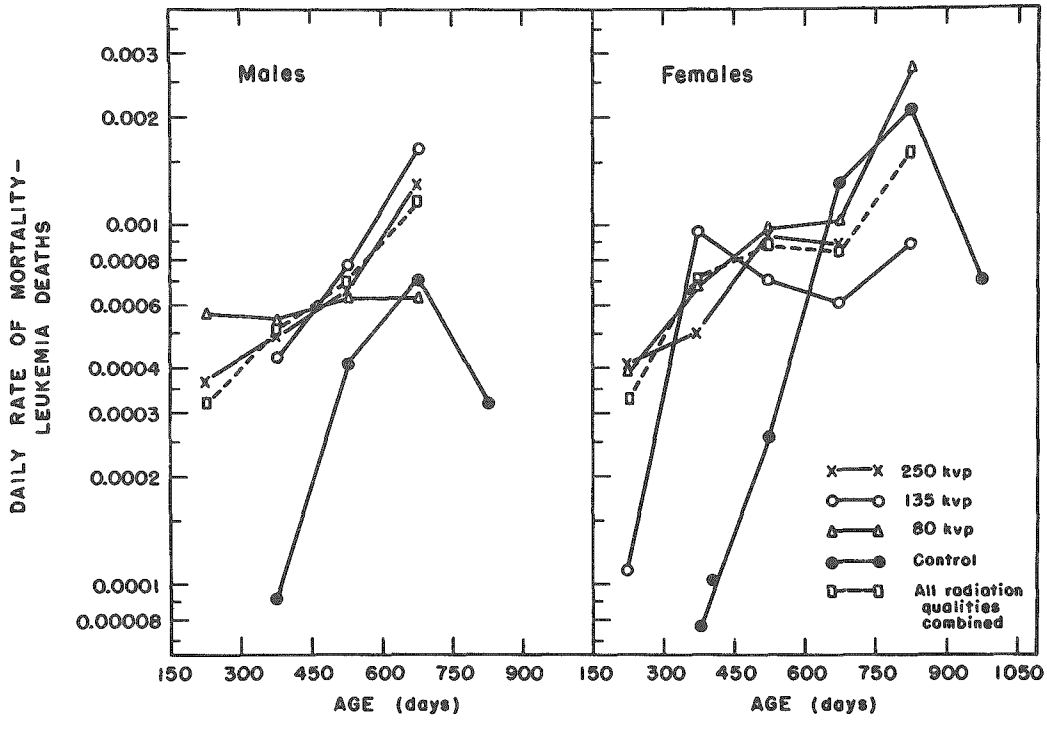

Figure 44. Age-specific rates of mortality for leukemia deaths. Mortality rates plotted on log scale. Age at exposure 100 days.

References

1. Grahn, D., G. A. Sacher, and H. Walton, Jr. Comparative effectiveness of several X-ray qualities for acute lethality in mice and rabbits. Radiation Research 4: 228-242 (1956).

2. Sacher, G. A. On the statistical nature of mortality, with especial reference to chronic radiation mortality. Radiology 67: 250-257 (1956).

SURVIVAL OF GIANT AMOEBAE AFTER SINGLE EXPOSURES TO Co^{60} GAMMA RAYS AND FISSION NEUTRONS

Edward W. Daniels and Howard H. Vogel, Jr

In a preliminary report[1] the survival of giant amoebae (Pelomyxa illinoisensis) was described after single exposures to fission neutrons. Since that time further irradiations have been carried out. Complete survival curves for the amoebae are presented here after single exposures to both Co^{60} γ-rays and fission neutrons at approximately equal intensities. The data are presented in Table 31 and the dose-mortality curves are illustrated graphically in Figure 45.

TABLE 31

Survival of Pelomyxa illinoisensis following irradiation with Co^{60} γ-rays or fission neutrons

Co^{60} γ-rays**			Fission neutrons***		
Total dose	Irradiation time, hr	10-day survival, %*	Total dose	Irradiation time, hr	10-day survival, %*
6	4	100	9.3	5	76
7.5	5	100	9.8	5.25	92
9	6	100	10.2	5.5	80
10.5	7	100	10.7	5.75	76
13.5	9	92	11.2	6	56
15	10	80	11.2	6	54
16.5	11	52	11.6	6.25	36
18	12	28	12	6.5	24
21	14	4	13	7	8
25	16.6	0	14.8	8	0
30	20	0			
40	30	0			

*Each datum represents 25 cells.

**Dose expressed in kr; all exposures made in high-level gamma room at an intensity of 25 r/min.

***Dose expressed in kilorep. All exposures made in the radiation chamber at CP-5 reactor. Reactor was operated at 2000 kw and boral shutter was pulled out of thermal column. Intensity of total dose (nuetrons + γ-rays) was 31 rep/min.

The amoebae were irradiated in 1-ml plastic centrifuge tubes which contained a phosphate buffer solution as described previously.(2) The exposures to Co^{60} γ-radiation were all carried out in the high-level gamma room at an intensity of 25 r/min. The data in Table 31 were obtained from four separate exposures. It is clear that the 10-day mortality range, at this intensity, lies between 10,500 r and 25,000 r of γ-rays. Irradiated cells which live 10 days usually give rise to mass cultures.

The neutron exposures were carried out in the radiation chamber at the thermal column of the CP-5 reactor, which was doubled in power (from 1000 to 2000 kw) in October, 1956. This resulted in an increase of intensity at the animal exposure position and a consequent decrease in the time required for irradiation. Comparative dosimetric methods (Sigoloff chemical dosimeters; Victoreen r-chambers calibrated against Rossi tissue-equivalent-chambers; photographic emulsion techniques developed by Tochilin at USNRDL) all indicated that the total dose received in the animal exposure position was approximately 31 rep/min. This total dose was composed of 25 rep/min of fission neutrons and 6 rep/min of γ-ray contamination. In this report the total dose of fission neutrons includes the γ-ray component. The neutron irradiations were carried out in two separate experiments, the first of which included the 5- to 6-hr irradiations represented by the top five figures in Table 31. The second exposures were from 6 to 8 hr, with a replicate exposure series at the 6-hr level. The lethal range for fission neutrons was found to be between approximately 9,000 and 14,000 rep.

Since the slopes of the two survival curves are not significantly different, an RBE for this biological effect can be determined. At the 50% survival figure, this would be:

$$\frac{17{,}000 \text{ rep (gamma)}}{11{,}000 \text{ rep (neutron)}} = 1.5$$

If the dose of fission neutrons alone is plotted, in which case the γ-ray contamination is ignored, the 50% survival figure is reduced to about 9,000 rep. In this case the RBE would still be less than 2.0.

These data indicate that, for this biological effect, i.e., killing these multinucleated cells, fission neutrons were approximately 1.5 times as effective as Co^{60} γ-rays under the conditions of this experiment.

Effects of Irradiation on Rate of Cell Division

In Figures 46 and 47 are illustrated the effects of single exposures of the two radiations on division rate of the amoebae.* It is clear that the

*The number of cell divisions is expressed as N_t/N_0; N_0 is the number of single cells isolated following irradiation; at time t this value is equal to the number of surviving clones. N_t is the total number of cells at time t.

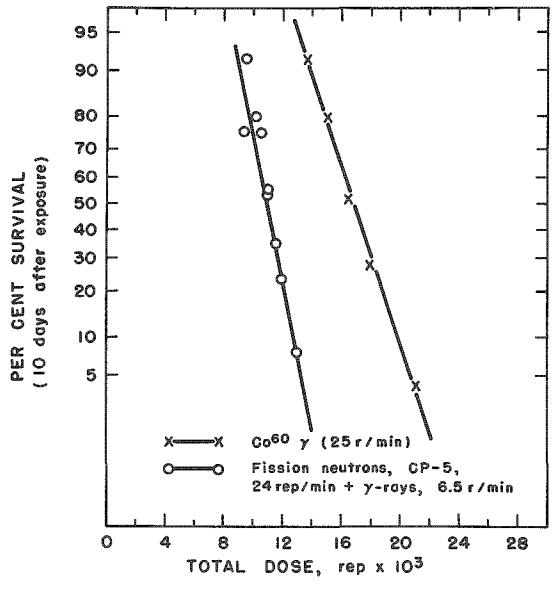

Figure 45. Per cent survival of Pelomyxa illinoisensis following exposure to fission neutrons or to Co^{60} γ-rays. Each point represents 25 cells which were irradiated and isolated at the beginning of the experiment. (The survival data are calculated on the exposed cells or their offspring.)

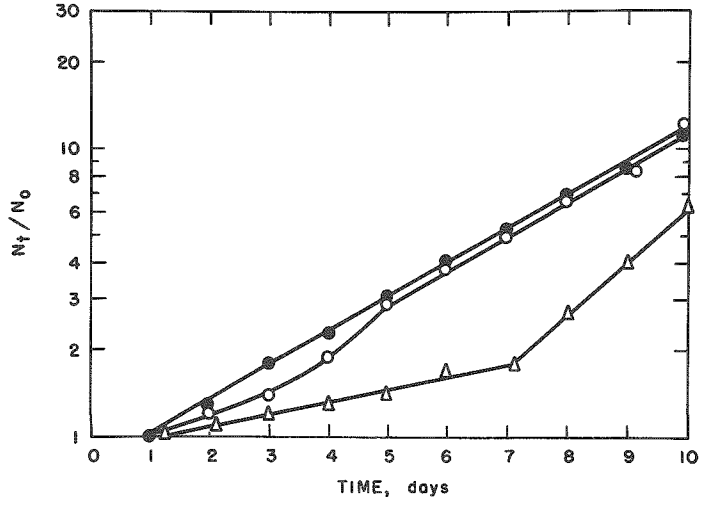

Figure 46. Rate of cell division in γ-irradiated Pelomyxa illinoisensis single cell clones. ●, nonirradiated controls (N_0 = 50); O, 15 kr γ-rays (N_0 = 25, 80% survival, Figure 45); △ 16.5 kr γ-rays (N_0 = 25, 52% survival, Figure 45).

Figure 47. Rate of cell division in fission neutron-irradiated amoebae, single cell clones. ●, nonirradiated controls (N_0 = 50); O, 9500 rep fission neutrons, exposure 5-1/4 hours (N_0 = 25, 92% survival, Figure 45); ⊖, 11,000 rep fission neutrons exposure 6 hours (N_0 = 50, 55% survival, Figure 45).

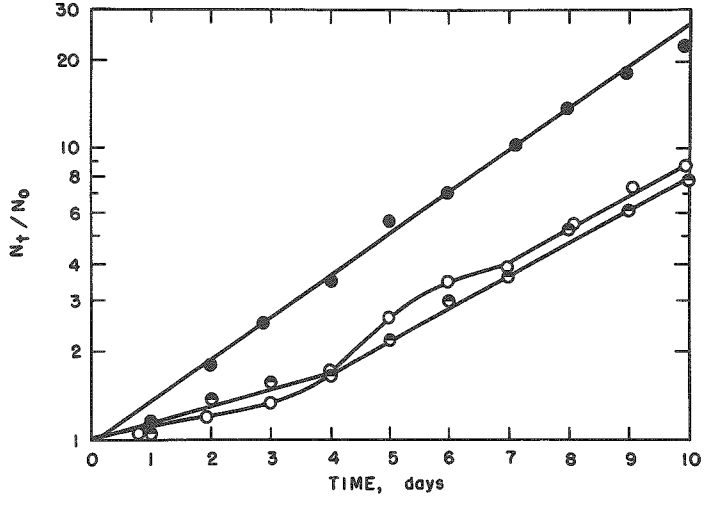

rate of division is inhibited in all four classes of irradiated cells, as compared to the controls. The two higher doses (16.5 kr γ-rays and 11 kilorep neutrons) were approximately equal in terms of 10-day survival (52% and 55%; Figure 45); in terms of inhibition of cell division, these neutron-irradiated cells seem to recover to the control rate of division earlier than the γ-irradiated amoebae. On the other hand, when the lower doses are compared, the γ-rays do not seem to depress cell division as markedly as the neutrons, even though the former radiation had a higher lethal effect (Table 31). In each case, the irradiated cells had essentially recovered to the control rate of division by 4-7 days.

Survival Effect of Nonirradiated Protoplasm after Microinjection into Single Cells Irradiated with a Lethal Dose of Fission Neutrons

Nonirradiated protoplasm prevents death when it is injected into lethally X-irradiated giant amoeba cells.[2] Therefore, we decided to investigate the possibility of similar recovery in amoebae of this species following lethal doses of fission neutrons.

Amoebae were taken from the same vial of organisms which was used to establish the zero survival point in Table 31 (8-hr irradiations with fission neutrons). Eight amoebae from this sample were successfully injected (by microfusion) with whole, nonirradiated protoplasm from cells of a control culture of Pelomyxa illinoisensis. Each injected cell was then isolated and fed with Paramecia.

Six of these 8 individuals survived and gave rise to mass cultures. The remaining 2 individuals died between the 3rd and 5th day after lethal neutron exposure without undergoing cell division. The survivors underwent the first postirradiation cell division after an average of 3.6 days. Later divisions appeared to occur within a normal period of time. The average first division in the control organisms was at 2.1 days.

The amount of protoplasm injected into each cell was estimated. Ratios of nonirradiated to neutron-irradiated protoplasm in the 6 survivors was 1:1, 1:1, 1:5, 1:6, 1:10, and 5:1, respectively. Within these limits, no relationship could be seen between the amount of nonirradiated protoplasm injected into the irradiated cell and the time of first cell division. The ratios in the two cells which did not survive were 1:1 and 1:1. Clearly, death in these two cells did not occur because of an inadequate amount of nonirradiated protoplasm. It is also clear that death did not occur because of inadequate mixture of nonirradiated with neutron-irradiated protoplasm. In each of the 8 amoebae, the injected protoplasm was seen to flow in with consequent mixing.

At the present time, the relative roles of the neutron-irradiated and the nonirradiated cell components in the experimental cell are not known.

In X-irradiated-nonirradiated systems, the exposed nuclei participate in cell division in a manner similar to that of the nonirradiated nuclei.(3)

References

1. Vogel, H. H. Jr., and E. W. Daniels. Survival of giant amoebae after single exposures to fission neutrons. Quarterly Report, Biological and Medical Research Division, Argonne National Laboratory. ANL-5597, pp. 70-73 (1956).

2. Daniels, E. W. X-irradiation of the giant amoeba, Pelomyxa illinoisensis. J. Exptl. Zool. 130: 183-197 (1955).

3. Daniels, E. W. Effect of nonirradiated centrifuged protoplasm on supralethally X-irradiated giant amoebae. III. Quarterly Report, Biological and Medical Research Division, Argonne National Laboratory. ANL-5576, pp. 77-78 (1956).

RECOVERY FOLLOWING INJECTION OF NONIRRADIATED PROTOPLASM INTO AMOEBAE IRRADIATED WITH FISSION NEUTRONS

Edward W. Daniels and Howard H. Vogel, Jr.

Multinucleated amoebae of the species Pelomyxa illinoisensis were exposed to about 30,000 rep of fission neutrons, twice the dose necessary to kill all amoebae in 6 days. The dose rate was approximately 31 rep/min (of which 6 rep/min were γ-rays). Death occurred in all of the nontreated, irradiated controls between the 3rd and 6th postirradiation days. The time of death is therefore the same as that which follows supralethal X-ray exposure in this species. There was no cell division in these controls prior to death.

Each of 32 supralethally irradiated cells was given whole homologous protoplasm by microfusion. This method combines the irradiated cell with the nonirradiated cell or some fraction of it. Ninety-one per cent of the experimentally fused cells recovered. They usually divided a few times within the 10-day period and appeared to be in good condition at its end. Eleven representative clones of these 10-day survivors were kept for further study, of which ten gave rise to mass cultures. The 11th cell lived several times longer than the nontreated controls but it did not undergo division.

At the time of each fusion, the volume ratio of nonirradiated to irradiated protoplasm was estimated. The ratios ranged from 25:1 on the one hand to 1:25 on the other. If an irradiated organism did not receive more than 1 part nonirradiated protoplasm to some 15 parts irradiated protoplasm, recovery was poor or failed completely.

AN ACCURATE MICROPIPETTE CUTTING DEVICE

Edward W. Daniels

In micrurgical operations involving the injection or removal of materials from single cells, it is essential that microtips of the proper size be used. Thus after a micropipette is made and checked for patency, it is essential to cut or break it at the proper place. For rough work, a good pair of scissors can be used while the micropipette is held under a dissecting microscope; however, for precise work, better results are obtained by clipping the microtip with a special trimming unit. The device described here incorporates some of the ideas used by Richter[1] in his design for a micropipette trimmer for use with a moist chamber.

The unit (Figure 48) operates by simultaneously bringing two opposing, parallel knife edges against the microtip, and the trimming is done in the field of a compound microscope, magnified 100 or more diameters. The unit is composed of two stainless steel parts, A and B in Figure 48. Part A is the size of an ordinary microscope slide (1 x 3 inches) except for the thickness which is 9 mm; the clamp projection extends slightly more than a centimeter from one side. Part B is 8 x 8 x 77 mm. Each clamp (Parts A and B) holds a 2- or 3-mm portion of a sharp edge of a thin double-edged razor blade (Figure 48, C). Part B is placed in a rack and pinion micromanipulator while part A is placed in the mechanical stage of the microscope. Thus, both A and B can be manipulated in the horizontal plane and Part B can also be manipulated in the vertical plane.

The micropipette is held in the chuck of another micromanipulator in such a manner that it can be brought into the microscopic field at right angles to the blades of the cutter. When a portion of the desired diameter, as measured with an eyepiece micrometer, is between the blades of the cutter, either part A or part B of the unit is moved toward the opposing blade until the glass is severed. Microtips 15 μ or less in diameter are very easily trimmed at precisely the point of contact with the blades. Short pieces of microtip glass, about 25μ long can also be trimmed off from a micropipette. This is convenient since it enables one to remove the contaminated tip of a long tapering micropipette so that the remainder can again be used. Thus, fewer micropipettes are needed.

The micropipette cutting unit described in this report was designed for use with the liquid micrurgy chamber described previously.[2] However, its use is not limited to use with this chamber. The liquid chamber can actually be mounted, with a thin film of vaseline, on top of part A of this unit instead of on top of a standard slide. This has certain advantages since there is more clearance between the chamber and the microscope stage. The liquid chamber is then removed if the micropipette needs to be trimmed.

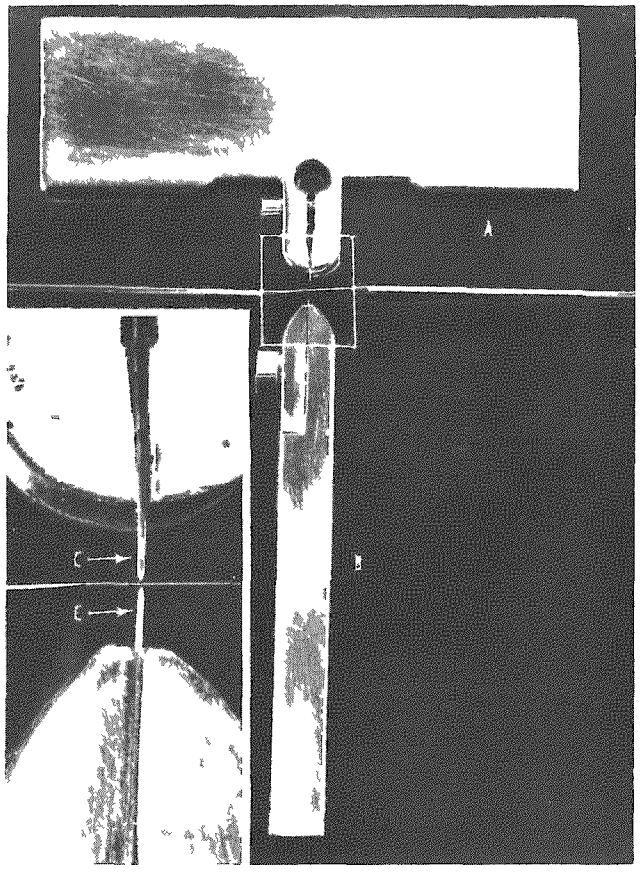

Figure 48

Micropipette cutter. Inset shows details of blade assembly.

The author expresses gratitude to A. Akerhaugen for constructing the micropipette cutter.

References

1. Richter, K. M. A precision micro-pipette trimmer. Science 106: 598-599 (1947).

2. Daniels, E. W. A liquid micrurgy chamber. Quarterly Report of Biological and Medical Research Division, Argonne National Laboratory. ANL-5486, pp. 23-25 (1955).

A MICROPIPETTE PULLING UNIT

Edward W. Daniels

During the past year micropipettes and microneedles have been made satisfactorily in this laboratory by the unit shown in Figure 49. There are two major parts to this unit, the microburners and the pulling device, which is a somewhat more complex form of the simple puller described previously.(1)

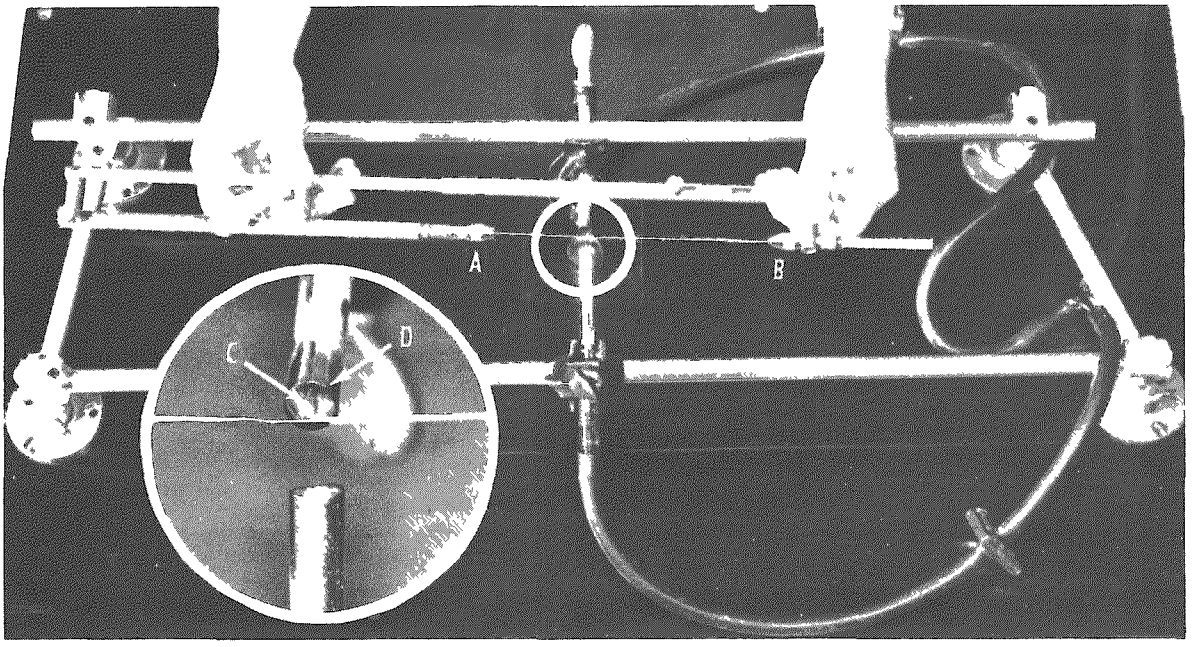

Figure 49

Micropipette pulling unit

A hidden spring, which supplies the pulling force, is attached to pin vice A (Figure 49). The spring tension can be adjusted by a set screw while the attached pin vice A remains in a fixed position. Pin vice B in Figure 49 is attached to a sliding arm which can be held in a given position either by hand or by a set screw. When a micropipette is made, a thin-walled glass capillary tube is held at each end by the pin vices. Then pin vice B (simultaneously with pin vice A) is moved out and held in any desired position within a 9-cm limit; the position is located by reading the scale on the shaft of pin vice A. The glass capillary tube, under tension, is then placed over the flame and removed as soon as the pulling begins. If, for example, a 10-μ microtip is to be made from an 0.8-mm thin-walled glass capillary tube, two "pulls" are recommended, the first from the

1.5-cm mark and the second from the 3-cm mark. Shorter and stronger microtips can be made in this manner by using two settings, and reproducibility in size is good.

The gas microburners are mounted at an angle of 110°from each other so that the flame of each microburner heats a different side of the glass capillary tube, and this angle can be increased by adjusting set screws. Each burner (Figure 49, C) was made from a 25-gauge hypodermic needle pulled out of its metal base, turned end for end and replaced; thus the sharp end is covered. In addition to this, a metal jacket (Figure 49, D) was placed over the microburner for protection and to reduce air currents at the base of the flame. The two microburners burn throughout the day without relighting.

The author gratefully acknowledges the assistance of A. Akerhaugen, who constructed the apparatus.

Reference

1. Daniels, E. W. A simple micropipette pulling device. Quarterly Report of Biological and Medical Research Division, Argonne National Laboratory. ANL-5486, pp. 21-22 (1955).

GRANULOCYTE BALANCE: RELATIVE NUMBERS OF CIRCULATING AND MARGINAL CELLS

Harvey M. Patt and Mary A. Maloney

There is reason to think that the detectable circulating granulocytes are in dynamic equilibrium with a large peripheral reservoir.(1) A part of this reservoir probably exists within the confines of the vascular system, perhaps to a considerable extent as marginal cells.(2) The present studies were undertaken in an attempt to approximate the number of intravascular cells that are not detected by conventional sampling techniques. The problem was approached by comparison of the dilution of erythrocytes relative to granulocytes when isotonic sodium chloride is infused rapidly through a limb for several minutes. In the first experiments, polyethylene cannulae were inserted into the femoral artery and vein of a dog, the animal was then sacrificed and saline was infused through the artery at a rate of about 50 ml/min. Samples were collected at frequent intervals from the femoral vein. Approximately twice the anticipated number of leucocytes was obtained in the three dogs studied in this way (Figure 50). Differential counts reveal that the added leucocytes are primarily granulocytes. The additional number of cells probably represents a minimal value. Present experiments are concerned with different perfusion media and different vascular beds.

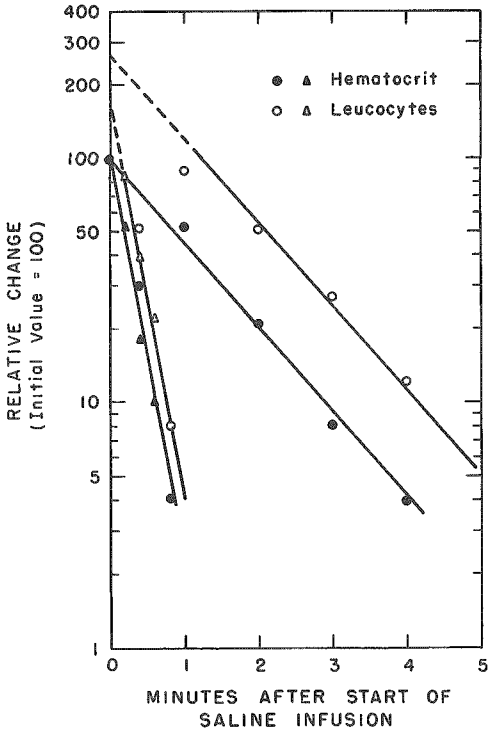

Figure 50

Change in hematocrit and leucocyte count during infusion of an isolated limb. The one-minute infusion represents two experiments, the first designated by circles, the second by triangles.

References

1. Patt, H. M. and M. A. Maloney. Control of granulocyte formation. Brookhaven Symposia in Biology No. 10, in press.

2. Vejlens, G. Distribution of leucocytes in vascular system. Acta Pathol. Microbiol. Scand., Suppl. 33: 1-241 (1938).

PROGRESS REPORT: RADIOSTRONTIUM REMOVAL. I

Arthur Lindenbaum, Marcia W. Rosenthal, and Joan F. Fried

The removal of radiostrontium from the body is difficult because of its close chemical resemblance to calcium and its rapid absorption and sequestration in bone.[1,2] These factors are responsible for in ineffectiveness of therapy aimed at reducing absorption from the gut by feeding phosphates,[3] or at promoting excretion by such measures as injection of large doses of nonradioactive "carrier" strontium.[3,4,5] Chelating agents of the ethylenediaminetetraacetic acid (EDTA) type are likewise ineffective against strontium in the body because of the vastly larger concentrations of calcium and magnesium available for complex formation.[4]

From the biochemical standpoint the ideal therapeutic agent would possess, in addition to the usual pharmacological requirements, the capacity to undergo rapid and preferential reaction with strontium in the presence of relatively massive amounts of other alkaline earth metals and to be readily excreted in combined form. One class of compounds offering some possibility of fulfilling these requirements is represented by rhodizonic acid and tetrahydroxyquinone (Figure 51). Sodium rhodizonate has been employed analytically for the detection of barium and strontium.[6] In neutral solutions these metals are preferentially precipitated in the presence of calcium. Although little is known about the chemistry of such compounds, metal binding is thought to occur through the mechanism of chelation and, presumably lake formation.

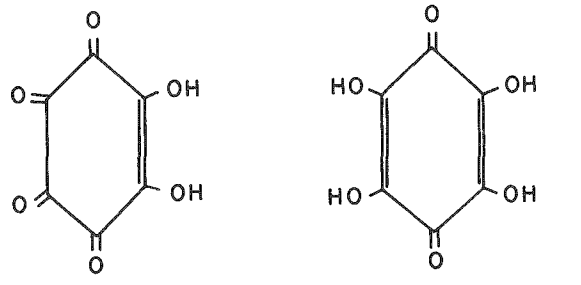

Rhodizonic Acid Tetrahydroxyquinone

Figure 51

Preliminary Observations

The dipotassium salt of rhodizonic acid (K_2R) and the tetrasodium salt of tetrahydroxyquinone (Na_4T) were used at pH 6-7. Both salts are

easily oxidized in air, and within a few days dilute solutions (0.01 M or below) lose their ability to precipitate Sr. However, a precipitate with Sr, once formed, remains indefinitely. When heparinized plasma made $\sim 10^{-3}$ M with respect to $SrCl_2$ is mixed with equimolar amounts of K_2R appreciable amounts of precipitate are formed.

Amounts of K_2R up to 30 mg/kg intravenously and 150 mg/kg intraperitoneally produce no toxic symptoms in adult female Sprague-Dawley rats. Since K_2R is a yellow-orange dye which fades upon oxidation, its fate in the body may be followed by observing the urine. Upon administration of 3 to 15 mg K_2R into rats by either route the unoxidized dye is observed in the urine almost immediately and continues to be excreted for approximately 1-2 hr.

A pilot experiment has been conducted in vivo with three 235-240 g rats injected intraperitoneally with 15 mg K_2R 3 min prior to an intravenous injection of 0.62 μc of carrier-free $Sr^{85}Cl_2$. Two control animals received the same amount of Sr^{85} plus an equivalent volume of water intraperitoneally. All animals were sacrificed after 24 hr. Significant differences were observed between control and treated groups with respect to excretion and skeletal content of Sr^{85}. Delayed urinary excretion by one treated rat was associated with elevated levels of strontium in all tissues of this animal compared to tissue levels in the other treated rats. Because of the inclusion of data from this animal, the difference in total body retention in favor of the treated group was made less significant. Despite inclusion of this data, however, treated rats excreted an average of 22.8% of the injected Sr^{85} in the urine, while controls excreted 12.9%. Skeletal retention of Sr^{85} (arbitrarily calculated as ten times the value for both femurs) was 51.2% for treated animals and 61.9% for controls. Retention in the liver, kidney, and spleen was very low ($<0.25\%$) in all animals, and always lower in the treated group than in controls.

Further in vivo studies aimed at increasing the therapeutic effectiveness of K_2R and its analogs are in progress. The route and time of treatment, as well as the amount given, may be of critical importance in effecting increased excretion of radiostrontium. It is conceivable, for example, that an unstable agent, however efficiently it binds Sr, if given as a single dose may be broken down before it can be excreted. Therefore, unless there is rapid excretion, the only observable effect might be a delay in the passage of Sr from the soft tissues to bone. Promotion of diuresis may thus be of value. In addition, fractionated dosage or extended administration through feeding might prolong effective concentrations in the body. Since K_2R is relatively tasteless and easily diffusible, the oral route may be feasible.

The physical-chemical aspects of the affinity of K_2R and Na_4T for Sr and Ca are also being investigated. Precipitation is not necessarily

a measure of affinity between a ligand and a metal, and it is quite possible that measurements of the true binding constants for rhodizonic acid may give similar values for both Sr and Ca, despite physical differences with respect to precipitation. It is therefore important to obtain such data in order to evaluate the possibility of a colloidal carrier effect, such as that which is observed in the use of zirconium citrate for promoting excretion of plutonium.(4)

References

1. Norris, W P , and W. Kisieleski Comparative metabolism of radium, strontium and calcium. Cold Spring Harbor Symposia Quant. Biol. 13:164-172 (1948)

2. Jones D. C., and D. H. Copp. The metabolism of radioactive strontium in adult, young, and rachitic rats J Biol Chem 189: 509-514 (1951).

3. Hamilton, J. G. Metabolism of fission products. Technical Information Division, Oak Ridge Operations. MDDC-1001 (1944).

4. Schubert, J Removal of radioelements from the mammalian body. Ann. Rev Nuclear Sci. 5: 369-412 (1955).

5. Copp, D H , D. J. Axelrod, and J G. Hamilton The deposition of radioactive metals in bone as a potential health hazard. Am. J. Roentgenol. 58: 10-16 (1947)

6. Feigl, F. Chemistry of Specific, Selective and Sensitive Reactions. Academic Press, Inc., New York (1949)

THE NATURE OF THE SECRETORY ACTIVITY OF THE TISSUE MAST CELL

Douglas E. Smith

Abstract

In the tissues of the peritoneal cavity the mast cell appears to be the only cell capable of releasing histamine.(1) Protamine sulfate, toluidine blue, stilbamidine, and curare when dissolved in Tyrode's solution and injected intraperitoneally into adult, male, albino rats resulted in the discharge into the peritoneal fluid of measurable quantities of histamine. When these stimuli were administered to rats whose peritoneal tissue mast cells had been destroyed by intraperitoneal injection of distilled water, no release of histamine was evoked. When toluidine blue injections (20 ml of 1:20,000 in Tyrode's solution, intraperitoneally) were repeated in otherwise untreated animals at intervals of from 5 min to 1 day over periods of 50 min to 5 days, respectively, significant quantities of histamine were released after each administration. The daily injections were followed by the discharge of relatively large amounts which were approximately the same from day to day. When the injections were repeated every 5 min, the amounts of histamine discharged became successively smaller as the administrations proceeded. These repeated injections of toluidine blue caused in the mast cells or other cells of the peritoneal tissues no changes which could be detected histologically.

It was concluded that secretion by the tissue mast cell does not require cell disruption and death, as most of the literature indicates, but rather that it is merocrine in nature. The mast cell appears to be an endocrine cell which can continuously elaborate and release histamine in response to appropriate stimulation.

Reference

1. Fawcett, D. W. Cytological and pharmacological observations on the release of histamine by mast cells. J. Exptl. Med. 100: 217-224 (1954).

STUDIES ON EFFECTS OF DEUTERIUM OXIDE

IV. Serum and Ascitic Fluid Transaminase in Tumor-Bearing Mice

Asher J. Finkel and Dorice Czajka

In a previous report[1] data were presented that indicated that when the deuterium content of the body fluids in mice was increased there was a reduction of growth of the Krebs-2A ascites tumor in CF No. 1 female mice This effect of deuterium on ascites tumor growth can be postulated to be a result either of an inhibition of cell division, or of destruction of the individual cells, or of both mechanisms operating together. It was thought that some insight in this matter might be afforded by an examination of the glutamic oxalacetic transaminase (GO-T) values since these have been shown to be elevated in serum in experimental and clinical disease states in which destructive lesions of specific tissues, such as myocardium and liver, occur.[2] GO-T was determined spectrophotometrically in serum and in ascitic fluid plasma according to the method of Steinberg et al.[3]

In a preliminary experiment, where an attempt was made to grow the Krebs-2A ascites tumor in the solid phase by subcutaneous injection of 23.2×10^6 cells, a number of the animals unexpectedly developed ascites tumors as well as solid phase tumors. Table 32 gives the mean GO-T values determined for the sera and ascitic plasma in these animals. In mice bearing only solid phase tumors the serum GO-T data fall within the range for normal mice (20 to 120 units in our experience), while the nondeuterated ascites-bearing animals have somewhat increased mean serum GO-T values. In ascites-bearing deuterated mice the serum GO-T values are appreciably increased above normal levels with increasing body deuterium content, and this elevation is even more marked in the ascitic fluid GO-T values.

Table 33 presents similar data for a second experiment for which the growth characteristics were given in Table 16 in a previous report.[1] These transaminase values were determined on mice that were sacrificed at the same time as those used for the measurement of the growth characteristics. The control groups that were deuterated but not inoculated with the ascites tumor had serum GO-T values that were well within the normal range. The tumor-bearing mice showed elevated serum GO-T values (SGO-T) and even more elevated ascitic plasma GO-T levels (AGO-T). The collective ratios of SGO-T to AGO-T very closely parallel the results of the preliminary experiment.

A third experiment was performed with a larger number of mice and with a greater range of deuteration of body fluids. In addition a larger inoculum was used than in the preceding experiment ($4\ 8 \times 10^6$ instead of

TABLE 32

Glutamic oxalacetic transaminase values*
of mouse sera and ascites plasma

Deuterium in body fluids, atom %	Ascites-phase tumors				Solid-phase tumors	
	No. of mice	Mean serum GO-T values	Mean ascites plasma GO-T values	Ratio $\frac{\text{SGO-T}}{\text{AGO-T}}$	No. of mice	Mean serum GO-T values
23-24	5	282	461	0.61	7	86
13-14	8	202	238	0.84	7	101
0	9	142	120	1.18	4	90

*Arbitrary units defined in Reference (3).

7×10^5 cells). From the data in Table 34, which corresponds to Table 17 in Reference (1), it can be seen that the mean serum GO-T level rises with increasing deuteration of the tumor-bearing mice and that there is a similar elevation of the ascites GO-T. In this case, however, the trend of the ratios of SGO-T to AGO-T is reversed and the spread between the nondeuterated group and the treated groups is narrower in spite of a greater span of degree of deuteration.

If GO-T values can be used as a measure of cell destruction, these data indicate that deuterium at appropriate levels in the body fluids, including the ascitic plasma, leads to tumor cell destruction. The enzyme, presumably released into the ascitic plasma with cell injury, is carried into the general circulation with consequent elevation of the serum GO-T values. Since deuteration of non-tumor-bearing mice does not lead to an elevation of the serum GO-T, it may be concluded that deuterium affects ascites tumor growth in part, at least, by injuring the tumor cells. Whether or not there is, in addition, an inhibitory effect on cell division of the tumor will be the subject of further investigation.

TABLE 33

Glutamic oxalacetic transaminase (GO-T) values* in serum and ascitic fluid in deuterated and nondeuterated mice inoculated with Krebs-2A ascites tumor**

Day after inoculation	Deuterium in body fluids, atom %	Tumor-bearing mice					Non-tumor mice	
		No. of mice	Mean SGO-T	No. of mice	Mean AGO-T	Ratio $\frac{\text{SGO-T}}{\text{AGO-T}}$	No. of mice	SGO-T
4	23-24	3	145	2	173	0.84	3	80
	13-14	3	79	3	169	0.47	3	85
	0	3	197	3	112	1.76	3	91
7	23-24	3	405	3	350	1.16	3	58
	13-14	3	193	2	333	0.58	3	61
	0	3	289	2	418	0.69	3	69
9	23-24	3	333	2	681	0.49	3	47
	13-14	3	377	1	688	0.54	3	41
	0	3	298	3	326	0.91	3	73
14	23-24	3	713	3	1311	0.54	2	30
	13-14	3	479	2	301	1.59	2	57
	0	3	534	3	263	2.03	2	52
Total	23-24	12	399.0	12	669.1	0.60	11	55.9
	13-14	12	282.0	8	307.9	0.92	11	61.4
	0	12	329.5	11	267.2	1.23	11	73.0

*Arbitrary units defined in Reference (3).

**Inoculated intraperitoneally with 7×10^5 tumor cells on the 7th day of deuteration.

TABLE 34

Glutamic oxalacetic transaminase (GO-T) values* in serum and ascitic fluid in deuterated and nondeuterated mice inoculated with Krebs-2A ascites tumor**

Day after inoculation	Deuterium in body fluids, atom %	No. of mice	Mean SGO-T	No. of mice	Mean AGO-T	Ratio $\frac{\text{SGO-T}}{\text{AGO-T}}$
3	27.5-29	5	117	5	294	0.40
	23-24	10	100	10	235	0.42
	13-14	10	118	10	240	0.49
	0	10	132	10	206	0.64
5	27.5-29	6	253	6	400	0.63
	23-24	10	155	10	222	0.70
	13-14	10	144	10	192	0.75
	0	10	143	9	204	0.70
7	27.5-29	5	1236	5	713	1.73
	23-24	5	838	4	688	1.22
	13-14	5	480	5	518	0.93
	0	5	246	5	254	0.97
10	27.5-29	-	-	-	-	-
	23-24	5	850	4	1031	0.82
	13-14	5	492	3	564	0.87
	0	5	220	5	175	1.26
12	27.5-29	-	-	-	-	-
	23-24	-	-	-	-	-
	13-14	2	406	1	924	0.44
	0	5	208	5	409	0.51
Total	27.5-29	16	517.7	16	464.7	1.11
	23-24	30	366.3	28	408.8	0.90
	13-14	32	259.1	29	328.4	0.79
	0	35	174.9	34	237.8	0.74

*Arbitrary units defined in Reference (3).

**Inoculated with 4.8×10^6 tumor cells on the 9th day of deuteration.

14 ..

References

1. Finkel, A. J. and D. M. Czajka Studies on effects of deuterium oxide. III. The effects of deuteration on ascites tumors in mice. Quarterly Report of Biological and Medical Research Division, Argonne National Laboratory. ANL-5696, pp. 74-76 (1957).

2. Mason, J. H., and F. Wroblewski. Serum glutamic oxalacetic transaminase activity in experiments and disease states. Arch. Internal Med. 99: 245-252 (1957).

3. Steinberg, D , D. Baldwin, and B. Ostrow. A clinical method for the assay of serum glutamic oxalacetic transaminase. J. Lab. Clin. Med. 48 144-151 (1956).

143

AN AUTOMATIC SCANNER FOR TRITIATED COMPOUNDS IN PAPER CHROMATOGRAMS

William Eisler, William Chorney, and Walter E. Kisieleski

Paper chromatography in conjunction with radioactive tracer techniques provides one of the more promising methods for study of the transport and metabolism of specific substances. Recently there has been an active interest in the preparation of labeled compounds using tritium.

Labeling of biologically interesting compounds by self-irradiation using tritium gas[1] is of considerable value because of the simplicity of the method and the high specific activities that can be obtained. Unfortunately many polymerization and breakdown products are formed during the tritium irradiation, necessitating a high degree of purification. Paper chromatography in conjunction with radioactive tracer techniques may be used to separate and localize these contaminants.

Because of the very weak β energy of tritium, one can obtain an autoradiograph on ordinary No-Screen X-ray film only at higher levels of activity Furthermore, in order to detect tritium on a paper chromatogram, it is necessary to cut the chromatograms into small sections 1-2 cm long, elute the material from the paper, and make activity measurements in a liquid scintillation counter. Alternatively, sections of the chromatogram can be counted under a windowless counter.

In order to facilitate the scanning of paper chromatograms containing a weak energy β-emitter such as tritium, or very low levels of C^{14}, an automatic strip counter has been designed and tested. This device scans the paper radiometrically and thus locates the labeled substances.

The automatic chromatogram scanner with its accompanying electronic equipment is shown in Figure 52. Similar scanners using somewhat different components have been previously reported in the literature.[2-4]

The electronic system for the scanner is mounted in a rack. It consists of a conventional Brown 0-10 MV strip recorder, a count-rate meter with a range of 20 to 10,000 cps, and a combination scaler and variable high voltage power supply (500-2500 volts). The preamplifier feeding the scaler is mounted in the box directly above the scanning chamber in order to keep the lead from the counter wire as short and direct as possible. The unit includes a two-stage amplifier and discriminator and has a negative output pulse of 0.5 volt. Inclusion of a scaler allows integrated counts to be taken for specific activity measurements at any point along the chromatogram strip.

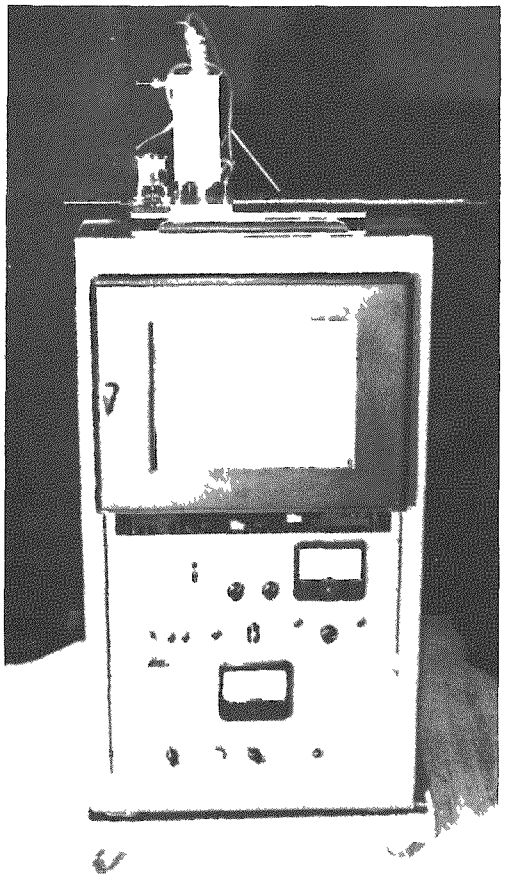

Figure 52

An automatic chromatogram scanner and its accompanying electronic equipment.

Figure 53

A detailed view of the scanner chamber and its assembly.

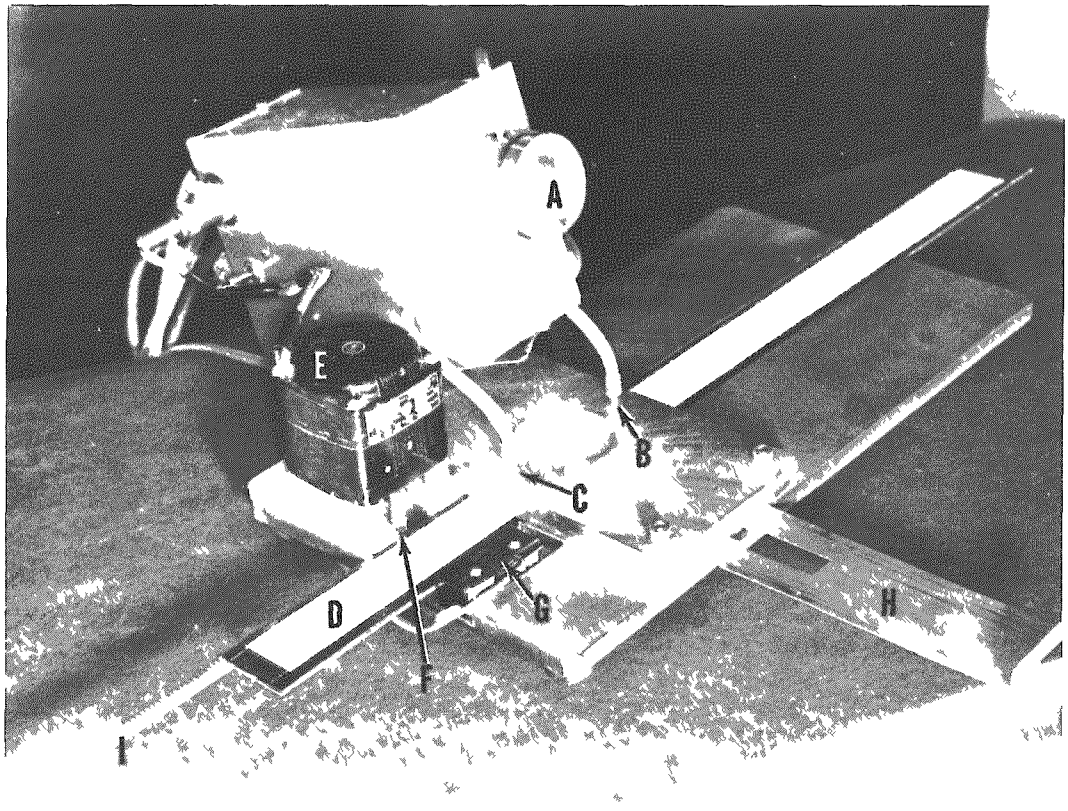

The scanner chamber, shown in detail in Figure 53, consists of a stainless steel hemisphere (A) containing a 1-cm stainless steel center wire loop. Argon-methane gas is used to flush the chamber which is operated at 2200 volts. Gas is also flushed at points of entrance (B) and exit (C) of the chromatogram strip in order to insure constant counting characteristics along the strip.

A paper chromatogram strip up to 4 cm wide and up to 60 cm long is attached to a geared carrier (D,I). The drive is operated by a Bodine #KC1-22RC reversible capacitor start spur gear motor (E) that has a pinion gear attached to its shaft (F), which, when engaged, can drive the carrier in either direction. The motor and gear combination is designed to synchronize the scanner mechanism to the speed of the chart recorder.

The starting position and successive 2-cm intervals of the paper strip are marked on the recorder by a marker pen which is operated by a micro switch (G) mounted on the base plate and activated by indentations cut into the paper carrier. This facility allows one to make R_f determinations directly from the recording chart.

Three window slits (H) of 0.5, 1.0, and 1.5 cm are available, positioned by a ball-bearing detent indicating the correct position. The smaller window slit, although it reduces the apparent counting rate, allows resolution of a number of components which may appear with the larger slits as broad bands of one component.

Figure 54 shows a typical recording of a chromatogram showing the high degree of resolution possible in cases in which the active zones are rather close together. Superimposed on the recording is a radioautograph of the same chromatogram, which required 11 days of exposure for development of the zones containing lower levels of activity. With this device, the activity in these zones can be determined within the time necessary to run the strip through the scanner, or about 15 min.

Measurements made by direct addition to Whatman No. 1 paper indicate that the minimal detectible concentration, discounting other factors of self-absorption and resolution, is in the order of 10^{-5} $\mu c/cm^2$ for C^{14} and 10^{-4} $\mu c/cm^2$ for tritium.

The simplicity and low cost of construction make this an ideal apparatus for scanning chromatogram strips containing C^{14} and tritium. The assembly provides easy access to parts coming in contact with the paper chromatograms and thus permits easy cleaning in case of any contamination.

The authors are indebted to Dr. K. Wilzbach of the Chemistry Division for his helpful advice and to A. Akerhaugen for his assembly of the scanner.

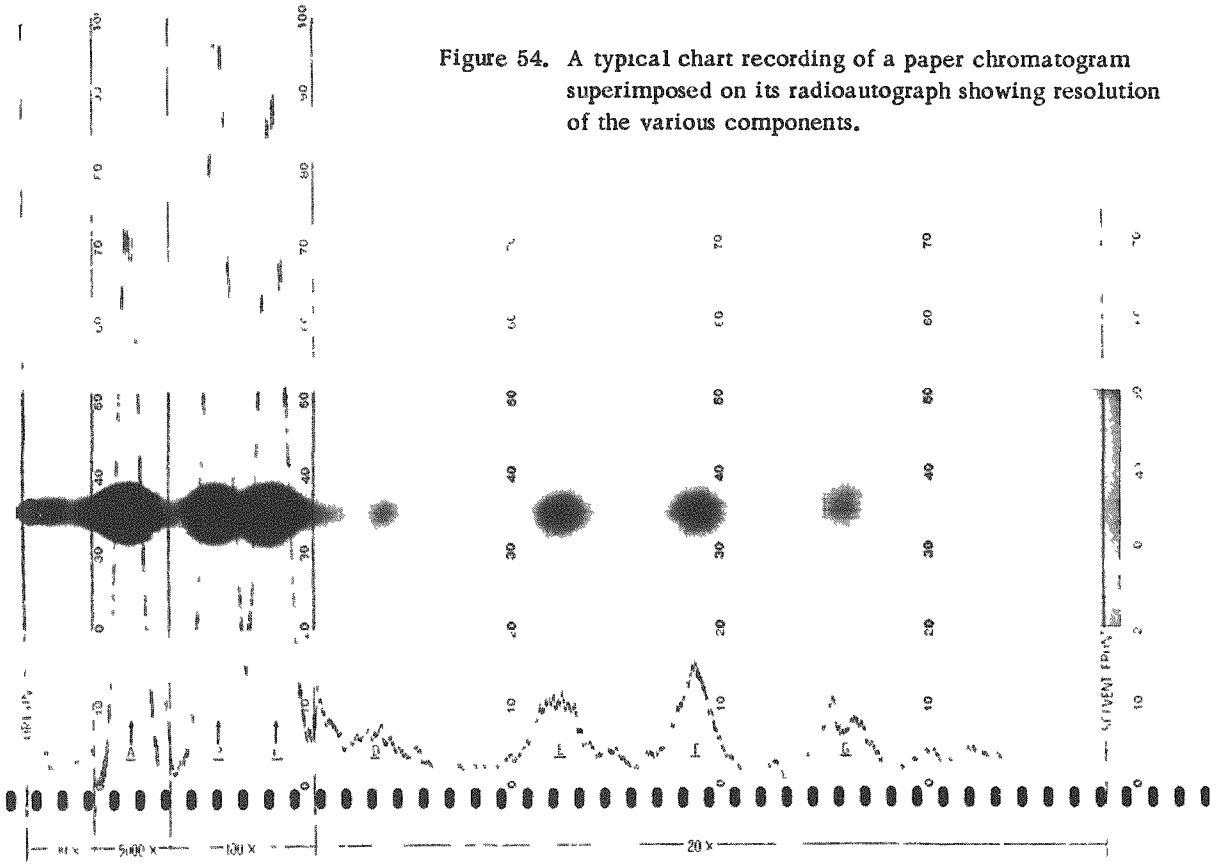

Figure 54. A typical chart recording of a paper chromatogram superimposed on its radioautograph showing resolution of the various components.

References

1. Wilzbach, K. Tritium-labeling by exposure of organic compounds to tritium gas. J. Am. Chem. Soc. 79: 1013 (1957).

2. Gray, I., S. Ikeda, A. A. Benson, and D. Kritchevsky. Detection of tritiated compounds in paper chromatography. Rev. Sci. Inst. 21: 1022 (1950).

3. Winteringham, F. P. W., A. Harrison, and R. G. Bridges. Radioactive tracer techniques in paper chromatography. Nucleonics 10 (No. 3): 52-57 (1952).

4. Soloway, S., F. J. Rennie, and S. DeWitt, Sr. An automatic scanner for paper radiochromatograms. Nucleonics 10 (No. 4): 52-53 (1952).

BACKGROUND DATA FOR THE BIOLOGY STEEL ROOM

S. S. Brar, Philip F. Gustafson and L. D. Marinelli

The major construction of the steel room located in the basement of the Biology and Medicine building is now completed. In structure and layout the room is identical to the room built by the Radiological Physics Division. The walls, floor, ceiling, and door are all constructed of quarter-inch steel plate with a total thickness of 9 inches.

The reduction of background has been followed using a $2\frac{1}{4}$ in. x 2 in. NaI crystal and a DuMont 6292 photomultiplier. The counting rate was analyzed using a single-channel pulse-height analyzer with different bias settings. For comparison, background data were taken at the center of the room before construction started. Further readings were taken as the construction of the room progressed, at 1/2, 1, 2, 4, 6, and 9 inches of shielding The spectral distribution of counts analyzed extends from 30 kev to 3.2 Mev

Table 35 shows background counts per minute (cpm) for two regions, 30 kev to 3.2 Mev, and 200 kev to 2.5 Mev. The second group serves as a basis for comparison with the work of Miller et al.[1] Counting rates were also obtained over the same portion of the spectrum with the counter in a lead cave with 4-inch lead walls.

TABLE 35

Background counting rates

Inches of steel*	30 kev to 3.2 Mev, cpm	200 kev to 2.5 Mev cpm
0	6008	3461
1/2	2314	1758
1	1436	1112
2	729	560
4	376	242
6 (door open)**	305	234
6 (door closed)	211	195
9 (door open)	284	207
9 (door closed)***	186	133
4 inches of lead	232	182

*9-inch steel floor was laid before walls were started.

**Door opening is 19 in. x 70 in., no door existed before 6 in. of steel were on walls and ceiling.

***An opening for an air conditioner duct (9 in. x 32 in.) is present in one wall.

We should like to take this opportunity to express our appreciation to the shop people involved in building the room for the many precautions taken to insure that no contamination occurred during construction. We are grateful also to J. W. Harrison for his sound advice and continuous assistance on this project.

Reference

1. Miller, C. E., L. D. Marinelli, R. E. Rowland, and J. E. Rose. Reduction of NaI background. Nucleonics 14 (No. 4):40-43 (1956).

THE EFFECT OF NEUTRON IRRADIATION UPON ANHYDROUS Na_2HPO_4 AND $Na_4P_2O_7$ IN QUARTZ, LIME, AND BORON-FREE GLASS TUBES

Takuya R. Sato and William P. Norris

Phosphate (PO_4) and pyrophosphate (P_2O_7) play critical roles in the metabolism of virtually all living organisms. Phosphate is one of the major components of bone, and both phosphate and pyrophosphate are essential components of enzyme systems that regulate the metabolism of the organisms themselves. Knowledge of the effect of neutrons upon phosphorus compounds might, therefore, yield results of significance to the interpretation of the effect of irradiation upon living organisms.

Thus far there has been considerable disagreement concerning the effect of neutrons and the concomitant γ-radiation upon phosphates. In most irradiations, the phosphate and pyrophosphate have been irradiated in air, and the resultant radioactive products have been isolated as insoluble chemical salts. On the basis of experiments carried out in this way, radioactivity has been reported in several different chemical species such as hypophosphorus and phosphorus acids.[1] Frequently less than half of the radioactivity has been found in the chemical species that was irradiated. These observations have led to the conclusion that the phosphorus to oxygen bonds (P-O bonds) in phosphate and in pyrophosphate are readily dissociated by the recoil of the phosphorus atom that takes place upon absorption of a neutron and emission of a γ-ray.[2-5]

In some of our earlier investigations, much of the radioactivity was found in the chemical species that were irradiated.[6-8] Recently, however, the radioactive products from certain phosphorus compounds were found to vary with the conditions of the irradiation, as for example, with the presence or absence of air and with the kind of glass from which the container was made. In view of the possible significance of these observations in biological effects produced by irradiation, we have now explored more exhaustively the effect of neutron irradiation of phosphorus compounds. We have also considered the associated effects produced by γ-rays in the reactor. To limit the number of the phosphorus compounds, we shall report here primarily the observations made with anhydrous Na_2HPO_4 and $Na_4P_2O_7$.

Materials and Methods

Materials. The salts employed for the irradiations were commercial anhydrous preparations. These salts (0.0001 formula weight) were placed in constricted tubes of various kinds of glass. The tubes were then attached to a vacuum line and evacuated overnight to a few microns of

pressure, thus removing most of the sorbed water and all but traces of air. Some of the tubes were sealed quickly with a hot flame so as not to heat the salts. Other tubes were filled with oxygen at atmospheric pressure and sealed. Those tubes containing the salts plus air were not evacuated before sealing.

Irradiations. The salts were exposed to neutron plus γ-rays in the vertical thimbles of the Argonne reactor CP-5, where the neutron flux was about 10^{13} neutrons per second, and the γ-ray radiation was roughly 500,000 r/min. The temperature was about 40 to 50°C. Most exposures were for 48 hr.

Analysis. The irradiation products were separated by electrochromatography. The irradiated salts were transferred to 10-ml volumetric flasks and dissolved in water to form 0.01 formula weight solutions. The various oxyacids contained in these solutions were separated by electrochromatography in a soft, acid-washed commercial filter paper moistened with dilute acids, for example, 0.1 M acetic or lactic acids. Semiquantitative estimation of the irradiation products was obtained by making radioautographs of the dried electrochromatograms. For acid leaching of the paper, Eaton-Dikeman filter paper (Grade 301, 0.03 inch thick) in sheets about 2 feet wide and 7 feet long was encased in a polyethylene sheet and washed with 1 M HNO_3 by siphonage and downward percolation for 24 hr. The paper was then washed with 1 M acetic acid and then with distilled water for 6 days. It was dried in air.

For the differential electrical migrations, a strip of polyethylene sheeting 2 feet wide was placed on a sheet of plywood 2 feet wide and 6 feet long, and a wide sheet of the acid-washed paper was placed on the polyethylene. The paper was moistened with 0.1 M acetic acid solution, and the excess solution was allowed to drain into large lucite electrode vessels at the ends of the tank. The moistened paper was blotted lightly with waste acid-washed filter paper, and each end dipped into about 8 liters of the acetic acid solution in each electrode vessel. The moist paper between the solutions in the electrode vessels (140 cm long), was covered with a sheet of polyethylene. The polyethylene cover was removed momentarily, and the solutions (50 μl) of the radioactive mixtures and of authentic inactive substance were placed at separate marked points 9 cm apart in a line about 15 cm from the starting end of the paper near the cathode. The paper was then covered again with the polyethylene, and D.C. electrical potential (5 volt per cm) was applied to the large graphite electrodes for 17-20 hr (current, about 10 ma). After this electrolysis, the ends of the paper in the electrode vessels were cut off; the upper polyethylene sheet was removed, and the paper was allowed to dry in air.

Detection of radioactive zones. For the detection and location of the radioactive products separated by migration in 0.1 M acetic acid, radioautographs were made with Kodak "No screen" X-ray film. The separated substances were identified by reference to authentic preparations submitted to migration in the same sheet of filter paper.

Detection of nonradioactive zones. Nonradioactive phosphorus compounds separated by electrical migration in moist paper were located by neutron activation. For this activation, the paper was dried, placed on a sheet of polyethylene, and the two sheets were rolled together, providing a roll about 3 inches in diameter. This rolled paper was wrapped in aluminum foil and placed in the thermal column of the reactor for two days at a neutron flux of approximately 10^{12} neutrons per second. When removed from the reactor, the paper was permitted to "cool" for some seven to fourteen days to reduce the background of the paper itself. Radioautographs were made with Kodak "No screen" X-ray film.

Results

Separation and identification of oxyacids of phosphorus. That some common acids of phosphorus migrate at different rates is shown by Figures 55 and 56. It was often observed, in studying irradiated phosphates, that a fraction incapable of migration in this apparatus was present. To test the possibility that this material is elemental red phosphorus, yellow phosphorus was irradiated in vacuo and then dissolved in .01 M HNO_3. Red phosphorus, in copious amounts, remained insoluble in the nitric acid and failed to move under the influence of electrochromatography. Other oxidation products of yellow phosphorus formed discrete, well-separated zones; since it is oxidized by HNO_3, one would predict that these are H_3PO_4, H_3PO_3 and H_3PO_2. However, the latter two are not distinguished from $H_4P_2O_5$ and $H_4P_2O_7$, respectively, under the experimental conditions. Irradiated phosphorus treated with bromine water yielded zones of radioactive H_3PO_4 and H_3PO_3, but no activity remained at the starting point.

Neutron-irradiated Na_2HPO_4. A typical electrochromatogram of Na_2HPO_4 after exposure to neutrons in the reactor for 2 days is reproduced as Figure 57. Comparisons with Oak Ridge $H_3P^{32}O_4$ and labeled $Na_4P_2^{32}O_7$ proved that the principal zone for the products of nonevacuated, air-containing Na_2HPO_4 consisted of pyrophosphate. Here the entire sample was converted to pyrophosphate as shown by neutron activation of the electrochromatogram. The container for the irradiation was lime glass. The small proportion of minor zones migrating slightly slower than the phosphate zone varied significantly in different irradiation experiments. The remaining small zone at the starting point was not found in solutions of the irradiated salt that had been allowed to stand in air for many days or that had been treated with bromine water, thus indicating that reduction

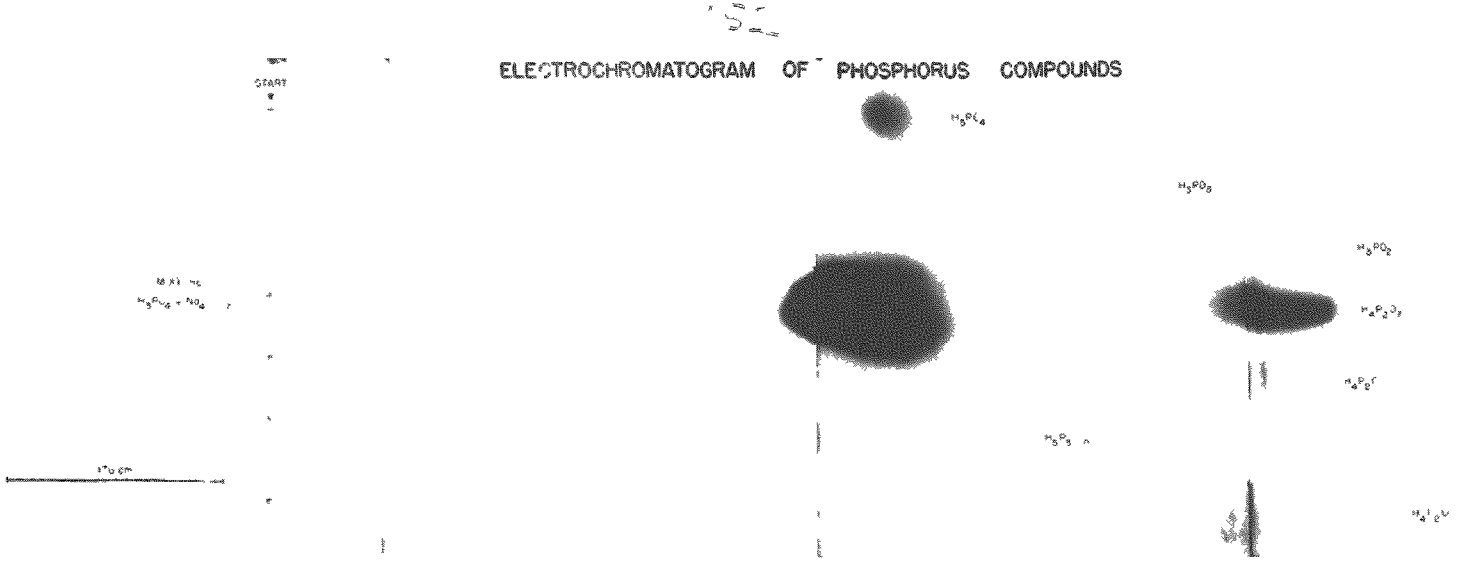

Figure 55. Radioautograph illustrating the comparative electrochromatographic position of authentic preparations of inactive H_3PO_4, Na_2HPO_3, NaH_2PO_4, $Na_4P_2O_5$, $Na_4P_2O_6$, $Na_5P_3O_{10}$, $Na_4P_2O_7$, and of neutron-irradiated K_2HPO_4. The inactive substances in the electrochromatogram were activated by exposure of the paper to neutrons, and the radioautograph was made of this activated electrochromatogram. Background solution 0.1 M acetic acid, time 20 hr, D. C. potential about 5 volts per cm.

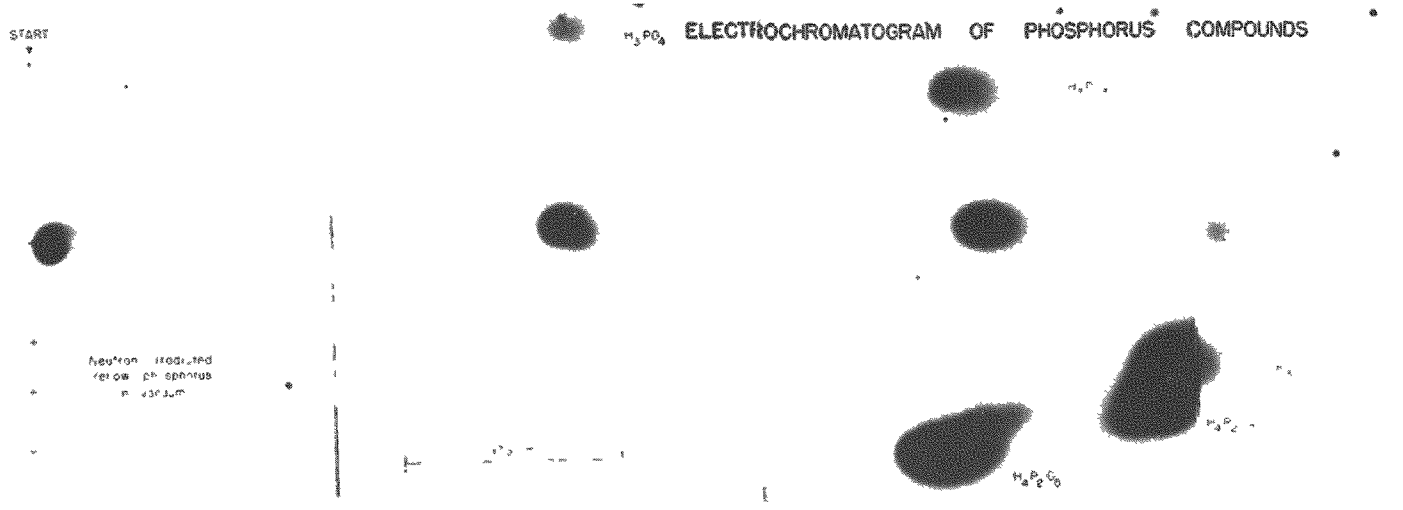

Figure 56. Radioautograph illustrating the comparative electrochromatographic position of authentic preparations of inactive H_3PO_4, Na_2HPO_3, NaH_2PO_2, $Na_4P_2O_7$, $Na_2H_2P_2O_5$, $Na_2H_2P_2O_6$, and of neutron-irradiated yellow phosphorus dissolved in .01 M HNO_3. The zones of the phosphorus compounds were located after activation of the electrochromatogram with neutrons. Background solution 0.1 M acetic acid, time 20 hr, D. C. potential about 5 volts per cm.

to elemental phosphorus does indeed occur to a limited degree. Separate experiments with the γ-ray irradiation of phosphate indicate that some, if not most, of these minor components may result from the action of the γ-rays that accompany the neutrons in the reactor.

When the container was boron-free glass and the gas was oxygen, the principal radioactive product was activated orthophosphate as indicated in Figure 57. When the boron-free glass container was evacuated, the principal radioactive product was also activated orthophosphate as shown in Figure 57.

In order to distinguish between the effects of glass and gas upon the conversion of Na_2HPO_4 into pyrophosphate, the phosphate was placed in containers of different kinds of glass which were then filled with different gases before irradiation. The results are summarized in Table 36. They show that in tubes of pure silica (quartz) and in tubes of boron-free glass (Corning 7280) there is no conversion of Na_2HPO_4 to $Na_4P_2O_7$ in air, oxygen, nitrogen, or vacuum. But in tubes of lime glass, there is complete conversion of Na_2HPO_4 to $Na_4P_2O_7$ in air, nitrogen, and oxygen, and partial conversion in vacuum.

TABLE 36

Irradiation products of anhydrous Na_2HPO_4 sealed in tubes of different kinds of glass

Container	Products of neutron irradiation under various conditions			
	In air	In vacuum	In oxygen	In nitrogen
Lime glass	$Na_4P_2O_7$	Na_2HPO_4 + $Na_4P_2O_7$	$Na_4P_2O_7$	$Na_4P_2O_7$
Boron-free glass	Na_2HPO_4	Na_2HPO_4	Na_2HPO_4	Na_2HPO_4
Quartz glass	Na_2HPO_4	Na_2HPO_4	Na_2HPO_4	Na_2HPO_4

Neutron-irradiated $Na_4P_2O_7$. A typical electrochromatogram of $Na_4P_2O_7$ after exposure to neutrons is reproduced as Figure 58. As in Figure 57 the principal zones from the compound irradiated under various conditions were identified by reference to authentic labeled $Na_4P_2^{32}O_7$. Here, however, the principal irradiation product was pyrophosphate regardless of the irradiation conditions (the container or the gas phase). The minor zone at the starting point was not found in solutions that had stood for a long time or that had been treated with bromine water.

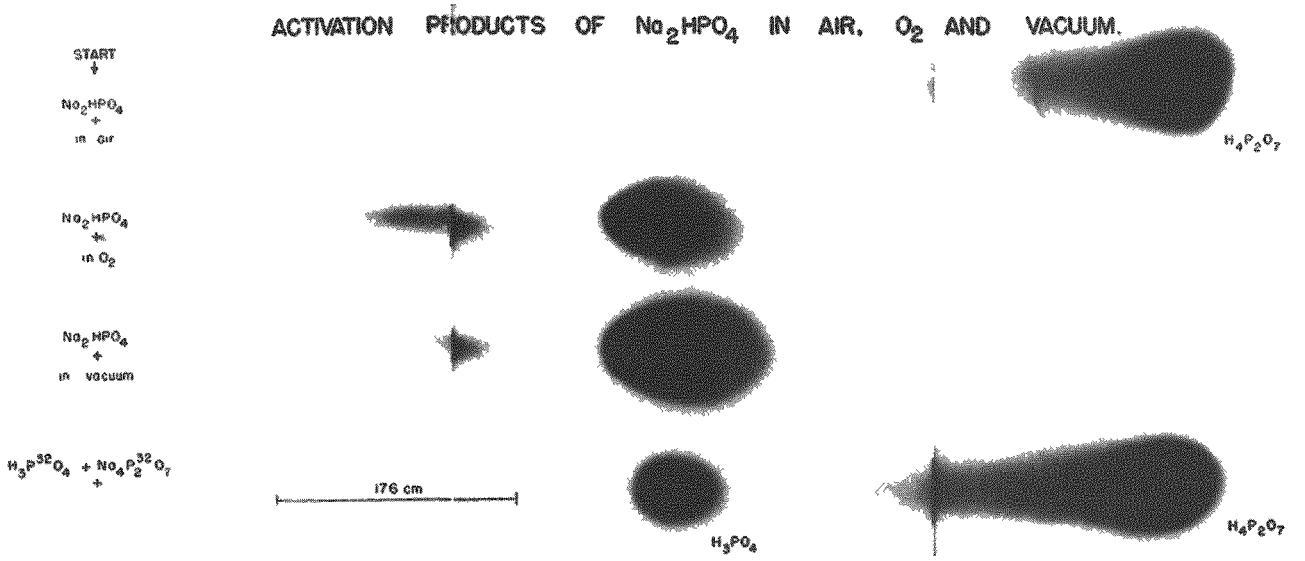

Figure 57. Radioautograph illustrating electrochromatographic separations of radioactive products formed by neutron plus γ-irradiation of Na_2HPO_4 in lime glass in air and in boron-free glass in oxygen and in vacuum. The zones were identified by simultaneous migrations of carrier-free radioactive phosphate obtained from Oak Ridge National Laboratory, and radioactive pyrophosphate obtained from the Atomic Energy Research Establishment at Harwell. Background solution 0.1 M acetic acid, time 20 hr, D.C. potential about 5 volts per cm.

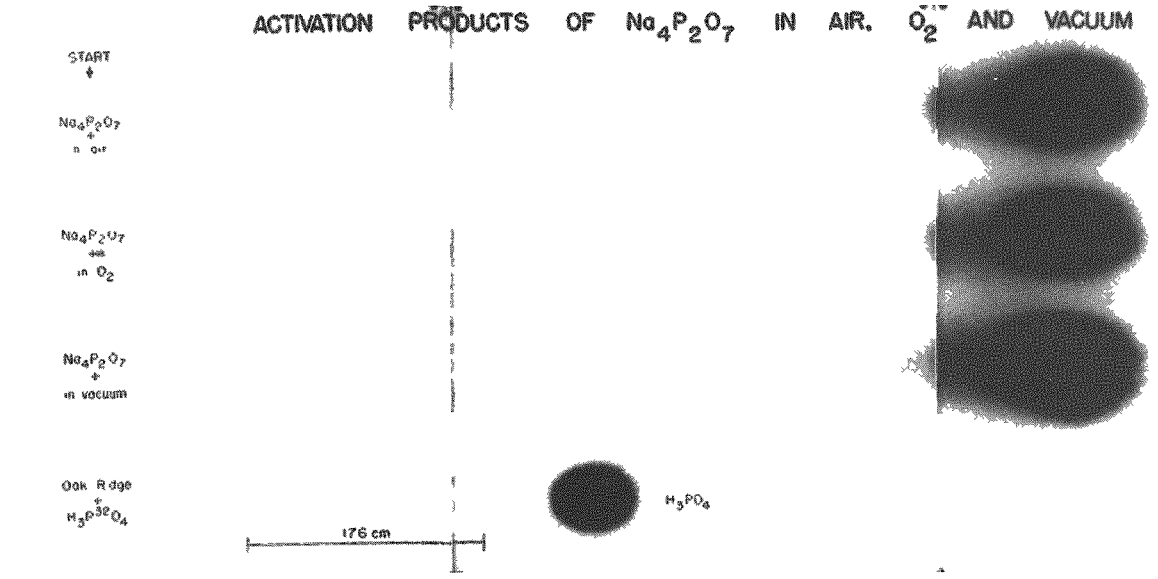

Figure 58. Radioautograph illustrating the electrochromatographic examination of radioactive products formed by neutron plus γ-irradiation of $Na_4P_2O_7$ in lime glass in air and in boron-free glass in oxygen and in vacuum. Zones identified by simultaneous migration of carrier-free radioactive phosphate, obtained from Oak Ridge National Laboratory and authentic pyrophosphate as in Figure 57. Background solution 0.1 M acetic acid, time 30 hr, D.C. potential about 5 volts per cm.

Other compounds. Neutron irradiation of various salts of phosphoric acid yielded primarily radioactive orthophosphate. For example the monoammonium, monopotassium, and tripotassium salts either in lime glass, in air, or in boron-free glass in vacuum yielded P^{32} phosphate. On the other hand, diammonium and dipotassium salts yielded much P_2O_7 when irradiated in lime glass in air, but not when irradiated in boron-free glass in vacuum.

Discussion

The parallel migrations shown in Figures 55 and 56 indicate that phosphate and phosphite should be separable from each other and from hypophosphite or pyrophosphate. They also demonstrate that hypophosphite, hypophosphate, and pyrophosphate should not be separable from each other except that pyrophosphate may be indicated by its trailing due to hydrolysis. As no secondary zones were detected in the paper sheet, large quantities of phosphorus-containing impurities could not have been present in the non-irradiated commercial salts.

Figures 57 and 58 show the relative amounts of radioactivity found in various substances produced by the action of neutrons plus γ-rays on Na_2HPO_4 and $Na_4P_2O_7$ under different conditions. These figures reveal the distribution of the radioactive phosphorus in the various products without regard to the quantity of the nonradioactive fraction of each substance present in the mixtures. They also show that the radioactive products varied with the glass of the container and with the gas contained therein.

Figure 57 shows that Na_2HPO_4 irradiated in lime glass in air yielded pyrophosphate almost completely. By contrast, Na_2HPO_4 in boron-free glass irradiated in vacuum or in oxygen yielded primarily radioactive phosphate with almost no trace of P_2O_7. Once formed, however, the pyrophosphate was remarkably stable. The mechanism for the formation of radioactive pyrophosphate from Na_2HPO_4 in air is being investigated. The formation of the $Na_4P_2O_7$ from the Na_2HPO_4 appears to be due largely to thermal effects because the entire sample of Na_2HPO_4 was condensed to pyrophosphate. (This extensive condensation has been further revealed by neutron activation of the electrochromatograms.)

156

References

1. Fiskell, J. G. A., W. A. Delong, and W. F. Oliver. The forms of phosphorus in neutron-bombarded phosphates. Can. J. Chem. 30:9-16 (1952).

2. Aten, A. H. W., Jr. Note on the chemical behavior of free ions in crystal lattices. Rec. trav. chimi. 61:467-468 (1942).

3. Thomas, W. D. E., and D. J. D. Nicholas. Radioactive phosphorus in biochemical research. Nature 163:719 (1949).

4. Libby, W. F. Reactions of high-energy atoms produced by slow-neutron capture. J. Am. Chem. Soc. 62:1930-1943 (1940).

5. Norris, W. P., T. R. Sato, and H. H. Strain. Complex phosphorus compounds of rat bone studied by neutron activation and electromigration. Quarterly Report, Division of Biological and Medical Research, Argonne National Laboratory. ANL-4745, pp. 69-70 (1952).

6. Sato, T. R., W. P. Norris, and H. H. Strain. Studies of phosphorus compounds and of bone by neutron activation plus electrical migration. Abstracts of Papers, 124th Meeting, Am. Chem. Soc., Chicago, September 6-11. pp. 43c-44c (1953).

7. Sato, T. R., W. P. Norris, W. E. Kisieleski, F. Smetana, and H. H. Strain. The effect of heat and radiation upon the condensation of carrier-free, radioactive phosphoric acid ($H_3P^{32}O_4$). Quarterly Report, Division of Biological and Medical Research, Argonne National Laboratory. ANL-5576, pp. 83-92 (1956).

THE EFFECT OF X-IRRADIATION ON S-ADENOSYLMETHIONINE

F. Schlenk

A survey of the literature failed to reveal investigations on the stability toward X-rays of sulfonium compounds of the general type,

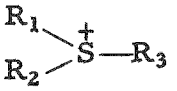

S-Adenosylmethionine was chosen as a representative of this class (for the formula see Reference (1)), because it has several important functions in cellular metabolism. Furthermore, the effects of X-irradiation on the component parts of this molecule have been studied previously; therefore, any observations beyond those recorded earlier for adenine, adenosine[2] and methionine[3] would have to be attributed to the sulfonium linkage of these units which shows unusual chemical properties[4].

Experimental

S-Adenosyl-L-methionine was obtained from yeast and purified by repeated chromatography[1]. Two concentrations were chosen for X-irradiation: 10 μmoles/ml and 0.05 μmoles/ml in water or 0.01 M phosphate buffer, pH 4.0 and 8.5; these conditions approximate the extremes of biological concentration and pH. At the high concentration, paper chromatography promised to reveal and identify split products if these were formed in excess of 1-2% of the parent material. The low concentration level was suitable for ultraviolet spectrophotometry.

The conditions of irradiation in both instances were 20,000 r at a rate of 920 r/min; 250 kv, 30 ma, filtration 0.25 mm Cu plus 1.0 mm Al; target distance 20 cm. The solutions were diluted with the requisite amounts of water or buffer, and aliquots were withdrawn before radiation and used as controls.

Paper chromatography was carried out with Whatman No. 1 paper and two solvent mixtures, ethanol, water, and acetic acid (65:34:1, v/v) and n-butanol, water, and acetic acid (60:25:15, v/v). Scanning with ultraviolet light and spraying with ninhydrin reagent were used to locate ultraviolet-absorbing material and amino acids, respectively. For each test, 10 and 30 μl (0.1 and 0.3 μmole) was applied to the papers. The threshold of response to the analytical methods after development is about 0.003 μmole per spot.

Results and Discussion

The change in the absorption spectrum of S-adenosylmethionine after irradiation with 20,000 r in 0.05 mM solution is shown in Figure 59. The decline in optical density at 260 mμ resembles qualitatively and quantitatively the changes observed by Barron and coworkers[2] with other adenine compounds. No decomposition was detected by paper chromatography in the solutions irradiated with 20,000 r at a concentration of 10 μmoles per ml of water or buffer. The efficiency of X-irradiation at this concentration was too limited to cause noticeable changes in the absorption spectrum.

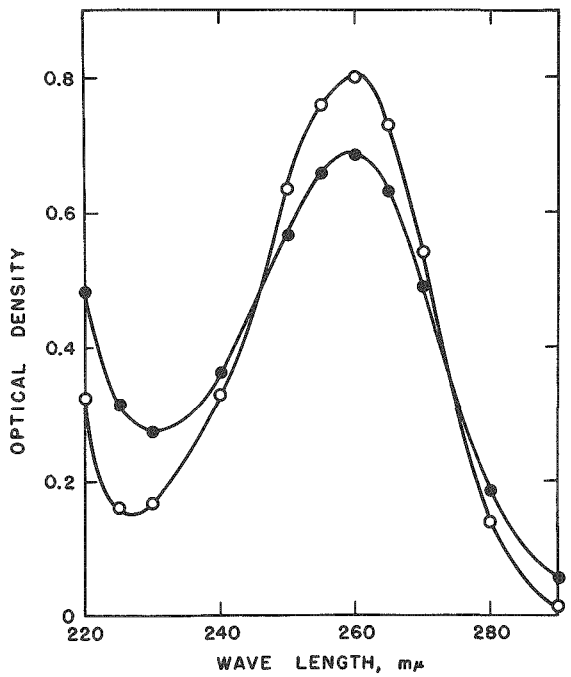

Figure 59.

The radiation-induced change in the ultraviolet absorption spectrum of S-adenosylmethionine. ○, control; ●, irradiated samples (20,000 r in 0.052 mM solution). The control samples showed identical absorption spectra in H_2O and 0.01 M phosphate buffer at pH 4.0 and 8.5; the spectra of material irradiated in water and in buffer at pH 8.5 were identical; at pH 4.0 the decline at 260 mμ (not shown here) was only 9% instead of 14%.

It may be concluded that the radiosensitivity of S-adenosylmethionine follows closely the pattern of other adenine compounds. The percentage of destruction becomes important only at levels which are at the lowest concentration range of biological material. No effects on the amino acid moiety of the molecule could be found under the present conditions; this is in accord with a recent report of Kolousek and coworkers[3] who found incipient decomposition of methionine by X-rays only with doses ranging from 10^6 to 10^7 r. The extreme chemical lability of the sulfonium bond in S-adenosylmethionine[4] apparently has no analogy in its sensitivity toward X-rays. Radiation effects on the metabolic systems involving S-adenosylmethionine and other sulfonium compounds remain to be investigated.

The author is indebted to Mr. J. E. Trier for performing the X-irradiations.

References

1. Schlenk, F., and R. E. DePalma. The metabolic relation between adenine and sulfur amino acids. Quarterly Report of the Biological and Medical Research Division, Argonne National Laboratory. ANL-5518, pp. 134-139 (1956).

2. Barron, E. S. G., P. Johnson, and A. Cobure. Effect of X-irradiation on the absorption spectrum of purines and pyrimidines. Radiation Research 1:410-425 (1954).

3. Kolousek, J., J. Liebster, and A. Babicky. Radiochemical degradation of DL-methionine. Nature 179:521-523 (1957).

4. Parks, L. W., and F. Schlenk. Hydrolysis of S-adenosylmethionine by alkali. Federation Proc. 16:231 (1957).

160

THE MEASUREMENT OF PROTEIN TURNOVER IN RAT LIVER

II. Glycine metabolism

Robert W. Swick

The first report in this series described some aspects of liver protein renewal and of arginine metabolism as measured by the incorporation of continuously administered, isotopic CO_2.[1] The present report is concerned with some kinetics of glycine metabolism in the same animals.

It was possible to study the incorporation of CO_2 into glycine in a manner similar to that employed for the study of CO_2 incorporation into the guanidine group of arginine. Benzoic acid is conjugated with glycine to form hippuric acid in the liver (and to some extent in the kidney), and excreted in the urine. Periodic measurement of the specific activity of urinary hippuric acid affords an estimate of the rise in specific activity of free glycine in the liver. This method gives only a minimal value for the rate of incorporation of isotopic CO_2 into free glycine; however, the process is still so rapid with respect to the rate of protein synthesis that only a small error in the estimation of protein turnover results.[1] The direct measurement of the rising curve of activity is undesirable for two reasons: because of the difficulties attendant to the isolation of the small amount of free amino acids present, and more seriously, because this procedure would require interanimal comparisons whereas with the method chosen, the data used in the calculations are obtained from the same animal. Thus the effects of biological variations are minimized.

Glycine metabolism in the liver may be represented by the scheme in Figure 60, which appears justified for the reasons discussed previously.[1]

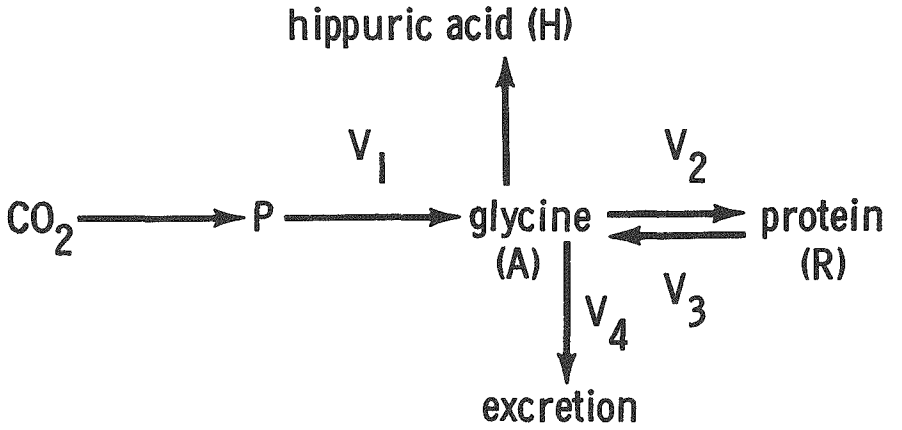

Figure 60. Glycine metabolism in liver.

The symbol V represents the reaction velocity in μM of the given compound formed by the reaction each day; the capital letters designate the specific activity of the component at any time, and were chosen to be consistent with those used in previous mathematical manipulations,[1] hence the apparent inconsistency of letters and the compounds they represent. The appropriate lower case letters will be used to indicate the amount of the component present. The rate of formation of the immediate precursors of glycine will be expressed as a single exponential since these reactions are very rapid with respect to the rate of protein synthesis and degradation.. V_2 is equal to V_3 because the animals used were in dynamic equilibrium, i.e., neither gaining nor losing weight during the experimental period.

The calculations were made according to Equations 1, 2, 3 and 4 of the previous report.[1] The data obtained were fitted to equation 4 of that report in the form below.

$$R = H\left(1 - \frac{k}{k - \frac{V_2}{r}} e^{-\frac{V_2}{r}t} + \frac{\frac{V_2}{r}}{k - \frac{V_2}{r}} e^{-kt}\right) \qquad (1)$$

where R is the specific activity of protein glycine at time t, H is the specific activity at equilibrium of the glycine excreted as hippuric acid, k is the rate of incorporation of isotopic carbon into urinary hippuric acid, and r is the amount of glycine per liver in μM; V_2 is the rate of incorporation of glycine into protein and presumably is related to the rate of protein formation.

If the experimental data are fitted to the equation

$$R = H\left[1 - \exp\left(-\frac{V_1}{V_1 + V_2} \cdot \frac{V_2}{r} t\right)\right] \qquad (2)$$

which has been derived previously,[1] an estimate of the ratio $V_1V_2/V_1 + V_2$ may be obtained. Since V_2 was measured directly, it then becomes possible to calculate V_1, the rate of synthesis of free glycine from its precursors. The computation of V_1 is subject to considerable error since it is the quotient of the product of two numbers divided by their difference. Nevertheless it was used to calculate a third relationship, viz., the reutilization of protein-derived glycine for protein synthesis, i.e., feedback, using the expression $V_2/V_1 + V_3$.

Methods

The management of the animals and the preparation of the materials has been described previously.[1,2] Liver glycine was isolated by one-dimensional descending paper chromatography on Whatman No. 17 filter paper fitted with a Whatman No. 1 wick and buffered at pH 12.[3] Phenol, nearly saturated with buffer, was the developing solvent. It was possible to

elute 4-5 mg of glycine free of other amino acid from a single sheet of paper. Hippuric acid was isolated from successive 3-hr samples of urine by extraction at pH 3.8 with ethyl acetate.[4] The ethyl acetate was removed by evaporation, and the hippuric acid was hydrolyzed with 2 cc of 3N HCl at reflux for 4 hr. Glycine was the only amino acid in these hydrolysates. The carboxyl group of glycine was liberated as CO_2 using ninhydrin, and its radioactivity was measured by proportional gas counting.[5]

Results

Incorporation of CO_2 into hippuric acid. The specific activity of the glycine excreted as hippuric acid was measured in each succeeding 3-hr sample of urine starting at t = 0 until the specific activity became constant. This required about 54 hr; a number of later samples were also analyzed to determine the equilibrium value for glycine (Table 37). The data were fitted to

$$\log (H-A) = \log H - kt \qquad (3)$$

where H is the equilibrium value for hippuric acid and A is the non-equilibrium value. The regression of log (H-A) on t was calculated and the slope k was found (Table 38). There are two factors which affect the significance of k. As mentioned above, k represents the rate of appearance of labeled body hippuric acid in the urine and not the rate of isotope incorporation into liver glycine. Secondly, the rat also conjugates benzoic acid in the kidney at about one third the rate in the liver.[6] However, the fixed carbon metabolism of kidney is much like that of liver[7] so the effect may be negligible.

TABLE 37

Radioactivity in glycine and hippuric acid

Days exposed	Protein glycine, μM	Specific activity	
		Glycine (R), cpm/mM COOH	Hippuric acid at equilibrium (H), cpm/mM COOH
4	1182	52.1	90.2
8	1182	74.8	100.7

TABLE 38

Measured parameters of glycine metabolism

k	V_2	V_2/r (glycine)	V_2/r (guanidine)
1.31	300	.253	.277
1.06	230	.194	.204

Incorporation of glycine into protein. Comparison of the specific activity of the glycine isolated from protein with the equilibrium value of hippuric acid glycine shows that protein glycine had been replaced to the extent of 58% after 4 days and to some 75% after 8 days (Table 37). When R, the specific activity of liver-protein glycine, H, the specific activity of hippuric acid, k as calculated, and r calculated from the data of Sauberlich and Baumann,[8] are fitted into Equation 1, V_2 may be calculated (Table 38). The fraction of protein glycine replaced each day is given by V_2/r; hence the rate of protein renewal may be inferred. The values for V_2/r for glycine are shown in Table 38. The agreement of the fraction of glycine replaced each day with the fraction of arginine-guanidine replaced in the same animals is excellent.

Synthesis and reutilization of glycine. V_1, the rate of synthesis of glycine from its precursors, was calculated, as was the extent of recycling of protein-derived glycine. These values are presented in Table 39, along with those obtained for arginine. The extent of feedback of glycine and the guanidine group of arginine is relatively small. It would appear that in studies designed to measure the turnover of various proteins by tracing the descending curve of radioactivity following a single exposure to isotope, it would be expedient to employ labeled non-essential amino acids, rather than the essential amino acids used heretofore in order to reduce the effects of feedback.

TABLE 39

Calculated parameters of glycine and arginine metabolism

	Glycine carboxyl	Arginine guanidine	Arginine carboxyl
V_1	1700	2490	85
	1590	2140	126
$V_2/V_1 + V_3$	.15	.06	.67
	.13	.06	.45

Summary

Adult rats were administered C^{14}-carbonate continuously for periods of 4 and 8 days. The rate of appearance of activity in the immediate precursors of liver protein, namely the free amino acids, was inferred from the rate of appearance of activity in urinary compounds formed in the liver from free arginine and glycine. At the conclusion of the experimental period, the isotopic content of protein arginine and glycine was determined and the rate of renewal was calculated. Glycine and the guanidine group of arginine gave essentially identical estimates of the average half-life of liver protein: 3 days. There was little re-utilization of either compound for protein synthesis.

References

1. Swick, R. W. The measurement of protein turnover in rat liver. I. Arginine metabolism. Quarterly Report of Biological and Medical Research Division, Argonne National Laboratory. ANL-5696, p. 112 (1957).

2. Swick, R. W., and D. T. Handa. The distribution of fixed carbon in amino acids. J. Biol. Chem. 218:577-585 (1956).

3. McFarren, E. F. Buffered filter paper chromatography of the amino acids. Anal. Chem. 23:168-174 (1951).

4. Chao, F. C., C. C. Delwiche, and D. M. Greenberg. Biological precursors of glycine. Biochim. et Biophys. Acta 10:103-109 (1953).

5. Buchanan, D. L., and A. Nakao. A method for the simultaneous determination of carbon-14 and total carbon. J. Am. Chem. Soc. 74:2389-2395 (1952).

6. Borsook, N., and J. N. Dubnoff. The biological synthesis of hippuric acid in vitro. J. Biol. Chem. 132:307-324 (1940).

7. Buchanan, D. L., and A. Nakao. Effect of growth and body size on fixed carbon turnover. J. Biol. Chem. 200:407-416 (1953).

8. Sauberlich, H. E., and C. A. Baumann. The amino acid content of certain normal and neoplastic tissues. Cancer Research 11:67-71 (1951).

INVESTIGATIONS UPON STRUCTURAL ELEMENTS OF UTERINE MUSCLE

Preliminary Observations on a Nucleic Acid-Protein Complex from Uterine Muscle

Mario A. Inchiosa, Jr., John F. Thomson, and Florence J. Klipfel

The structural proteins of skeletal muscle are generally found free of nucleic acids by the common methods of isolation[1] except for the reports by Hamoir of a nucleotropomyosin from carp muscle.[2,3] The extraction of uterine muscle by procedures commonly used for the isolation of actomyosin from skeletal muscle[4,5] have yielded what appears to be a nucleic acid-protein complex. A complex of this nature has already been observed for uterine muscle which appears similar in some respects to actomyosin of skeletal muscle.[6] Studies have been initiated to characterize this complex and consideration will be given to the possibility that it may pre-exist in smooth muscle.

Methods

Disintegration of uterine muscle was accomplished either by homogenization in the Waring blender or by fine mincing in the Latapie mincer in the presence of about 3 volumes of solution 0.3 M in KCl, 0.15 M in KH_2PO_4, and 0.15 M in K_2HPO_4. The homogenates were stirred briefly before being centrifuged, and the minces were allowed to stand for 20 hr in the cold before centrifugation. The supernatants were diluted with water to a KCl concentration of 0.025 M and allowed to stand overnight. The protein was collected by centrifugation and dissolved in 2.0 M KCl. The solution was next diluted with water to a KCl concentration of 0.44 M and centrifuged. The supernatant was saved, filtered through glass wool, and diluted with water to a KCl concentration of 0.22 M which resulted in precipitation of the nucleic acid-protein complex. The precipitate was collected by centrifugation and dissolved in 2.0 M KCl. The purification procedure was repeated. The above procedure is a modification of methods by Szent-Györgyi,[4] Mommaerts,[5] and others[5] for the extraction of the structural proteins of skeletal muscle. Storage of the protein was found to be better at concentrations of approximately 0.2% (in 1.4 M KCl) than when more concentrated.

Adenosin triphosphatase (ATPase) activity was assayed by the rate of accumulation of inorganic phosphate in the presence of added ATP under anaerobic conditions in Warburg flasks. The assays were carried out in $NaHCO_3$ buffer at pH 7.5.

Results

Within the range of ultraviolet (UV) light from 260 mμ to 290 mμ, uterine muscle preparations showed a maximum absorption at 260 mμ compared with a maximum at 280 mμ for skeletal muscle actomyosin.[7] Data on the UV absorption patterns and phosphorus and nitrogen contents of the uterine preparations are listed in Table 40.

TABLE 40

Ultraviolet absorption data, and nitrogen and phosphorus contents of the uterine muscle preparations

Extraction procedure	Source	No. of samples	Ratio 260mμ/280mμ (Av.)	Ratio N/P (Av.)
Homogenization	Cow uteri	3	1.37	8.29
Mincing	Cow uteri	5	1.42	7.99
Mincing	Guinea pig uteri	1*	1.33	7.93

*This sample was prepared from the pooled uteri of eight castrated animals.

The influence of magnesium was tested on the ATPase activity of two preparations of the nucleic acid-protein complex of uterine muscle prepared by the homogenization method of extraction. These results are presented in Table 41.

TABLE 41

The influence of magnesium on the ATPase activity of two uterine muscle preparations

	μM P accumulated / 150 μg N / hr	
	0.5 M KCl	0.5 M KCl + 0.002 M $MgCl_2$
Extract I	1.47	4.66
Extract II	2.24	5.31

Discussion

In addition to the UV absorption maxima observed at 260 mμ and the high phosphorus contents of the uterine preparations, it was found that extraction of the protein samples with hot trichloroacetic acid (TCA) decreased the nitrogen content of the residue by an amount which approximated closely that which could be accounted for as nucleic acid nitrogen on the basis of the phosphorus content of the preparations.(8) These observations taken together suggested a nucleic acid-protein complex.

The stimulatory action observed for magnesium upon the ATPase activity of the nucleic acid-protein complex appears interesting in view of the report of a stimulatory action of magnesium upon the ATPase activity of collagenase-prepared myofibrils of skeletal muscle, as compared to an inhibitory effect of magnesium upon the isolated actomyosin when these preparations were assayed in the presence of KCl.(9) The similar influence of magnesium in the case of the nucleic acid complex and the intact myofibril suggests that the complex may represent an organized smooth muscle element and lends credence to the possibility that it is pre-existing in muscle.

References

1. Szent-Györgyi, A. Chemical Physiology of Contraction in Body and Heart Muscle. Academic Press Inc., New York (1953).
2. Hamoir, G. Fish tropomyosin and fish nucleotropomyosin. Biochem. J. 48:146-151 (1951).
3. Hamoir, G. Further investigations on fish tropomyosin and fish nucleotropomyosin. Biochem. J. 50:140-144 (1951-52).
4. Szent-Györgyi, A. Chemistry of Muscular Contraction. 2nd Ed. Academic Press Inc. New York (1951).
5. Mommaerts, W. F. H. M. Muscular Contraction. Interscience Publishers Inc., New York (1950).
6. Snellman, O., and M. Tenow. A contractile element containing tropomyosin (actotropomyosin). Biochim. et Biophys. Acta 13:199-208 (1954).
7. Neurath, H., and K. Bailey. The Proteins, Vol. IA. Academic Press Inc., New York (1953).
8. Schneider, W. C. Phosphorus compounds in animal tissues. I. Extraction and estimation of desoxypentose nucleic acid and of pentose nucleic acid. J. Biol. Chem. 161:293-303 (1945).
9. Perry, S. V. The adenosinetriphosphatase activity of myofibrils isolated from skeletal muscle. Biochem. J. 48:257-265 (1951).

INVESTIGATIONS UPON STRUCTURAL ELEMENTS OF UTERINE MUSCLE

II. Influence of Various Extraction Conditions upon the Nature and Enzymatic Activity of Certain Elements of Uterine Muscle.

Mario A. Inchiosa, Jr., and Florence J. Klipfel

Earlier work with preparations of structural protein from uterine muscle, obtained by techniques common to the extraction of actomyosin from skeletal muscle, gave indications that the material was rich in nucleic acid.(1) In this part of the study an attempt was made to test the effect of various extraction conditions upon the amount of nucleic acid present in these preparations, on a roughly quantitative basis. It was felt that this type of information would contribute to an appraisal of the importance of such nucleic acid-protein complexes as pre-existing components of uterine muscle. The adenosine triphosphatase (ATPase) activity of the various preparations was also assayed.

Methods

The uterine myometrium from four cows was pooled, finely divided and mixed thoroughly. Four extracts were prepared using 25 g of the composite uterine muscle sample for each extract. Eighty-three ml of solution were used in each of the following respective extractions:

Extraction I: Homogenization of tissue for 3 min and extraction with 0.3 M KCl - 0.15 M K_2HPO_4 - 0.15 M KH_2PO_4.

Extraction II: Mincing of tissue in Latapie mincer and extraction with 0.3 M KCl - 0.15 M K_2HPO_4 - 0.15 M KH_2PO_4.

Extraction III: Mincing of tissue in Latapie mincer and extraction with 0.6 M KCl, containing approximately 1.5 μM of adenosine triphosphate (ATP) per ml.

Extraction IV: Mincing of tissue in Latapie mincer and extraction with 0.6 M KCl - 0.01 M Na_2CO_3 - 0.04 M $NaHCO_3$.

The details of extraction and purification have been discussed previously.(1) The supernatant obtained upon centrifugation of the 0.22 M KCl material in the first purification of the extract was examined in this present work as well as the precipitate obtained upon centrifugation of the 0.22 M KCl material in the second purification. The precipitate is the nucleic acid-rich material.

The ATPase activity of the extracts was assayed by measurements of the rate of accumulation of inorganic phosphate under anaerobic conditions in $NaHCO_3$ buffer at pH 7.5 in the presence of added ATP.

Pentose was determined by a modification of the procedure of Mejbaum.[2] Calculation of the total pentose was made on the basis of the purine to pyrimidine ratios obtained by Hamoir[3] for the nucleic acid of nucleotropomyosin from carp muscle.

The extraction and purification procedures and the age of the preparations at the time of the respective assays were carefully standardized in order to increase the validity of comparisons among the four extractions.

Experimental

Table 42 presents total nitrogen yields, ultraviolet absorption data, and results of ATPase assays for the 0.22 M KCl supernatant and precipitate fractions obtained under four different extraction conditions. The concentration of added ATP for the ATPase assays was 0.005 M.

The concentration of pentose was determined for the nucleic acid-rich fraction from Extraction III. The phosphorus pentose ratio (atom/mole) was calculated to be 1.17.

Discussion

Although differences were observed in the 260-mμ/280-mμ absorption ratios of the precipitate fractions obtained in the four extractions (Table 42), in each case the deficiency in nucleic acid in the precipitate was approximately accounted for in the supernatant. The good agreement among the average 260-mμ/280-mμ ratios suggests a somewhat constant pattern in the presence of nucleic acid in preparations of this nature, especially in consideration of the rather gross differences in the total nitrogen yields by the different extraction methods.

In all of the extracts, calcium stimulated the ATPase activity of both the 0.22 M KCl precipitate and supernatant fractions. Also in every case, magnesium inhibited the ATPase activity of the 0.22 M KCl precipitate fractions but stimulated the activity of the 0.22 M KCl supernatant fractions. Marked differences were found among the ATPase activities of the preparations and the relative effects of calcium and magnesium. It appears that the method of extraction has important influences upon the enzymatic activity of these preparations.

TABLE 42

Total nitrogen, ultraviolet absorption data, and ATPase activity of two fractions of uterine muscle obtained under four different extraction conditions

Extraction	Fraction	Total N, mg	Absorption ratio 260-mμ/280-mμ	Absorption ratio 260 mμ/280 mμ (Av.)	ATPase activity		
					Control 0.5 M KCl, μMP accumulated per 150 μg N/hr	0.5 M KCl± 0.002 M $CaCl_2$, % of control	0.5 M KCl + 0.002 M $MgCl_2$, % of control
I	0.22 M KCl precipitate	13.90	1.454	1.232	3.10	170	66
	0.22 M KCl supernatant	14.25	1.011		0.80	398	404
II	0.22 M KCl precipitate	13.10	1.464	1.210	3.06	127	34
	0.22 M KCl supernatant	9.38	0.955		0.19	1258	1342
III	0.22 M KCl precipitate	16.64	1.411	1.244	7.31	127	15
	0.22 M KCl supernatant	11.40	1.076		0.60	425	410
IV	0.22 M KCl precipitate	2.48	1.302	1.248	4.72	168	29
	0.22 M KCl supernatant	4.05	1.194		0.57	446	421

In earlier work[1] magnesium was found to stimulate the ATPase activity of two preparations comparable to the 0.22 M KCl precipitate fractions of the work reported here. The reason for this discrepancy has not been ascertained, but it is possible that ageing of the preparations in the earlier work and/or the effects of a more extensive purification procedure which was used at that time may have been factors.

From the results of the pentose determination it appears that probably the major part, at least, of the nucleic acid present is ribonucleic acid.

References

1. Inchiosa, M. A., Jr., J. F. Thomson, and F. J. Klipfel. Investigations upon structural elements of uterine muscle. I. Preliminary observations on a nucleic acid-protein complex from uterine muscle. This report, p. 165.

2. Albaum, H. G., and W. W. Umbreit. Differentiation between ribose-3-phosphate and ribose-5-phosphate by means of the orcinol-pentose reaction. J. Biol. Chem. 167: 369-376 (1947).

3. Hamoir, G. Further investigations on fish tropomyosin and fish nucleotropomyosin. Biochem. J. 50: 140-144 (1951-52).

TRITIUM LABELING OF ORGANIC COMPOUNDS BY SELF-IRRADIATION

Walter E. Kisieleski and Frank Smetana

Tritium, already an important tool in biological studies, has taken on an added degree of importance since the recent work of Wolfgang et al.[1] and Wilzbach.[2] The techniques of nuclear recoil and self-irradiation provide a possibility for direct tritium labeling of biologically interesting compounds. The self-irradiation method, however, yields tritiated products of high activity without the extensive radiation damage that takes place in the nuclear-recoil method from the γ-rays and the α-particles and tritons associated with pile irradiation of the sample.

We have undertaken to label some biologically useful compounds, especially those associated with bone metabolism, using the self-irradiation method. The method consists of sealing a gram of an organic compound with a few cubic centimeters of tritium gas and allowing the sample to stand at room or slightly elevated temperature for from 3 to 10 days. The labeled product can then be recovered by distillation, recrystallization, and/or chromatography.

The vacuum system shown in Figure 61 was therefore devised to handle the addition of variable amounts of tritium gas (1-100 curies) to organic compounds and, further, to combust tritium-containing samples into water for absolute activity determinations using a liquid scintillation counter.[3]

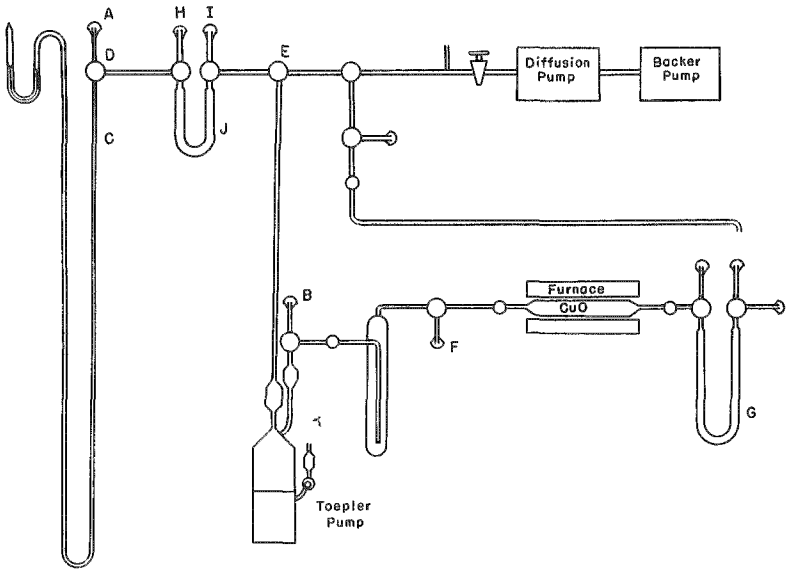

Figure 61. Vacuum apparatus for dispensing and assaying tritium gas.

General Procedure for Transferring and Handling the Tritium Gas in This System

A bulb containing tritium gas (2.59 curies/cc at STP) is attached at point A and the sample to be irradiated at point B. The entire system is then evacuated by means of a mercury diffusion pump to 10^{-6} mm/of Hg. The tritium gas is allowed to expand into a calibrated manometer C at which time temperature, pressure, and volume readings are made to calculate the activity of the tritium gas. Stopcocks D and E are then opened allowing the tritium gas from the manometer to be compressed by means of the Toepler pump into the sample to be irradiated at point B. This procedure can than be repeated for any number of samples.

After the samples have been sufficiently irradiated, based on curie-days calculation, the tritium gas can be removed by either of two methods. The irradiated sample is attached at point F and the tritium gas and any volatile products formed during the irradiation are combusted by CuO (600° C) into water and frozen out in trap G with liquid air. The alternative method allows one to attach the irradiated samples at points A, H, and I, and the tritium gas can be pumped into an evacuated bulb at point B for reuse. Volatile products during this procedure are removed by trap J.

In preliminary investigations, samples of ascorbic acid, estradiol, calciferol, galacturonic and glucuronic acids, quercetin, and rutin have been irradiated with 3 to 10 curies of tritium gas for from 1 to 10 days per sample. Direct assays of tritium activity of these samples immediately after irradiation ranged from 100 to 1000 mc/g.

Samples recrystallized from water lost from 70 to 85% of their initial activity and from 5 to 25% following a second recrystallization. These results indicate that successive recrystallizations are of little value, and in cases where other methods of purification are used initial recrystallization may be unnecessary.

In an effort to purify calciferol and ascorbic acid, paper chromatography was used.(4,5) The tritium activity on the chromatograms was located using an automatic chromatographic scanner of our own design.(6) In each case the zones of interest contained tritium activity; however, a considerable amount of activity was associated with the starting zone as well as with the solvent front. The specific activities of the zones of interest were determined by elution and absolute measurement in a liquid scintillation counter.

In the case of ascorbic acid the biological activity was determined and found to be identical to that of the pure compound.

These results indicate that following irradiation there is considerable fragmentation and polymerization, and it is certain that labeled contaminants in the parent product must be dealt with. These contaminants are present in submicrogram quantities, and great care must be taken to insure the radiochemical purity of the original compound.

These results will be reported later in more detail.

The authors are indebted to Dr. K. Wilzbach of the Chemistry Division for his helpful advice.

References

1. Wolfgang, R., F. S. Rowland, and C. N. Turton. Production of radioactive organic compounds with recoil tritons. Science 121: 715-717 (1955).

2. Wilzbach, K. Tritium-labeling by exposure of organic compounds to triton gas. J. Am. Chem. Soc. 79: 1013 (1957).

3. Kisieleski, W. E., and F. Smetana. Liquid scintillation counting of low energy β-emitters. Quarterly Report of Biological and Medical Research Division, Argonne National Laboratory. ANL-5426, p. 125 (1955).

4. Kodicek, E., and D. R. Ashby. Paper chromatography of vitamin D and other sterols. Biochem. J. 57: xii-xiii (1954).

5. Mapson, L. W., and S. M. Partridge. Separation of substances related to ascorbic acid. Nature 164: 479-480 (1949).

6. Eisler, W., W. Chorney, and W. E. Kisieleski. An automatic scanner for tritiated compounds in paper chromatograms. This report, p. 143.

OBSERVATIONS ON THE METABOLISM OF ALKYLMERCAPTANS IN YEAST

F. Schlenk

The formation of volatile mercaptans by the decomposition of sulfur-containing organic matter has been known for centuries, but details of the chemical processes leading to these compounds have been studied only in recent years. Methylmercaptan is formed by enzymatic splitting of methionine by methionase, an enzyme which is present in various microorganisms.(1) This information, however, does not explain the origin of ethylmercaptan because the amino acid analogue ethionine is not found in nature under ordinary circumstances. An entirely different mechanism of mercaptan formation has been elucidated by Neuberg in experiments with yeast: a reduction of thioaldehydes to the corresponding mercaptans.(2)

In the present paper some attempts to identify the reducing enzyme responsible for mercaptan formation will be reported. Furthermore, some observations on the assimilation of mercaptans will be described. The aliphatic mercaptans of short chain length usually have been considered as catabolic products only. However, in a survey of organic sulfur compounds for ability to serve as precursors of 5'-thioadenosine derivatives it was noted(3) that the presence of methyl- and ethylmercaptan in yeast cultures stimulates the formation of adenine sulfur compounds. The experimental conditions will be reported in this paper and the significance of the present observations will be discussed.

Materials and Methods

The culture conditions and type of yeast employed in the experiments on mercaptan assimilation have been described in an earlier report.(4) The following methods of providing mercaptan in the culture medium were used:

A. Methylmercaptan was generated from methylisothiourea and admixed in small quantity to a stream of air which was dispersed in the culture medium by a sintered glass sparger.

B. Commercial mercaptan, stored in dry ice, was pipetted at suitable intervals into the vigorously agitated solution. Sodium mercaptide, freshly precipitated from its alcoholic solution by ether, was an alternative.

C. The disulfides CH_3SSCH_3 and $C_2H_5SSC_2H_5$, of commercial origin, were used. Because of their relatively high boiling points they are handled with ease. The metabolizing yeast reduces the -S-S- linkages gradually to -SH groups.

The formation of adenine and sulfur-containing compounds by metabolizing yeast was demonstrated by extraction of the washed cells with water in a boiling water bath for 20 min, followed by qualitative and quantitative paper chromatography. S-Adenosylmethionine and S-adenosylethionine are converted under these conditions into methyl- and ethylthioadenosine. In other experiments, extraction at low temperature after treatment of the cells with liquid nitrogen yielded the thionium compounds which were determined by spectrophotometry after chromatographic separation on Dowex 50 ion exchange resin.(5)

For the experiments with alcohol dehydrogenase the crystallized enzyme of commercial origin was used after dialysis. Mercaptan from a generator was collected in 0.1 M sodium pyrophosphate; its concentration in the solution was determined by iodimetry. The addition of this solution to the alcohol dehydrogenase system resulted in a pH of 8.9, which was maintained also in the control experiments with ethanol as the substrate.

Experiments with Alcohol Dehydrogenase and Mercaptan

While the rapid reduction of thioacetaldehyde to ethylmercaptan by yeast has been well established(2) the enzyme responsible for this reaction has not yet been identified. Alcohol dehydrogenase during fermentation catalyzes the reaction

$$CH_3CH_2OH + DPN^+ \rightleftharpoons CH_3CHO + DPN\text{-}H + H^+ \qquad (1)$$

It may be surmised to catalyze also the analogous system

$$CH_3CH_2SH + DPN^+ \rightleftharpoons CH_3CHS + DPN\text{-}H + H^+ \qquad (2)$$

To test this possibility, spectrophotometry at 340 mμ with crystallized alcohol dehydrogenase from yeast, DPN, and methyl- and ethylmercaptan were carried out in the customary fashion. Figure 62 shows some results of comparative experiments with ethanol and ethylmercaptan. It may be seen that ethylmercaptan does not react in the expected fashion. The response of the mercaptan-containing system to subsequent addition of ethanol shows that the enzyme is not damaged by the sulfur compound although some inhibition is apparent. One may conclude that the alcohol dehydrogenase system does not provide the mechanism for mercaptan formation from thioaldehydes, unless under the experimental conditions used here the equilibrium thioaldehyde $\rightleftharpoons$ mercaptan is very different from that observed with ethanol and acetaldehyde. Methylmercaptan in analogous experiments was likewise found to be inert; this is less surprising, however, because its analogue methanol is almost devoid of reactivity. Unfortunately, the properties of mercaptan preclude measurements under widely varied conditions of pH and substrate concentration. Experiments with thioaldehydes were not attempted because of the inaccessibility of these compounds.

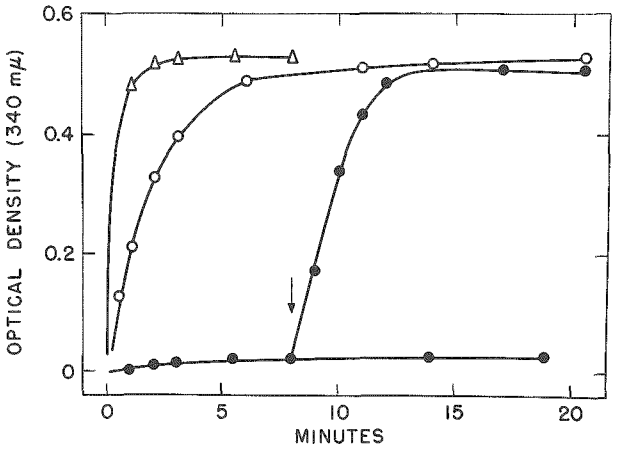

Figure 62

Examination of ethylmercaptan in the alcohol dehydrogenase spectrophotometry. The concentrations per ml were as follows: △—△, 20 μg of dehydrogenase, 3.0 μM of ethanol, 0.3 μM of DPN; ○—○, 2 μg of dehydrogenase, 3.0 μM of ethanol, 0.3 μM of DPN; ●—●, 20 μg of dehydrogenase, 3 μM of C_2H_5SH, 0.3 μM of DPN in a parallel experiment. 3.0 μM of ethanol was added after 8 min, as indicated by the arrow.

Reaction between Adenine Compounds and Mercaptans

Table 43 shows the results of experiments with yeast cultures which had been exposed to mercaptans and related compounds. To ascertain that the effects are not caused merely by an increment in readily assimilated sulfur, or by a special source of one-carbon compounds, some control experiments with substances of this type are included. Experiments with methyl- and ethylmercaptan using bakers' yeast gave virtually identical results.

In all experiments measuring S-adenosylmethionine or its homologues by extraction at low temperature it was ascertained by paper chromatography that the corresponding alkylthionucleosides were present only in insignificant amounts; conversely, in experiments involving heat extraction only the nucleosides were obtained, and the level of the parent thionium compounds was insignificant.

Discussion

In view of the negative results of the present attempts to demonstrate dehydrogenation of ethylmercaptan by alcohol dehydrogenase (Equation 2) one must assume a highly different equilibrium constant for this reaction compared with the system containing ethanol or acetaldehyde as substrate (Equation 1). An alternative would be to assume that some other reducing enzyme system is responsible for the production of mercaptan observed by Neuberg.(2)

The utilization of methyl- and ethylmercaptan in the formation of adenosine thionium compounds constitutes one of the few examples of assimilation of these substances.

The reaction mechanism by which S-adenosylmethionine and S-adenosylethionine are formed is obscure. It may be recalled that

TABLE 43

The effect of mercaptans and related compounds on the formation of thioadenosine derivatives by yeast (Torulopsis utilis)

Precursor in culture medium, procedure, and concentration*	Yield of yeast, g/100 ml culture medium	Sulfur adenine compounds extracted from yeast, μM/g	
		at 20° C**	at 100° C
None	3.0 to 3.7	0.5 to 1.0	0.5 to 1.0
CH_3SH (Procedure A)	1.5	2.6	-
CH_3SNa (Procedure B, 4 μM/ml at times zero, 6 hr and 24 hr)	2.4	-	5.6
C_2H_5SH (Procedure B, 30 μM/ml	1.2	-	2.3
$CH_3CH_2CH_2SH$ (Procedure B, 30 μM/ml)	2.5	-	$<0.3^{\dagger}$
$CH_3CH_2CH_2CH_2SH$ (Procedure B, 30 μM/ml)	2.3	-	$<0.3^{\dagger}$
$CH_3S\text{-}SCH_3$ (Procedure C, 10 μM/ml)	3.2	2.2	-
$C_2H_5S\text{-}SC_2H_5$ (Procedure C, 6 μM/ml)	3.1	2.7	-
$Na_2S_2O_3$ (4.0 μM/ml	3.7	0.8	-
$(NH_4)_2S$ (10 μM/ml)	2.1	0.4	-
CH_3OH (8 μM/ml)	2.8	0.9	-
CH_3NH_2 (8 μM/ml)	3.6	0.7	-
HCOOH (8 μM/ml)	3.1	0.4	-

*Details of the procedures are given under Materials and Methods. The culture time was 48 hr at 30° C.

**Extraction with water at 20° C after thermal shock of the cells by liquid nitrogen yields S-adenosylmethionine or its alkyl homologues; extraction for 20 min at boiling temperature yields 5'-methylthioadenosine or its homologues.

† No sulfur adenine compound could be detected.

S-adenosylmethionine is obtained by the reaction of methionine with adenosine triphosphate (ATP). An analogous reaction with methylmercaptan would lead to methylthioadenosine:

$$ATP + HSCH_3 \longrightarrow \text{Methylthioadenosine} + 3\ P_{(i)} \qquad (3)$$

However, the extraction at low temperatures of yeast treated with methyl- or ethylmercaptan shows the presence of S-adenosylmethionine or S-adenosylethionine rather than of the nucleosides; the latter are formed mainly by thermal decomposition during extraction with heating. Therefore, the utilization of the mercaptans for methionine or ethionine formation, followed by the condensation with ATP, appears more likely.

In summary, experiments with alcohol dehydrogenase have failed to yield evidence for its role in mercaptan formation by yeast. Methyl- and ethylmercaptan are incorporated by yeast into S-adenosylmethionine and S-adenosylethionine.

References

1. Kallio, R. E., and A. D. Larson. Methionine degradation by a species of Pseudomonas, in a Symposium on Amino Acid Metabolism. W. D. McElroy and B. Glass, eds. pp. 616-634. The Johns Hopkins Press, Baltimore (1955).

2. Neuberg, C. Biochemical reductions at the expense of sugars, in Advances in Carbohydrate Chemistry 4:75-117 (1949).

3. Schlenk, F., and J. A. Tillotson. Metabolism of methyl- and ethylmercaptan in yeast (Torulopsis utilis). Federation Proc. 13:290-291 (1954).

4. Schlenk, F. Method for the preparation of 5'-methyl and 5'-ethylthioadenosine. Quarterly Report of Biological and Medical Research Division, Argonne National Laboratory. ANL-5378, pp. 126-127 (1955).

5. Schlenk, F., and R. E. DePalma. Progress Report: The metabolic relation between adenine and sulfur amino acids. Quarterly Report of Biological and Medical Research Division, Argonne National Laboratory, ANL-5518, pp. 134-139 (1956).

UNSATURATED FATTY ACIDS AND CHOLESTEROL METABOLISM

I. Influence of Linoleic Acid in Diet on Cholesterol Levels in Liver and Blood

Peter D. Klein

This report deals with the first phase of a study intended to explore the relationships of dietary fat level, unsaturated fatty acid content, and dietary cholesterol in the rat. Some aspects have been previously described by other authors;(1) however, in order to establish a firm basis for future studies, some repetition was unavoidable.

Methods

Animals. Male weanling Holtzmann rats, received at an age of 20 days were placed immediately on the experimental diets, in 5 groups consisting of 20 animals each. The composition of the diets is given in Table 44. For purposes of convenience, they will be abbreviated as follows: FF, "fat free"; 5 H, 5% Crisco; 5 U, 5% corn oil; 30 H, 30% Crisco; 30 U, 30% corn oil; and ST, stock diet.

TABLE 44

Composition of experimental diets

	Percentage composition				
	FF	5 H	5 U	30 H	30 U
Salts, Wesson	4.0	4.0	4.0	4.0	4.0
Vitamin mixture*,**	0.50	0.50	0.50	0.63	0.63
Casein**	18.0	18.0	18.0	22.50	22.50
Hydrogenated fat		5.0		30.0	
Corn oil			5.0		30.0
Anhydrous glucose	77.5	72.5	72.5	41.87	41.87
	100.0	100.0	100.0	100.0	100.0

*Vitamin mixture:

Calciferol	2 mg	Niacin	1.0 g	α-tocopherol	20 g
Biotin	50 mg	Riboflavin	1.2 g	Choline	50 g
Folic acid	50 mg	Thiamine	1.8 g	Inositol	50 g
β-carotene	400 mg	B_{12} concentrate	2.0 g	Sucrose to	500 g
Menadione	1000 mg	Calcium panthothenate	6.0 g		

**Ingredient adjusted to compensate for increased caloric value of diet.

Cholesterol determinations. Free and total cholesterol determinations were performed on plasma, red blood cells, and liver by the revised method of Schoenheimer and Sperry.(2) Blood obtained by cardiac puncture was collected with a small amount of potassium oxalate to prevent clotting, after which it was centrifuged and the plasma drawn off in the usual manner. Small samples of liver were obtained without sacrificing the animal by means of a lateral incision in the right side through which a portion of the small triangular lobe of the liver was removed. Operated animals recovered quickly and appeared to be normal in weight gain and other respects thereafter.

Analysis of unsaturated fatty acids. Determination of linoleic, linolenic, arachidonic and pentaenoic acids were carried out by the method of Herb and Riemenschneider.(3)

Results and Discussion

Table 45 lists the values for free and total cholesterol in plasma and liver, and free cholesterol (only form present) in the red blood cells. Table 46 lists the content of unsaturated fatty acid in the diets used. Figure 63 is a plot of the cholesterol values versus the logarithm of the linoleic acid content of the diet.

TABLE 45

Cholesterol values in rats on various diets*

Group	Plasma			RBC	Liver		
	Free	Total	F/T	Free	Free	Total	F/T
FF	8.2	28.3	.290	88.0	152	389	.389
5 H	10.8	37.8	.310	83.5	158	207	.763
5 U	17.3	51.3	.338	102.5	149	250	.595
30 H	18.2	58.2	.312	105.1	144	253	.569
30 U	16.5	62.3	.266	106.2	172	366	.471
Stock	26.8	72.8	.368	174.9	162	222	.729

*All values are in mg%. Five animals were tested per group. With the exception of the plasma values, the standard deviations were usually of the order of 3%; plasma values varied up to a standard deviation of 10%.

TABLE 46

Unsaturated fatty acid contents of experimental diets*

	FF	5 H	5 U	30 H	30 U	ST
Linoleic acid	0.43	3.49	14.05	19.42	81.23	11.75
Linolenic acid	0.23	0.19	1.92	0.11	2.09	1.08
Arachidonic acid	0.12	0.00	0.38	0.00	0.12	0.53
Pentaenoic acid	0.18	0.05	0.17	0.87	0.12	1.01

*All values are in mg/g of diet.

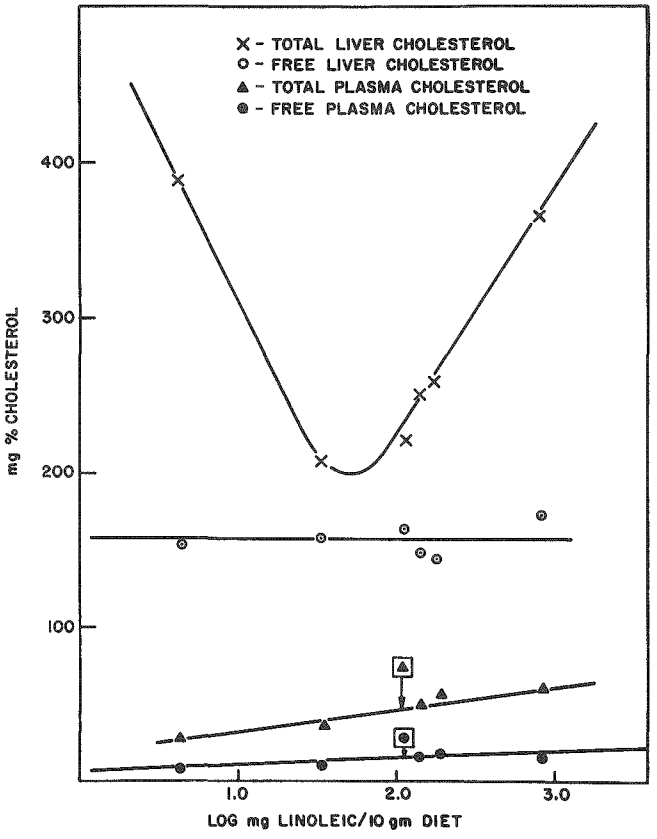

Figure 63.

Blood and liver cholesterol values as a function of dietary linoleic acid. In order of increasing linoleic acid content, the points represent FF, 5 H, ST, 5 U, 30 H and 30 U. Note deviation of plasma values in stock animals.

The following observations are pertinent: first, the effect of increasing fat (and linoleic acid) levels of the diet is a slow increase in both forms of plasma cholesterol. The esterified cholesterol (total minus free) rises at a slightly faster rate than the free form. Second, the stock diet has an effect on both of these values as well as on the red blood cell cholesterol, raising them significantly above those of the other diets. This matter will be discussed subsequently. Third, while the free form of liver cholesterol is seemingly unaffected in these experiments, the esterified cholesterol displays a behavior which must be regarded as biphasic. In the right half of the graph it is evident that the appearance of esterified cholesterol in the liver is proportional to the concentration of linoleic acid in the diet, not to total fat content (compare, for example, 30 H with 30 U in Table 45). Below 5 U the trend levels off, and then reverses itself. A suitable explanation for this phenomenon can not be given at this time; however, there is the following possibility. The metabolism of cholesterol and the unsaturated fatty acids are intimately linked with each other, and the availability of linoleic acid may determine the amount of esterified cholesterol in the liver. When linoleic acid drops below a certain level, cholesterol esters are perhaps transported back to the liver where the vital unsaturated fatty acids esterified with them are reclaimed. Substitution of a saturated fatty acid may then lead to the accumulation of a new ester because of its altered physicochemical properties. Work now in progress is expected to reveal the type of lipid esterified with cholesterol at both dietary extremes and should make possible the acceptance or rejection of this possibility.

It should be noted that with respect to the liver cholesterol values, the data obtained from the stock animal are in every way consistent with those obtained from the other diets. In light of the deviations noted in values for plasma and red blood cells, one may note that some nutrient other than linoleic acid must be affecting the blood values. This is not surprising, since increased cholesterol levels are known to result from a deficiency of several other factors, including methionine, choline and nicotinamide. Adequate levels of these may not be present in the stock diet.

It should be noted that these diets, with the possible exception of the stock diet, are essentially cholesterol-free. The absence of cholesterol may explain the differences encountered between the actions of the unsaturated and hydrogenated fats. Here a definite cholesterogenic tendency on the part of the unsaturated fat was observed, contrary to the results reported by Shapiro and Freedman.(4)

References

1. Alfin-Slater, R. B., L. Aftergood, A. F. Wells, and H. J. Deuel, Jr. The effect of essential fatty acid deficiency on the distribution of endogenous cholesterol in the plasma and liver of the rat. Arch. Biochem. and Biophys. 52:180-185 (1954).

2. Sperry, W. M., and M. Webb. A revision of the Schoenheimer-Sperry method for cholesterol determination. J. Biol. Chem. 187:97-106 (1950).

3. Herb, S. F., and R. W. Riemenschneider. Spectrophotometric micro-method for determining polyunsaturated fatty acids. Anal. Chem. 25:953-955 (1953).

4. Shapiro, S. L., and I. Freedman. Effect of essential unsaturated fatty acids and methionine on hypercholesteremia. Am. J. Physiol. 181:441-444 (1955).

UNSATURATED FATTY ACIDS AND CHOLESTEROL METABOLISM

II. Influence of Linoleic Acid in Diet on the Unsaturated Fatty Acid Content of Cholesterol Esters in Liver and Plasma

Peter D. Klein

In the first report in this series[1] an investigation was carried out on the effect of linoleic acid levels in the diet on plasma and liver cholesterol levels. It was found that, as reported by other workers,[2] there is an accumulation of cholesterol esters in the livers of fat-deficient animals; in addition, on high linoleic acid diets, there was also an accumulation of liver cholesterol esters. The present report deals with the analysis of the unsaturated fatty acids of the cholesterol esters of these animals both in liver and in plasma.

Methods

Animals. The dietary groups described in the first report[1] were used. These consisted of five groups; FF, "fat-free;" 5 H, 5% Crisco; 5 U, 5% corn oil; 30 H, 30% Crisco; and 30 U, 30% corn oil.

Analytical procedures. Cholesterol determinations and unsaturated fatty acid analyses were carried out as previously described.[1] Chromatographic separation of the cholesterol esters following precipitation of the phospholipides was done according to the method of Hanahan and Barron.[3] During the chromatographic separation, elution of the esters was followed by the method of Brown et al.[4] because of the shorter time required for this determination. In all cases, the final fraction of cholesterol esters resulting from the combination of eluates was measured by the previously used method of Sperry and Webb.[5] Isolation of cholesterol esters from livers was carried out on five animals from each group. The plasmas were pooled by groups to provide sufficient material for analysis.

Results and Discussion

In Table 47 the values for liver cholesterol esters are given in terms of the unsaturated fatty acids esterified with the cholesterol. Values are calculated in terms of moles per 100 moles of cholesterol, thus yielding directly the percentage composition of each acid. The relationship between ester linoleic acid and dietary linoleic acid has been plotted in Figure 64.

The values clearly indicate a smooth relationship between ester linoleic acid and the dietary content of this ingredient. Thus there are no discontinuities which could account for the accumulation of ester cholesterol

at either end of the dietary extremes. The data also indicate that the variation in ester content is purely a function of the linoleic content, and does not follow the absolute dietary fat content.

TABLE 47

Unsaturated fatty acid composition of cholesterol esters in rat liver
(Values as moles of fatty acid per 100 moles of cholesterol)

Group	FF	5 H	5 U	30 H	30 U
Linoleic	2.1	5.4	14.3	13.4	32.5
Linolenic	0.7	1.3	1.6	1.3	1.7
Arachidonic	0.1	1.0	1.2	2.6	1.2
Pentaenoic	0.1	0.0	0.2	0.2	0.8
Total fatty acid (moles)	3.0	7.7	17.3	17.5	36.2

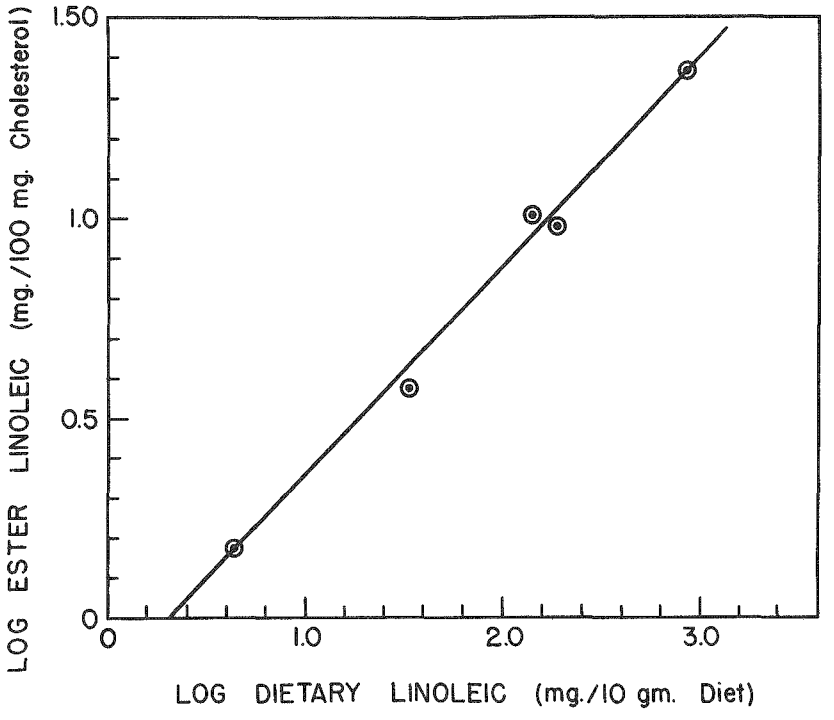

Figure 64

Relationship between cholesterol ester content of linoleic acid and dietary concentration of linoleic acid.

It should be noted here, for comparison later, that the major unsaturated fatty acid component in liver esters is linoleic acid; furthermore, even at the highest levels measured, the total unsaturation of the esters amounts to only 36%, i.e. approximately 60% of the fatty acids esterified with liver cholesterol are saturated or monoethenoic.

In contrast to the values obtained in liver, the composition of plasma esters (Table 48) indicated a much higher concentration of unsaturated fatty acids which could not be related in a simple manner to the diet. Linoleic acid in the esters increase twofold between a fat-free and a 5% Crisco diet but thereafter increased only slightly. On the other hand, arachidonic acid, not present to any great extent in liver esters, underwent a tenfold increase between the lowest and the highest fat levels. The most striking portion of this rise took place between 5% Crisco and 30% Crisco. It may be recalled from the previous report that these two diets contained 3.49 and 19.4 g of linoleic/g diet respectively and no arachidonic acid. This remarkable increase is suggestive of some critical level in unsaturated fatty acid in the diet which suddenly makes unsaturated fatty acid available for plasma esters. Finally it may be noted that the total ester content of unsaturated fatty acids, even in the fat-deficient plasma, is higher than those encountered in liver; in fact, at a 30% Crisco level, cholesterol is esterified exclusively with unsaturated fatty acids.

TABLE 48

Unsaturated fatty acid composition of cholesterol esters in rat plasma
(Values as moles of fatty acid per 100 moles cholesterol)

Group	FF	5 H	5 U	30 H	30 U
Linoleic	21.0	40.0	41.5	42.6	51.7
Linolenic	11.0	11.2	6.3	8.5	12.1
Arachidonic	3.3	2.5	15.9	45.0	35.7
Pentaenoic	3.3	1.4	1.6	2.5	2.5
Total fatty acid (moles)	38.6	55.1	65.3	98.6	102.0

With these relationships in mind, it should prove fruitful to examine the plasma lipides of humans consuming comparable amounts of dietary fat. The American diet is roughly comparable to that of the 30 H group in terms of fat composition. The report[6] of the isolation from human plasma of cholesterol oleate in yields of 50% suggests significant differences between the two species in their metabolism of cholesterol and unsaturated fatty acids.

References

1. Klein, Peter D. Unsaturated fatty acids and cholesterol metabolism. I. Influence of linoleic acid in the diet on cholesterol levels in liver and blood. This report, p. 180.

2. Alfin-Slater, R. B., L. Aftergood, A. F. Wells, and H. J. Deuel, Jr. The effect of essential fatty acid deficiency on the distribution of endogenous cholesterol in the plasma and liver of the rat. Arch. Biochem. and Biophys 52: 180-185 (1954)

3. Hanahan, D J., and E. J. Barron. Chromatographic separation of acetone-soluble lipides. Federation Proc. 16: 191 (1957).

4. Brown, H. H , A. Zlatkis, B. Zak, and A. J. Boyle. Rapid method for determination of free serum cholesterol. Anal. Chem. 26:397-399 (1954).

5. Sperry, W. M., and M. Webb. A revision of the Schoenheimer-Sperry method for cholesterol determinations. J. Biol. Chem. 187:97-106 (1950).

6. Keegan, P., and R. G. Gould. Isolation of a crystalline cholesteryl ester from normal plasma. Federation Proc. 12:228 (1953)

UNSATURATED FATTY ACIDS AND CHOLESTEROL METABOLISM

III. Distribution of Unsaturated Fatty Acids in Liver and Plasma of Rats Fed Varying Levels of Linoleic Acid

Peter D. Klein

In the previous report, the unsaturated fatty acid composition of cholesterol esters in liver and plasma of five dietary groups was reported.(1) It appeared of interest to examine the distribution of unsaturated fatty acids between phospholipides and cholesterol esters as related to the total amount of these acids present. It might be expected that some insight into the mobility and metabolism of these compounds could be gained.

Methods

The animals used, the dietary conditions and the analytical procedures were described in the previous report.(1)

Results and Discussion

The analysis of unsaturated fatty acids in the total lipide, phospholipide and cholesterol esters of liver was carried out, using five animals in each group. The pooled plasma samples were used for a single analysis for each group. Using the values found for cholesterol esters in the first report of this series,(2) the concentrations of unsaturated fatty acids as esters were calculated; total lipide and phospholipide concentrations were calculated from the weight of tissue analyzed. No noteworthy variations in tissue dry weight or organ weight were found in any of the groups.

The results for liver and plasma are shown in Tables 49 and 50. Considering the liver values first, it will be noted that the bulk of the total unsaturated lipide found in liver is located in the phospholipide fraction. The unsaturated fatty acids in phospholipides contain approximately 90% of the total linolenic, arachidonic and pentaenoic acids. The total linoleic acid, on the other hand, is apportioned between the phospholipides and the cholesterol esters in the ratio of 75 to 25 until a dietary level of 30% corn oil is reached, whereupon the percentage found in cholesterol esters rises to about 60%.

In plasma, however, the picture is reversed. The phospholipides are conspicuous by their almost complete lack of unsaturated fatty acids. Indeed, the cholesterol esters contain better than 90% of all unsaturated fatty acids, with the exception of the 30% corn oil group, in which triglycerides apparently make up a sizeable contribution to the total unsaturated lipide.

TABLE 49

Distribution of unsaturated fatty acids in rat liver lipides.
All values are expressed in mg/100 g liver.

Group	FF*	5 H*	5 U*	30 H*	30 U*
Total					
Linoleic	89	176	407	292	717
Linolenic	235	79	37	39	44
Arachidonic	127	347	555	375	385
Pentaenoic	42	73	135	92	54
Acetone-Insoluble (Phospholipide)					
Linoleic	106	218	310	244	295
Linolenic	247	124	43	109	69
Arachidonic	132	293	466	360	331
Pentaenoic	42	76	130	80	62
Cholesterol Esters					
Linoleic	36	19	104	106	455
Linolenic	12	4	11	10	24
Arachidonic	1	4	10	22	18
Pentaenoic	2	7	2	2	13

*FF, "fat-free;" 5 H, 5% Crisco; 5 U, 5% corn oil; 30 H, 30% Crisco; 30 U, 30% corn oil.

TABLE 50

Distribution of unsaturated fatty acids in rat plasma lipides.
All values are expressed in mg/100 ml plasma.

Group	FF*	5 H*	5 U*	30 H*	30 U*
Total					
Linoleic	2.5	7.1	7.7	11.0	26.6
Linolenic	1.8	1.2	0.0	0.3	0.3
Arachidonic	0.9	4.8	6.8	9.2	11.6
Pentaenoic	0.3	0.2	0.3	0.6	0.6
Acetone-Insoluble (Phospholipide)					
Linoleic	0.0	0.1	0.2	1.2	1.8
Linolenic	0.1	0.1	0.0	0.2	0.1
Arachidonic	0.1	0.1	0.2	0.5	0.9
Pentaenoic	0.1	0.1	0.1	0.1	0.2
Cholesterol Esters					
Linoleic	3.0	4.9	10.2	12.3	17.1
Linolenic	1.6	1.4	1.5	2.4	4.0
Arachidonic	0.5	0.3	4.2	13.7	12.8
Pentaenoic	0.6	0.2	0.5	0.9	1.0

*FF, "fat-free;" 5 H, 5% Crisco; 5 U, 5% corn oil; 30 H, 30% Crisco; 30 U, 30% corn oil.

Thus we are faced with an unusual picture with respect to the percentage of total unsaturated lipide carried by a given fraction. There is a greater resemblance between liver phospholipide and plasma cholesterol esters than between either liver and plasma phospholipides or liver and plasma cholesterol esters. Exactly how this may be interpreted in terms of lipide metabolism is not clear; however it suggests that the esters of rat plasma are used almost exclusively as the means of carrying unsaturated fatty acids to other portions of the body, since the rat apparently does not utilize plasma phospholipides to carry out this function. One might indeed visualize these two carriers as highly specialized individuals, keeping the two types of lipide relatively separated.

It is of equal interest, however, to consider the source of the plasma cholesterol esters. They closely resemble liver phospholipides in composition, not only in terms of total unsaturated fatty acids, but also in terms of the relative concentrations of the individual fatty acids. Liver ester cholesterol, on the other hand, is low in the more highly unsaturated members. This might suggest that some form of transesterification takes place before the liver ester cholesterol is secreted from the liver into the plasma. While this possibility cannot be ruled out, a more likely possibility presents itself on examination of the absolute concentrations of ester in liver and plasma. Assuming that the weights of plasma and liver are of the same order of magnitude, it appears that liver ester cholesterol could supply the plasma with sufficient esters of the given composition to account for all of the plasma esters found. Thus, in no case does the total amount of any fatty acid esterified with plasma cholesterol exceed its concentration in liver. It must be added, of course, that the production by the liver of cholesterol esters of the composition found in plasma would involve a highly selective process. Such a production mechanism would play an important role in the control of plasma cholesterol.

References

1. Klein, P. D. Unsaturated fatty acids and cholesterol metabolism II. Influence of linoleic acid in diet on the unsaturated fatty acid content of cholesterol esters in liver and plasma. This report, p. 185.

2. Klein, P. D. Unsaturated fatty acids and cholesterol metabolism. I. Influence of linoleic acid in diet on cholesterol levels in liver and blood. This report, p. 180.

PROGRESS REPORT· THE GIBBERELLINS

III. The Biogenesis of C^{14}-Gibberellic Acid

Ronald Watanabe

Preliminary fermentation experiments using the NURB-2284 strain* of the fungus, Gibberella fujikuroi, have produced satisfactory yields of gibberellic acid.[1] These procedures were utilized for the biosynthesis of uniformly labeled C^{14}-compounds for use in physiological studies related to their action in the plant.

A small inoculum from an actively growing colony of the fungus G. fujikuroi (NURB-2284) was submerge-cultured for 14 days at 76°F in 25 ml of Raulin-Thom medium[2] containing 2.636 mc of uniformly labeled C^{14}-sucrose. The specific activity of the medium was 9.39 μc of C^{14} per mg of carbon. During the fermentation, CO_2-free air was passed over the culture media and subsequently bubbled through normal alkali and saturated $BaCl_2$ solutions. The distribution of C^{14} activity after the 14-day culture period is shown in Table 51.

TABLE 51

Distribution of C^{14} activity after 14-day culture period

(Total activity incorporated, 2.636 mc)

Fraction	Activity, % of total used
Supernatant	8.5
Fungal cells	28.0
Respired CO_2	55.0
Unaccounted	8.5†

†This may have been respired CO_2 which was unabsorbed by the alkali as indicated by the turbidity in the $BaCl_2$ trap on the fourth day of fermentation.

The extraction procedure (Fig. 65) of Borrow et al.[3] was used for the isolation of gibberellic acid. The relative efficiency of the extraction procedure is shown on the autoradiogram (Fig. 66) of an ascending chromatogram of aliquots from each fraction. The numbers at the bottom of the autoradiogram correspond to the numbers of the fraction in Figure 66. The arrow corresponds to the position of an authentic sample of gibberellic acid** which had been chromatographed alongside the labeled fractions on

*Kindly supplied by Dr. Frank Stodola, Northern Utilization Research Branch, United States Department of Agriculture, Peoria, Illinois.

**Kindly supplied by Dr. Kurt Leben, Eli Lilly and Company, Indianapolis, Indiana.

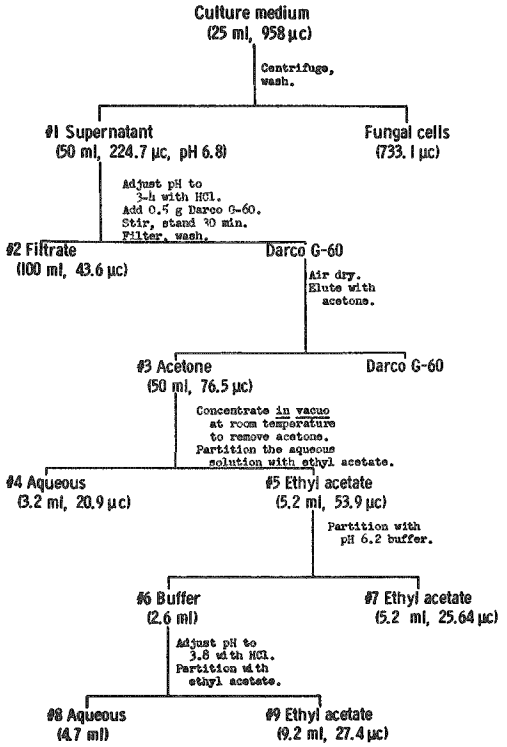

Figure 65. Isolation scheme for gibberellic acid.

Figure 66. Autoradiogram of fractions obtained during isolation of gibberellic acid.

Whatman No. 1 paper with n-butanol:propionic-acid solvent.[4] Fractions 6 and 8 were not chromatographed because of their high salt concentration. The autoradiogram indicates that fractions 4 and 7 retained a small amount of gibberellic acid, and fraction 9 contained not only a spot corresponding to gibberellic acid but also several unknown substances. This fraction is currently being processed to obtain pure gibberellic acid for translocation and metabolism studies. Preliminary bioassay[1] of fraction 9 with pinto bean indicates a yield of about 2 mg of labeled gibberellic acid.

References

1. Watanabe, R., and N. J. Scully. A preliminary report: the gibberellins. Quarterly Report of the Biological and Medical Research Division, Argonne National Laboratory. ANL-5696 pp. 104-105 (1956).

2. Brian, P. W., P. J. Curtis, and H. G. Hemming. A substance causing abnormal development of fungal hyphae produced by Penicillium janczewskii Zal. I. Biological assay, production, and isolation of "curling factor." Trans. Brit. Mycol. Soc. 29:173 (1946).

3. Borrow, A., P. W. Brian, V. E. Chester, P. J. Curtis, H. G. Hemming, C. Henehan, E. G. Jeffreys, P. B. Lloyd, I. S. Nixon, G. L. F. Norris, and M. Radley. Gibberellic acid, a metabolic product of the fungus Gibberella fujikuroi: Some observations on its production and isolation. J. Sci. Food Agri. 6:340-348 (1955).

4. Benson, A. A., J. A. Bassham, M. Calvin, T. C. Goodale, V. A. Haas, and W. Stepka. The path of carbon in photosynthesis. V. Paper chromatography and radioautography of the products. J. Am. Chem. Soc. 72:1710 (1950).

PROGRESS REPORT: THE GIBBERELLINS

IV. The Translocation of C^{14}-Gibberellic Acid and/or Its Metabolic Fragments in the Pinto Bean

Ronald Watanabe and Norbert J. Scully

The biosynthesis and isolation of C^{14}-gibberellic acid (GA) have been described in a previous report.(1) An aliquot of the final fraction, which contained not only the labeled GA but several unknown substances, was chromatographed by the streak technique on Whatman No. 1 paper using an n-butanol-ammonia (1.5 N NH_4OH) solvent. The autoradiogram (Fig. 67) shows a band marked AA corresponding to the position of what is currently accepted as authentic GA and, in addition, a closely following unknown band BB. The AA band was cut out of the chromatogram and eluted with ethanol and water. The eluate was concentrated in vacuo at room temperature to dryness. The residue was dissolved in 50% ethanol-water to give a final concentration of approximately 1 μg of GA per μl.

Ten-μl aliquots, equivalent to 186,000 cpm each, were applied to the first internodes of 6 young pinto bean plants. Twenty-four and 48 hr after application, the plants were harvested by drying in a plant press at 70° C for 24 hr. The dried plants were exposed to No-Screen X-ray films for 3 weeks. The C^{14} distribution patterns for a representative plant of each harvest period are shown on the autoradiograms (Figures 68 and 69). The figures show that radioactivity was distributed throughout the plant including the roots, although the true pattern in roots is not fully defined due to the loss of fine root tissues by handling. The higher concentrations of radioactivity in young actively growing tissues above the site of application, particularly in the two youngest leaves expanded from the bud, suggests that, unlike the auxins, gibberellic acid does not show polar movement within the plant. This conclusion has been suggested by other investigators(2) who have demonstrated by more indirect methods that the plants respond to gibberellin treatment only in tissues above the site of application. The fact that radioactivity is present in the tissues below the site of application does not exclude this conclusion in present or other studies since it is not demonstrated that the GA molecule is translocated per se. Further experiments are contemplated to determine the nature of the transported radioactive materials and to determine whether the site of application would change the distribution pattern.

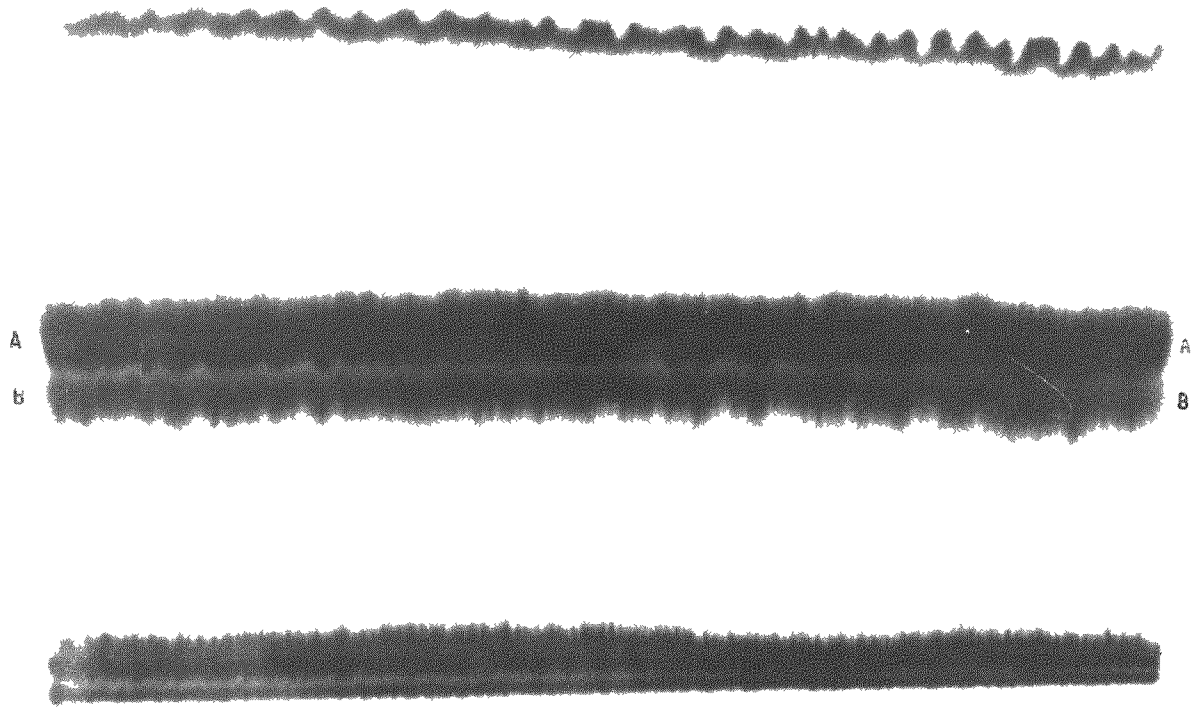

Figure 67. Autoradiogram of the final fraction obtained in the isolation of gibberellic acid. Band AA represents the position corresponding to accepted authentic GA. Band BB represents a closely following unknown substance.

Figure 68. Autoradiogram of a pinto bean plant which was harvested 24 hr after application of C^{14}-GA.

Figure 69. Autoradiogram of a pinto bean plant which was harvested 48 hr after application of C^{14}-GA.

References

1. Watanabe, R. The gibberellins. III. The biosynthesis of C^{14}-gibberellic acid. This report, p 192.

2. Stowe, B. B., and T. Yamaki. The history and physiological action of the gibberellins. Ann. Rev. Plant Physiol. 8:181-216 (1957).

PROGRESS REPORT: GROWTH OF ALGAE IN HIGH CONCENTRATIONS OF DEUTERIUM OXIDE

William Chorney, Norbert J. Scully, Henry Crespi,*
and Joseph J. Katz*

Earlier workers[1-3] have reported that they were unable to grow algae in concentrations of D_2O above 75-85%. Meyer,[4] to the contrary, reported normal growth and morphological development of Chlorella vulgaris in 99.2% D_2O. Meyer's results were disputed by Bonhoeffer.[5] More recently Holm-Hansen et al.[6] and Moses and Holm-Hansen[7] have found normal growth of algae to occur in D_2O concentrations up to about 35%, good growth in concentrations up to about 60%, and some growth in concentrations as high as 90%. The experiments reported here show that algae will grow in 99.6% D_2O, although morphologic development and growth rate are adversely affected. The present effort was undertaken with the initial purpose of determining the highest concentration of D_2O in which algae would make a substantial net gain in weight, and also of ascertaining, if possible, the conditions required to attain maximum growth in 99.6% D_2O. These algae would then serve as a source for fully deuterated compounds.

Methods

Two species of algae, Chlorella vulgaris and Scenedesmus obliquus, were used. They were grown at 28° C under continuous light of an intensity of 600 foot-candles supplied by a fluorescent panel. The algae were agitated continuously by shaking. They were supplied a gaseous mixture composed of 95% N_2 and 5% CO_2 bubbled through a complete inorganic nutrient solution at about 200 ml/min. New cultures were started by inoculating from a rapidly growing culture of algae in a water medium. As D_2O algae cultures were obtained, they were used to inoculate subsequent cultures of the same and higher concentrations of D_2O. They were not grown under sterile conditions.

Growth of the algae was followed by measurements of dry weight. Periodic microscopic examinations were also made to estimate the number of cells in division and the increase in number of cells. At the end of a culture period, which varied from 400 to 700 hr, the organisms were harvested by centrifugation. Assays were made of D_2O concentration of the nutrient solutions and for hydrogen/deuterium ratio in wet and dry cells; the latter was determined by combustion. The results of the assays are shown in Table 52.

*Chemistry Division

TABLE 52

D_2O concentrations of various fractions of cultures of algae

Experiment	Species	Deuterium oxide, %			Ash, %
		Nutrient solution	Cell water	Dry cells*	
1	Chlorella	69.5	67.5	57.4	4
3	Chlorella	0	-	-	4
3	Chlorella	70.7	70.2	66.2	6
3	Chlorella	88.4	87.5	77.7	5
4	Chlorella	99.6	99.6	83.0	9
3	Scenedesmus	0	-	-	3
3	Scenedesmus	70.0	68.9	58.0	7
3	Scenedesmus	88.0	86.6	73.6	7
4	Scenedesmus	99.6	98.8	91.0	8

*% D_2O by combustion of dry cells.

Results

Figures 70 and 71 show typical growth curves for Chlorella and Scenedesmus, respectively, in various concentrations of D_2O. The algae in 70% D_2O made greater gains in weight than algae in H_2O. In 85% D_2O, Chlorella grew essentially as well as in ordinary water. However, in 85% D_2O the initial growth of Scenedesmus was delayed markedly for 200 hr; after this period of time growth started and continued at a normal rate. In 99.6% D_2O the growth of Chlorella and Scenedesmus was very markedly inhibited for the first 200 hr. After this initial period with no weight gain, growth began but continued at a much slower rate than that of the water controls.

When highly deuterated algae grown in 85% and 99.6% D_2O media were transferred back to H_2O, their growth rates were retarded to a marked degree for 60-70 hr. At the end of this initial period their growth rates returned essentially to normal.

Many morphological changes occurred in the deuterated algae. The most striking was a change in the shape of the Scenedesmus cell. Although normally it is ellipsoid, in high concentrations of D_2O one can find forms ranging from ellipsoids to spheres. In both Chlorella and in Scenedesmus, some of the cells grow two or three times larger than normal. Another striking difference is in the chloroplasts; in normal cells the pigmentation

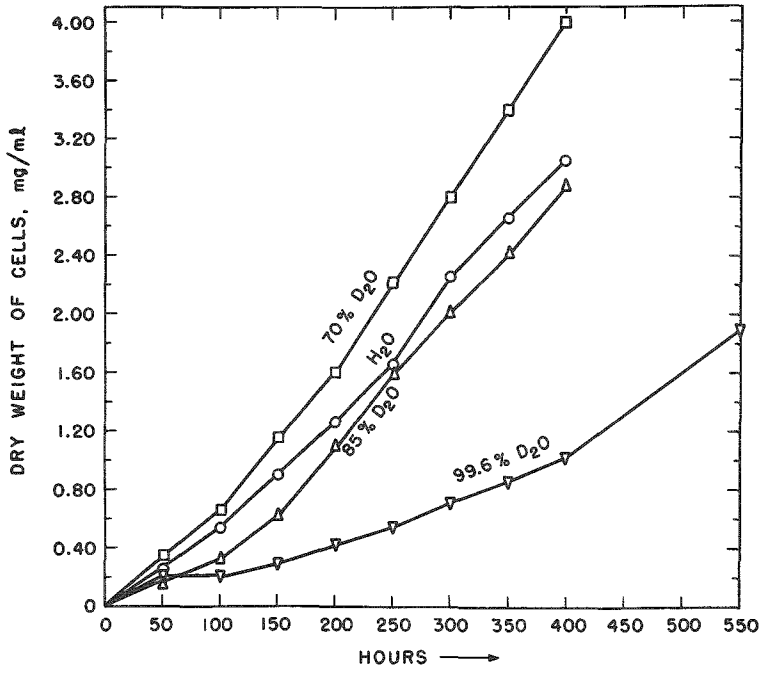

Figure 70

Growth of Chlorella vulgaris in various concentrations of D_2O

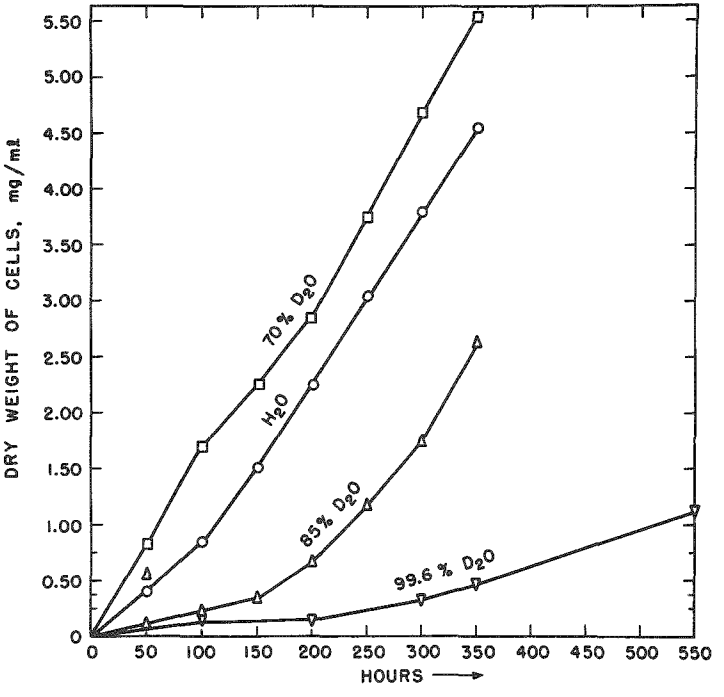

Figure 71

Growth of Scenedesmus obliquus in various concentrations of D_2O

is rather diffuse throughout the cell, but in deuterated algae it becomes quite granular. After the deuterated algae were returned to H_2O, they still had not regained their normal appearance after 3 days although they had gone through 8 to 10 cell devisions.

From the analyses (Table 52) it appears that the cell water is in equilibrium with the nutrient solution with respect to percentages of D_2O. It is apparent, however, that hydrogen is incorporated preferentially to deuterium in the organic compounds of the algae.

It appears feasible to grow algae in very high concentrations of deuterium oxide. This procedure should afford a practical source of highly deuterated organic compounds.

Experiments are in progress to determine whether the initial delay in growth of algae in 99.6% D_2O can be overcome and whether the growth rate can be increased by altering certain environmental factors.

References

1. Reitz, C., and K. F. Bonhoeffer. The incorporation of heavy hydrogen in growing organisms. Naturwissenschaften 22: 744 (1934).

2. Pratt, R. Influence of D_2O on the growth of Chlorella vulgaris. Am J. Botany 25: 699-701 (1938).

3. Calvin, M. Personal communication (1956).

4. Meyer, S. L. Further contributions on the study of the biological effects of heavy water. J. Tenn. Acad. Sci. 11: 269 (1936).

5. Bonhoeffer, K. F. Physiological-chemical investigation with deutero compounds. Z. Elecktrochem. 44: 87-98 (1938).

6. Holm-Hansen, O., V. Moses, and E. Yarberry. Growth of algae in media containing D_2O. Quarterly Report of Chemistry Division, University of California Radiation Laboratory. UCRL-3629, pp. 31-34 (1956).

7. Moses, V., and O. Holm-Hansen. Physiology of Chlorella grown in heavy water. Quarterly Report of Chemistry Division, University of California Radiation Laboratory. UCRL-3710, pp. 22-25 (1957).

PROGRESS REPORT: STUDY OF THE ACTIVATION OF THE CHEMICAL CONSTITUENTS OF THE HUMAN BODY BY A LOW NEUTRON FLUX

Sarmukh S. Brar and Philip F. Gustafson

A preliminary study of the neutron activation of Na, Cl, and K at low flux levels has been carried out at the CP-5 research reactor. Twenty-gram samples of NaOH, $CaCl_2$, and KOH placed in polyethylene bottles were exposed for 24 hr at various locations in the pile room at Bldg. 330. One sample of each compound along with an empty polyethylene bottle was placed at each exposure site. Only the NaOH showed measurable activation in the 24-hr period. The mass of Na irradiated was roughly one-tenth that present in the human body (105 g Na in a 70-kg man). Thus there is a good probability of being able to detect the neutron-activated Na in persons exposed to less than a tolerance dose of thermal and fast neutrons.

PROGRESS REPORT: SCINTILLATION SPECTROSCOPY OF THE X-RAY BEAM FROM A GENERAL ELECTRIC MAXITRON 250

Philip F. Gustafson, Joseph E. Trier, and Sarmukh S. Brar

Preliminary X-ray spectra have been obtained using a $1\frac{1}{2}$ in. diam. by 1/2 in. thick NaI crystal canned in aluminum and a DuMont 6292 photo-tube. Data were collected and analyzed by a 256-channel analyzer. Rather thick (3.12 mm) aluminum filtration or none at all was employed and the X-ray tube current was of the order of a few hundred microamperes.

Since there is reason to suspect that the emission spectrum depends upon the operating current of the X-ray tube, a collimator and baffle assembly is being constructed which will allow using the normal operating current of 10-30 ma. A 2 x 2-in. NaI crystal with a beryllium window will be used with this assembly so that most of the photons will be totally absorbed.